

Dissertation zur Erlangung des Doktorgrades
der Fakultät für Chemie und Pharmazie
der Ludwig-Maximilians-Universität München

**Development of a novel T cell engaging antibody derivative
for local PD-1/PD-L1 immune checkpoint blockade
in acute myeloid leukemia**

Monika Herrmann

aus

Ehingen (Donau), Deutschland

2018

Erklärung

Diese Dissertation wurde im Sinne von § 7 der Promotionsordnung vom 28. November 2011 von Herrn Prof. Dr. Karl-Peter Hopfner betreut.

Eidesstattliche Versicherung

Diese Dissertation wurde eigenständig und ohne unerlaubte Hilfe erarbeitet.

München, den 25.03.2018

.....
(Monika Herrmann)

Dissertation eingereicht am 26.03.2018

1. Gutachter: Prof. Dr. rer. nat. Karl-Peter Hopfner
2. Gutachter: PD Dr. med. Sebastian Kobold

Mündliche Prüfung am 18.06.2018

This thesis has been prepared from September 2013 to March 2018 in the laboratory of Professor Dr. Karl-Peter Hopfner at the Gene Center of the Ludwig-Maximilians-Universität München.

Parts of this thesis are included in the following publication

Herrmann M, Krupka C, Deiser K, Brauchle B, Marcinek A, Ogrinc Wagner A, Rataj F, Mocikat R, Metzeler KH, Spiekermann K, Kobold S, Fenn NC, Hopfner KP and Subklewe M. Bifunctional PD-1 x α CD3 x α CD33 fusion protein reverses adaptive immune escape in Acute Myeloid Leukemia. *Blood*. 2018;132(23):2484-2494.

Parts of this thesis have been presented at international conferences

Herrmann M, Deiser K, Subklewe M, Hopfner KP. Novel antibody derivative locally blocking the PD-1/PD-L1 immune checkpoint in Acute Myeloid Leukemia.

Poster presentation at i-Target Kubus Conference: 29.06.2017 in Munich, Germany.

Herrmann M, Deiser K, Subklewe M, Hopfner KP. Novel antibody derivative locally blocking the PD-1/PD-L1 immune checkpoint in Acute Myeloid Leukemia.

Poster presentation at Third CRI-CIMT-EATI-AACR International Cancer Immunotherapy Conference: Translating Science into Survival: 06.-09.09.2017 in Mainz, Germany.

Third CRI-CIMT-EATI-AACR International Cancer Immunotherapy Conference 2017 Abstracts, 6-9 September 2017: A140.

Herrmann M, Deiser K, Krupka C, Subklewe M, Hopfner KP. Novel antibody derivative to reduce side effects of PD-1/PD-L1 blockade in Acute Myeloid Leukemia.

Poster presentation at PEGS Europe: Protein & Antibody Engineering Summit: 13.-17.11.2017 in Lisbon, Portugal.

PEGS Europe: Protein & Antibody Engineering Summit Abstracts, 13-17 November 2017: A30.

Herrmann M, Krupka C, Deiser K, Subklewe M, Hopfner KP. Novel PD-1 fusion protein to enhance cytolysis of Acute Myeloid Leukemia cells and reduce adverse events.

Poster presentation at the International Symposium Cancer Evolution: Genetic and Epigenetic Evolution of Hematopoietic Neoplasms: 01.-03.03.2018 in Munich, Germany.

Parts of this thesis contributed to the following patent application

LMU Munich, Hopfner KP, Subklewe M, Moritz N, Fenn N (09.11.2015):

“Trispecific molecule combining specific tumor targeting and local immune checkpoint inhibition.”

WO 2017081101 A1

TABLE OF CONTENTS

Table of contents

Summary.....	1
Zusammenfassung	3
1. Introduction	5
1.1. Cancer immunotherapy	5
1.1.1. History of cancer immunotherapy	5
1.1.2. Monoclonal antibodies.....	7
1.1.3. Bi- and multispecific antibodies and derivatives	9
1.1.4. T cell engaging antibody formats	11
1.2. Cancer immunity and the role of immune checkpoints.....	13
1.2.1. Regulation of T cell activation.....	13
1.2.2. Cancer immunoediting and immune escape	14
1.2.3. The PD-1/PD-L1 immune checkpoint	15
1.2.4. Success and drawbacks of PD-1/PD-L1 blockade.....	18
1.3. Acute myeloid leukemia.....	20
1.3.1. AML pathogenesis and conventional therapy	20
1.3.2. The immunosuppressive microenvironment in AML.....	21
1.3.3. Immunotherapeutic approaches in AML	23
2. Objectives.....	27
3. Materials and methods	29
3.1. Materials.....	29
3.1.1. <i>E. coli</i> strains and cell lines	29
3.1.2. Plasmids.....	30
3.1.3. Oligonucleotides	30
3.1.4. Amino acid sequences	32
3.1.5. Commercial antibodies	34
3.1.6. Buffers and media.....	35
3.1.7. Technical equipment.....	35
3.1.8. Software	36
3.2. Molecular biology methods.....	37
3.2.1. Molecular cloning.....	37

TABLE OF CONTENTS

3.2.2.	PCR and site-directed mutagenesis.....	37
3.3.	Microbiology methods.....	39
3.3.1.	Transformation in <i>E. coli</i>	39
3.3.2.	Recombinant periplasmic protein expression	39
3.4.	Cell culture methods	40
3.4.1.	Cell lines	40
3.4.2.	Cell line maintenance.....	41
3.4.3.	Recombinant protein expression in HEK293-based expression systems	41
3.4.4.	Generation of stable Expi293F™ and FreeStyle™ 293 expression cell lines	42
3.4.5.	Generation of stable Flp-In™ T-REx™ 293 cell lines	43
3.4.6.	Generation of stable PD-L1 ⁺ AML cell lines.....	43
3.4.7.	Patient and healthy donor (HD) material	44
3.4.8.	Isolation of peripheral blood mononuclear cells (PBMCs) and T cells	44
3.4.9.	T cell expansion	45
3.5.	Protein biochemistry methods	45
3.5.1.	Purification of poly-Histidine tagged proteins from <i>E. coli</i> periplasm.....	45
3.5.2.	Purification of poly-Histidine tagged proteins from cell culture supernatant.....	46
3.5.3.	Protein purification for analysis in murine NSG xenograft model	47
3.5.4.	Denaturing polyacrylamide gel electrophoresis (SDS-PAGE).....	47
3.5.5.	Western blot analysis	47
3.5.6.	Fluorescence-based thermal shift (ThermoFluor) assay	48
3.6.	Flow cytometry methods	48
3.6.1.	Detection of cell surface antigens	48
3.6.2.	Determination of surface antigen density	49
3.6.3.	Binding studies and determination of dissociation constants (K_D).....	49
3.6.4.	Internalization assay.....	50
3.7.	Biological assays	50
3.7.1.	Redirected lysis assay with pre-activated T cells.....	50
3.7.2.	Preferential lysis assay with pre-activated T cells	51
3.7.3.	Redirected lysis assay with non-stimulated T cells.....	51
3.7.4.	T cell proliferation assay.....	53
3.7.5.	T cell activation assay	54

TABLE OF CONTENTS

3.7.6.	<i>Ex vivo</i> redirected lysis assay of primary AML patient samples	54
3.7.7.	Determination of cytokine levels	55
3.8.	Mouse studies	55
3.8.1.	Study design.....	55
3.8.2.	Cell isolation from murine organs and extraction of murine whole blood	56
3.8.3.	Flow cytometry analysis of murine cells	56
3.9.	Plotting and statistical analysis.....	57
4.	Results	59
4.1.	Design of CiTE antibody format	59
4.2.	Generation and stability of CiTE antibody and scfb	60
4.2.1.	Expression and purification of CiTE antibody and scfb	60
4.2.2.	Protein stability of CiTE antibody, scfb and BiTE [®] -like molecule	62
4.3.	Characterization of target cell lines	63
4.3.1.	Generation of PD-L1 ⁺ AML target cell lines.....	63
4.3.2.	Generation of stable PD-L1 ⁺ , CD33 ⁺ and CD33 ⁺ PD-L1 ⁺ target cell lines	66
4.4.	Binding and internalization of CiTE antibody	67
4.4.1.	Binding of CiTE antibody to target and effector cells.....	67
4.4.2.	K _D determination of scFv modules in CiTE antibody and scfb	68
4.4.3.	Internalization of CiTE antibody	69
4.4.4.	CiTE-mediated PD-L1 blockade on AML cells	70
4.5.	Functional characterization of CiTE antibody on cell lines	71
4.5.1.	Activation of resting T cells.....	71
4.5.2.	Induction of cytotoxic lysis of AML cells by pre-activated T cells	72
4.5.3.	CiTE-mediated increase in redirected lysis of PD-L1 ⁺ AML cell lines	74
4.5.4.	CiTE-mediated increase in T cell proliferation	78
4.5.5.	Sterical influence of N-terminal module in CiTE antibody.....	80
4.5.6.	CiTE-mediated increase in proinflammatory cytokine secretion	80
4.5.7.	Selective lysis of CD33 ⁺ PD-L1 ⁺ target cells	83
4.6.	Selective lysis of primary AML patient samples	85
4.7.	Evaluation of the CiTE antibody in a murine AML xenograft model.....	87
5.	Discussion	93
5.1.	Rationale for the novel CiTE format	93

TABLE OF CONTENTS

5.2.	The CiTE format mediates T cell activation and cytotoxicity	94
5.3.	Differences between CiTE and BiTE [®] format.....	96
5.4.	The CiTE format increases selectivity for PD-L1 ⁺ AML cells.....	97
5.5.	Benefit and risk of CiTE-mediated T cell activation.....	99
5.6.	Optimization potential of the CiTE format.....	101
5.7.	Future directions of the CiTE format.....	102
6.	References	105
7.	List of abbreviations	121
8.	Acknowledgements	125

SUMMARY

Summary

Acute myeloid leukemia (AML) is a severe hematopoietic malignancy with fatal outcome if untreated. Although most patients initially respond to intensive chemotherapy, relapse rates are high and succeeding treatment is challenging. Older patients often do not tolerate conventional therapies and die from their disease within a short time. Thus, new therapeutic strategies are urgently needed. In recent years, improvements in immunotherapy have drastically changed cancer therapy and led to the broad application of immunotherapeutic agents in the clinics. A highly promising approach in AML treatment is the administration of monoclonal antibodies that target the leukemia-associated antigen CD33. Some of these agents redirect endogenous immune effector cells to leukemic cells to trigger their specific elimination. However, not all patients respond to targeted immunotherapy since the destructive anti-cancer activity of immune cells is often impeded by the upregulation of inhibitory checkpoints such as programmed death-1 (PD-1) and its main ligand programmed death-ligand 1 (PD-L1) in the tumor microenvironment. In AML, the expression of these molecules is caused by an inflamed milieu, and it results in an adaptive immune resistance against T effector mechanisms. The application of monoclonal antibodies that interfere with this inhibitory checkpoint can restore the cytolytic T cell activity. Yet, inhibitory ligands are expressed in almost every tissue as natural reaction to inflammation. Therefore, current checkpoint inhibitors frequently cause immune-related adverse events (irAEs) that can develop into a severe state or even lead to death.

The present work establishes a new concept to limit the blockade of the PD-1/PD-L1 axis to the leukemic site and thus to prevent the development of irAEs. This was accomplished by generating a novel molecular format for AML treatment, which is named “Checkpoint inhibitory T cell Engager” (CiTE). The CiTE antibody combines high-affinity targeting of the AML antigen CD33 with low-affinity PD-1/PD-L1 blockade. We took advantage of the naturally occurring weak binding of PD-1_{ex}, which is not sufficient to target PD-L1 alone. Consequently, CiTE-mediated checkpoint blockade is conditional on the avidity contribution of the CD33 binding arm and thus limited to the surface of antigen-positive cells. *In vitro* evaluation of the molecule demonstrates efficient T cell activation and specific induction of cytotoxic lysis of AML cell lines as well as primary AML patient samples. Further, the CiTE antibody reveals a high specificity for PD-L1 expressing AML cells, whereas non-AML cells that are positive for PD-L1 are not addressed. These findings are substantiated *in vivo* in a murine xenograft model, where the CiTE induces the

SUMMARY

depletion of AML cells but does not cause measurable adverse events such as tumor-independent T cell activation or body weight loss. Thus we consider the CiTE format as highly promising strategy to fight AML and lower the risk of irAEs that result from immune checkpoint blockade.

Zusammenfassung

Akute Myeloische Leukämie (AML) ist eine schwerwiegende hämatopoetische Krebserkrankung, die ohne Behandlung tödlich endet. Obwohl die meisten Patienten zunächst auf eine intensive Chemotherapie ansprechen, treten häufig Rezidive auf, die nur schwer zu therapieren sind. Ältere Patienten verkraften konventionelle Therapieformen oft nur schwer und sterben innerhalb kurzer Zeit an ihrer Krankheit, weshalb dringend neue therapeutischen Strategien benötigt werden. In den letzten Jahren fand durch Verbesserungen in der Immuntherapie bereits eine drastische Veränderung der Behandlung von Krebserkrankungen statt, sodass Immuntherapeutika mittlerweile eine breite Anwendung in der Klinik finden. Ein besonders vielversprechender Ansatz bei der Therapie von AML ist der Einsatz von monoklonalen Antikörpern, die das Leukämie-assoziierte Antigen CD33 adressieren. Einige dieser Therapeutika lenken endogene Immuneffektorzellen an Leukämiezellen, um diese spezifisch zu eliminieren. Jedoch sprechen bei weitem nicht alle Patienten auf eine zielgerichtete Immuntherapie an, da die destruktive Aktivität von Immunzellen gegen Krebszellen oft durch die Hochregulation von inhibitorischen Checkpoints in der Tumorumgebung behindert wird. Hierzu zählen insbesondere „Programmed death-1“ (PD-1) und sein Hauptligand „Programmed death-ligand 1“ (PD-L1). Bei AML wird die Expression dieser Moleküle durch ein entzündliches Milieu ausgelöst, welches zu einer adaptiven Immunresistenz gegen T-Effektormechanismen führt. Der Einsatz von monoklonalen Antikörpern, die mit diesem inhibitorischen Checkpoint interferieren, kann die zytolytische Aktivität von T-Zellen wiederherstellen, jedoch verursachen gegenwärtige Checkpointinhibitoren häufig immunassoziierte Nebenwirkungen, die schwerwiegend sein können oder sogar zum Tod führen. Dies liegt darin begründet, dass inhibitorische Liganden als natürliche Reaktion auf Entzündung in fast jedem Gewebe exprimiert werden.

Die vorliegende Arbeit etabliert ein neues Konzept, welches die Blockade der PD-1/PD-L1 Achse auf Leukämiezellen beschränkt und so die Entwicklung von immunassoziierten Nebenwirkungen verhindert. Dies wird durch die Herstellung eines neuen Molekülformats erreicht, das als „Checkpoint inhibitory T cell Engager“ (CiTE) bezeichnet wird. Der CiTE-Antikörper kombiniert hochaffines Targeting des AML-Antigens CD33 mit niedrigaffiner PD-1/PD-L1-Blockade. Wir machen uns die natürliche schwache Bindung der extrazellulären Domäne von humanem PD-1 (PD-1_{ex}) zunutze, die nicht ausreicht, um alleine mit PD-L1-positiven Zellen zu interagieren. Folglich ist die CiTE-vermittelte Checkpointblockade von dem Aviditätsbeitrag des CD33-

ZUSAMMENFASSUNG

Bindearms abhängig, was den Effekt auf die Oberfläche von antigenpositiven Zellen begrenzt. Die *in vitro* Evaluierung des Moleküls zeigt eine effiziente T-Zell-Aktivierung und das Auslösen einer spezifischen zytotoxischen Lyse von AML-Zelllinien sowie primären Patientenproben. Weiterhin beweist der CiTE-Antikörper eine hohe Spezifität für PD-L1-exprimierende AML-Zellen, während andere PD-L1-positive Zellen nicht adressiert werden. Diese Ergebnisse werden *in vivo* in einem murinen Xenotransplantationsmodell bestätigt. Hier verursacht der CiTE-Antikörper die Eliminierung von AML Zellen, jedoch keine messbaren Nebenwirkungen wie übermäßige T-Zell-Aktivierung oder Gewichtsabnahme. Deshalb betrachten wir das CiTE-Format als vielversprechende Strategie für die Therapie von AML, die zur Verringerung von immunassoziierten Nebenwirkungen führt, welche bei der systemischen Blockade von Immuncheckpoints auftreten.

1. Introduction

1.1. Cancer immunotherapy

1.1.1. History of cancer immunotherapy

The opinion about the role of the immune system in cancer has drastically changed over the last century.¹ In 1893, William B. Coley proclaimed that cancerous malignancies can be treated by activating the host immune system. He observed that the injection of streptococcal cultures into primary tumors of patients was able to cause tumor regression after the development of erysipelas.² Hundreds of patients were treated with the so-called “Coley’s toxin”, inducing durable clinical responses even in inoperable tumors. However, the occurrence of severe fever as well as low cure rates soon resulted in clinical replacement of the bacterial injections by surgery and radiotherapy.³ Still, in 1976 the idea of using attenuated bacteria as cancer vaccine was taken up again for treatment of invasive bladder cancer with Bacille Calmette-Guérin (BCG) therapy, which is in clinical use until today.⁴⁻⁶ Another early milestone towards cancer immunotherapy was provided by Paul Ehrlich. He stated in 1909, that the outgrowth of cancerous cells is usually suppressed by the immune system.⁷ Yet, this finding moved into the background until Thomas and Brunet revived the hypothesis of cancer immunosurveillance in the early 1960s. They both claimed that immune cells are able to eliminate malignant cells that were transformed by somatic mutations.⁸⁻¹⁰ Especially Brunet put the opinion forward that lymphocytes continuously guard healthy tissues by depleting cancer cells based on the presence of tumor-associated antigens (TAAs).⁹ However, due to technical limitations this theory could not be substantiated by experimental data in those days and it was not until the early 1990s that the existence of immunogenic TAAs was proven.^{1,11,12} Along with the description of genetic instability that can lead to mutations which favor the escape of tumors from immune surveillance, immunotherapy moved into focus again and is nowadays considered indispensable in the successful treatment of cancer.^{13,14}

The development of the so-called hybridoma technology was essential for the manufacture of monoclonal antibodies (mABs) for cancer immunotherapy.¹⁵ Naturally, antibodies are secreted by terminally differentiated B cells (i.e. plasma cells) as part of the adaptive immune response, and each plasma cell produces antibodies with one particular specificity.¹⁶ For the generation of recombinant mABs, mice were immunized with target antigen, and emerging B cells were

INTRODUCTION

subsequently fused with immortalized myeloma cells to give rise to hybridoma cells secreting one specific antibody.¹⁶ Of hybridoma-derived mABs, muronomab-CD3 (i.e. Orthoclone OKT3[®]; Janssen-Cilag) was the first to be approved by regulatory authorities in 1986 to reduce organ transplant rejection.¹⁷ Still, all early antibodies encountered serious problems when it came to their therapeutic application. These were issues in production and the frequent occurrence of immune responses against the foreign antibody framework regions (FR), which were designated HAMA (human anti-mouse antibody) responses and resulted in rapid elimination by the human immune system and subsequent therapy resistance.^{18,19} In addition, the efficiency of these mABs in patients was poor due to lack of cross-reactivity of the rodent fragment crystallizable (Fc) region with human Fc receptors (FcRs) or factors of the complement cascade.¹⁹ An important step to solve these problems was the ability to clone the genetic sequences of Immunoglobulins (Igs) into eukaryotic expression vectors, which paved the way for the modification of antibodies and overexpression in cell lines or *E. coli*.²⁰⁻²² The immunogenicity of mABs could be lowered by fusing the rodent variable domains of heavy and light chain (V_H and V_L) to the constant regions of a human IgG backbone, resulting in chimeric antibodies with a human content of 70% and a fully human Fc part.^{19,23} In 1985, Jones and colleagues introduced a new methodology that further increased the human proportion to 85-90%. These so-called “humanized” antibodies were generated by the engraftment of the murine complementarity-determining regions (CDR) to a human antibody scaffold.^{19,24} Later, fully human antibodies were generated by using panning strategies such as phage display, with which a multitude of antibodies could be screened based on their binding affinities.^{25,26}

Since the approval of the first recombinant mAB in 1986, the market of biopharmaceuticals, and especially antibodies, is rapidly increasing. Whereas in 2008 global sales of monoclonal antibodies were almost \$35 billion, in 2016 they already reached \$106.9 billion.^{27,28} Starting from highest market strength, the six top sellers in 2016 were adalimumab (Humira[®]; AbbVie), etanercept (Enbrel[®]; Amgen, formerly Immunex), infliximab (Remicade[®]; Johnson & Johnson/ Merck), rituximab (Rituxan[®], MabThera[®]; Genentech/ Roche), trastuzumab (Herceptin[®]; Genentech/ Roche) and bevacizumab (Avastin[®], Roche).^{27,28} Since many novel therapeutic antibodies are currently evaluated in clinical trials and new therapeutic targets are identified continuously, the antibody market is expected to grow steadily.²⁷

INTRODUCTION

1.1.2. Monoclonal antibodies

Based on their constant (C) regions, immunoglobulins (Igs) can be assigned to five different classes (i.e. isotypes). Molecules of the IgA class are present as monomers in the serum and as dimers in the mucosa, IgD antibodies either exist as B cell receptor (BCR) on naïve mature B cells or as soluble monomers. IgE as well as IgG classes exhibit a monomeric form, whereas IgM antibodies are either bound to the surface of B cells as BCR or they are secreted as pentamers. IgG is the most commonly utilized format in therapeutic approaches and can again be categorized into four subclasses (IgG1, IgG2a/b, IgG3, IgG4) that possess differences in FcR binding.^{16,29} A schematic illustration and the crystal structure of the IgG format are depicted in Figure 1.

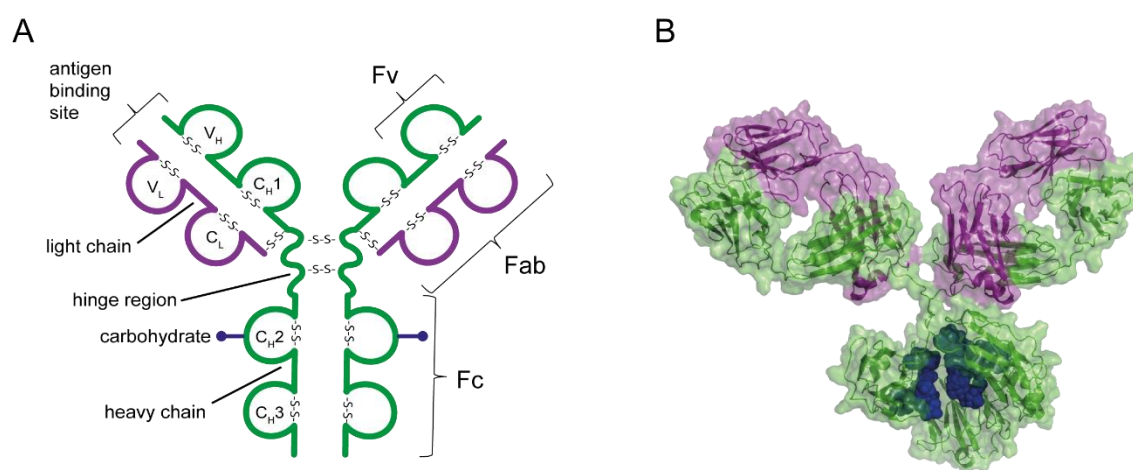


Figure 1: Schematic representation and crystal structure of an IgG antibody.

(A) IgG antibodies consist of two homodimerized heavy and two light chains that are stabilized by intramolecular disulfide bridges. The variable domains at the N-terminus of heavy and light chain (V_H and V_L) represent the variable fragment (Fv) of an antibody and form the specific antigen binding site. They are connected to the constant (C) domains C_H1-3 or C_L, respectively. Digestion with papain cuts the antibody at the flexible hinge region and separates it into two fragments for antigen binding (Fab) and one glycosylated fragment crystallizable (Fc).¹⁶ (B) Crystal structure of IgG1 monoclonal antibody (PDB 1IGY). Heavy chains (green), light chains (violet), carbohydrates (blue). Panel (A) was adapted from Ioscani Jimenez del Val *et al.* (2012), originally published in InTech, Copr. 2012 Kontoravdi *et al.*, licensed by CC BY 3.0 (<http://creativecommons.org>).³⁰

IgGs are composed of four polypeptide chains that are connected to each other by disulfide bridges and have a total molecular weight of roughly 150 kDa. They consist of two homodimerized 50 kDa heavy (H) and two 25 kDa light (L) chains of either kappa (κ) or lambda (λ) type, and have a flexible hinge region.¹⁶ The variable parts of heavy and light chain (V_H and V_L) represent the two identical antigen binding pockets (i.e. paratopes) of an antibody. They form a surface complementary to the binding epitope, which can either be a conformational protein shape, a linear peptide or a carbohydrate.¹⁶ By treating the molecule with the protease papain, it is cleaved into

INTRODUCTION

three functional parts, two fragments for antigen binding (Fab), which correspond to the light chain and the variable and constant 1 domains of the heavy chain (V_H - C_{H1}), and one Fc fragment, which consists of paired C_{H2} and C_{H3} domains.¹⁶ The Fc region exhibits oligosaccharides at Asn297, which are important for the exertion of Fc effector functions.^{31,32}

The separate domains of an IgG molecule reveal a similar and unique fold, which is known as Ig fold. Each Ig domain consists of two β -sheets that are stabilized by an intramolecular disulfide bridge and form a β -barrel structure.¹⁶ C and V domains share a significant similarity, however, the essential difference between the two is that the V domain is extended by two β -strands and possesses an extra loop.¹⁶ Each V domain contains three hypervariable regions (HV1-3) or CDRs, of which HV3 demonstrates the greatest variability. HV regions are connected by four framework regions (FR1-4) that show less variability and are located in close proximity due to the distinct domain fold.¹⁶ Accordingly, six hypervariable loops, three from V_H and three from V_L , form a hypervariable binding surface. Some but not necessarily all loops are responsible for antigen specificity of an antibody and define its binding affinity.¹⁶

Therapeutic mABs either operate by binding and subsequent blocking or activation of a signaling cascade, as antibody-drug conjugate (ADC) through a coupled drug or toxin, or by the initiation of an Fc-mediated immune response.^{33,34} Naturally, the most direct effect of an antibody is mediated by neutralization (i.e. opsonization) of pathogens or toxins to block the interaction with host cell receptors and prevent the infection of healthy cells.^{16,29} For immunotherapy, mABs are further tailored to block cell surface receptors, to trigger internalization or to induce activation or apoptosis of target cells.³⁴ Fc-dependent effector functions are conferred by binding to specific receptors, and the triggered effect crucially depends on the type of receptor as well as the respective immune cell on which it is present. Receptors are either classical FcRs, which are differentially expressed on cells of the innate and adaptive immune system, or C-type lectin receptors (CLRs).²⁹ Binding to the CLR C1q or mannose-binding lectin (MBL) leads to the destruction of target cells by complement-dependent cytotoxicity (CDC).^{29,33} Interaction with FcRs on innate immune cells triggers antibody-dependent cellular cytotoxicity (ADCC) or antibody-dependent cellular phagocytosis (ADCP).^{16,29,35} By utilizing these effector mechanisms in immunotherapeutic mABs, cancer cells can be specifically eliminated or suppressive immune cells such as regulatory T cells (T_{regs}) can be depleted.^{34,35} Notably, Fc-dependent mechanisms result in antigen cross-presentation

INTRODUCTION

by antigen presenting cells (APCs), such as dendritic cells (DCs) and macrophages, to T cells, which are able to initiate a potent anti-tumor immune response.^{33,35-38}

1.1.3. Bi- and multispecific antibodies and derivatives

Over the last years a multitude of bi- and multispecific antibody derivatives has been developed. In contrast to the conventional IgG format, these molecules are able to simultaneously address two or more target antigens and recruit distinct immune effector cells.^{39,40} This increases target cell specificity, impairs resistance formation and potentially leads to synergistic effects compared to combination therapies.⁴¹ Bispecific antibodies typically consist of two different heavy and light chains.⁴¹ As demonstrated at the example of the Triomab[®] format, the constant regions neither have to originate from the same species nor do they have to be of the same isotype. Here, hybridoma cells of mouse and rat are fused to generate a chimera of two full-length half-antibodies of murine IgG2a and rat IgG2b subclass.⁴² Yet, the generation of a bispecific antibody is challenging since it initially leads to complex mixtures.^{41,43,44} To overcome this problem, the knobs-into-holes (kih) technology was an important development ensuring correct heterodimerization of heavy chains.⁴⁵ Furthermore, the correct assembly of light chains can be achieved by engineering a common light chain or by implementing the CrossMab technology, which exchanges C_{H1} with C_L domains in one of the two binding arms.^{46,47} Recent approaches of correct chain pairing also include the forced asymmetric assembly by electrostatic steering or the introduction of specific point mutations at the interface of V_H-V_L and C_{H1}-C_L to generate an orthogonal Fab surface.⁴⁸⁻⁵⁰

Besides antibody derivatives that resemble the classical IgG architecture, various alternative formats are currently investigated. They can be subdivided into Fc-containing and Fc-deficient molecules, of which the latter lack the ability to induce Fc-mediated effector functions such as ADCC or ADCP.^{39,46} The large flexibility in antibody formats allows for tailoring of potential immunotherapeutics to different requirements, by e.g. variations in intramolecular flexibility, size, number of valencies and specificities, and type of effector cell. Fc-containing antibodies can resemble the classical IgG format or contain modifications such as additional binding sites or engineered Fc regions.^{39,46} Figure 2 depicts a selection of bispecific antibodies, of which most are either already approved by regulatory authorities or are currently undergoing clinical evaluation. Depending on the format, molecules can be manufactured from four or less polypeptide chains. Especially recent developments focus on molecular formats that lack an Fc region and are encoded by one (or two) polypeptides. They consist of a modular arrangement of targeting moieties, such

INTRODUCTION

as Fab fragments, scFvs or nanobodies.³⁹ ScFvs represent the minimal binding modules of a human antibody with a molecular weight of roughly 25 kDa and they are generated by connecting V_H and V_L by a flexible polypeptide linker.^{51,52} Nanobodies are single-domain antibodies of 11-15 kDa that originate from variable camelid V_{HH} domains and are similar to shark V_{NAR} domains.^{39,53}

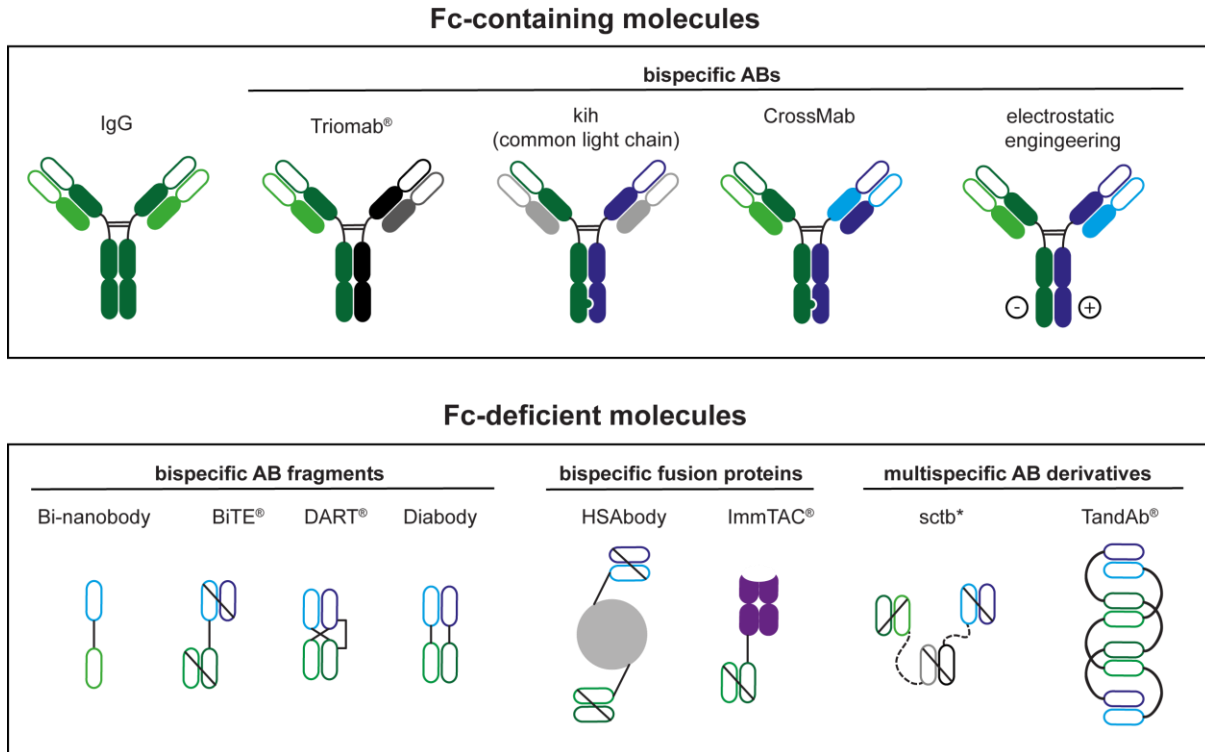


Figure 2: Selection of advanced bispecific antibodies and derivatives.

Molecules that are not yet applied to humans are indicated as *. The upper row depicts ABs containing an Fc region and two arms for bivalent target antigen binding. The lower row illustrates Fc-deficient bispecific AB fragments, fusion proteins and multispecific AB derivatives of smaller size that differ from the classical IgG format. kih, knobs-into-holes; BiTE[®], bispecific T cell engager; DART[®], dual-affinity re-targeting; HSA, human serum albumin; ImmTAC[®], immune mobilizing monoclonal T-cell receptors against cancer; sctb, single-chain triplebody; TandAb[®], tetravalent bispecific tandem diabodies.

Established bispecific molecules include bispecific T cell engagers (BiTE[®]s; Amgen, formerly Micromet) diabodies and dual-affinity re-targeting antibodies (DART[®]s; MacroGenics).^{39,54-56} Besides cell surface antigens, these formats can be extended to target human leukocyte antigen (HLA)-presented intracellular peptides, as implemented in the ImmTAC[®] format (Immunocore).⁵⁷ In contrast to conventional mABs, the smaller molecular weight of Fc-deficient molecules might bear advantages regarding the penetration of tumor tissues.^{58,59} However, they also hold a short plasma retention time due to rapid renal clearance.⁵⁸ Although the BiTE[®] format is the only of these molecules that has hitherto been approved by regulatory authorities, there are many more that

INTRODUCTION

undergo investigation at present, including multispecific molecules such as single-chain triplebodies (sctb) or tetravalent bispecific tandem diabodies (TandAbs[®]; Affimed), which might reveal a higher specificity for tumor cells and beneficial effects regarding cytotoxicity.⁶⁰⁻⁶³

1.1.4. T cell engaging antibody formats

Aside from monoclonal antibodies that trigger an immune response via their Fc region, the direct activation and redirection of antigen-experienced T cells turned out to be a highly successful strategy for cancer eradication.⁵⁶ The great potential of T cells as immune effectors lies within their plasticity, their ability to potentiate immune responses at different levels and the formation of immunologic memory.¹⁶ Notably, the first T cell bispecific (TCB) antibodies were already described more than 30 years ago.⁶⁴ A representative of these early formats is the EpCAM-targeting Triomab[®] catumaxomab (Removab[®]).⁴² However, this molecule leads to the induction of CRS due to Fc gamma receptor (FcγR)-dependent mechanisms as well as an immune response against the mouse/rat antibody backbone.^{65,66} A more recently developed T cell engaging antibody is the trivalent carcinoembryonic antigen (CEA)-TCB, which was designed for the treatment of CEA⁺ cancers.⁶⁷ The use of a human IgG1 backbone and Fc silencing mutations prevent the adverse events that have been described for catumaxomab.⁶⁷ The molecule contains a dual specificity for CEA and CD3ε. By the head-to-tail fusion of a second CEA-targeting Fab fragment to the N-terminus of the CD3ε binding arm, it possesses two valencies for its TAA.^{67,68} Due to promising preclinical data, this format is currently investigated in two phase I clinical trials (NCT02650713, NCT02324257) on advanced or metastatic CEA⁺ solid tumors.^{67,68}

In recent years, particularly BiTE[®] antibodies emerged as efficient TCB format. BiTE[®]s are 55-60 kDa fusion proteins that consist of two scFvs connected by a short peptide linker. One of the two scFvs is directed against the T cell coreceptor CD3 to redirect T cells to the tumor cell, whereas the second scFv specifically addresses a TAA.^{56,69-71} Notably, the BiTE[®] mode of action is independent of the specific interaction between major histocompatibility complex (MHC):peptide and T cell receptor (TCR) or additional stimuli and therefore has the potential to access a large effector T cell pool.^{69,72} T cell activation is accompanied by the transient release of proinflammatory cytokines such as interferon (IFN)-γ, tumor necrosis factor (TNF)-α, IL-2, IL-4, IL-6 and IL-10, T cell proliferation and the cytotoxic lysis of target cells.^{56,69,70,73} Recent findings indicate that BiTE[®]s not only induce tumor cell depletion but extend their effect to bystander cells that are TAA-negative.⁷⁴ Yet, since *in vitro* T cell activation crucially depends on the physical

INTRODUCTION

crosslink to target cells, T cell effector functions are expected to be mainly limited to the tumor milieu. This implies avoiding severe damage to distant organs by sole CD3 stimulation.⁷³ An important feature of the molecular BiTE[®] scaffold is the balanced affinities between the two scFvs. Whereas the tumor-targeting scFv holds a high affinity for the TAA with a K_D value in the range of 10^{-9} M, the T cell redirecting CD3 scFv binds with lower affinity ($K_D = 10^{-7} - 10^{-9}$ M).^{70,75} This difference results in stronger binding to targets than to T cells and leads to the formation of a tumor-immobilized matrix of BiTE[®] molecules, on which T cells migrate between tumor cells to induce serial lysis.⁶⁹ BiTE[®]-mediated target cell depletion is very efficient with measured EC_{50} values in the range of $10^{-11} - 10^{-13}$ M, indicating that low numbers of bound molecules are sufficient to induce T cell effector functions.^{75,76}

Various BiTE[®] constructs have been tailored to address different TAAs.^{56,69,75-81} Of these, the CD19xCD3 BiTE[®] antibody blinatumomab was the first to achieve clinical approval by the U.S. Food and Drug Administration (FDA) and European Medicines Agency (EMA) in 2014 and 2015, respectively, for the treatment of relapsed or refractory (r/r) CD19⁺ B-cell acute lymphoblastic leukemia (B-ALL) under the trade name BLINCYTO[®].⁶³ Blinatumomab has demonstrated its high clinical efficacy at very low concentrations. Due to its low molecular weight and the associated fast renal clearance, it is administered as continuous infusion over several weeks.^{63,82} Blinatumomab-mediated T cell activation is often accompanied by immune-related adverse events (irAEs), mostly represented by mild inflammation that manifests in flu-like symptoms.⁸³ However, some patients develop characteristics associated with cytokine release syndrome (CRS), which in a small group of adult patients can adopt a severe state.⁸⁴ Commonly observed irAEs include pyrexia, lymphopenia, an increase in C-reactive protein as well as neurotoxic effects that are expected to be associated with increased cytokine levels in the central nervous system (CNS).⁸² Most adverse events can be reduced by stepwise dosage and counteraction with e.g. corticosteroids and pentosane polysulfate.^{82,85} Besides blinatumomab, the CD33xCD3 antibody AMG 330 is the second most advanced BiTE[®] and a promising candidate for the therapy of r/r AML. In preclinical studies, AMG 330 demonstrated its high potential to specifically deplete AML cell lines and primary AML patient blasts in allogeneic as well as autologous settings and therefore entered clinical trials in August 2015 (NCT02520427).^{75,79} Furthermore, other T cell redirecting formats such as scTbs are under preclinical evaluation.^{86,87}

1.2. Cancer immunity and the role of immune checkpoints

1.2.1. Regulation of T cell activation

Priming and activation of naïve T cells takes place in lymphoid organs through the contact with APCs. Three distinct signals are required: Signal one is provided by the interaction of the TCR with its specific MHC:peptide complex expressed on the APC. Signal two is a co-stimulatory signal that regulates T cell survival and expansion and is mostly delivered by binding of B7 molecules on APCs to CD28 on T cells. Signal three is represented by the cytokine milieu, which determines T cell proliferation and differentiation.¹⁶ In particular, cytokine interleukin-2 (IL-2) binds to the high-affinity version of its receptor on activated T cells, which are in turn triggered to produce IL-2 themselves and thereby amplify the signal.¹⁶ In case of low-level TCR crosslinking (i.e. signal one) in the absence of co-stimulatory signals, T cells become anergic or undergo apoptosis.^{16,88,89} Generally, T cell fate is largely determined by the composition of the cytokine microenvironment that the cell encounters, which in turn is shaped by factors released by innate and adaptive immune cells.¹⁶ While CD8⁺ naïve T cells differentiate into cytotoxic T lymphocytes (CTLs) that specifically induce cytolysis of target cells, CD4⁺ T cells can develop into different effector subclasses. These are divided into T helper cells T_{H1}, T_{H2}, T_{H17} and regulatory T cells (T_{reg}).¹⁶ T_{H1} cells act by triggering the elimination of intracellular pathogens by macrophages. Both T_{H1} and T_{H2} cells trigger antibody production by plasma cells, and T_{H17} cells stimulate neutrophils to eliminate extracellular bacteria. Contrarily, T_{regs} function as natural opponents of an immune response and suppress T cell effector functions.¹⁶ Although it was previously stated that T_{regs} originate from CD4⁺ T cells, lately also CD8⁺ T_{reg} cells have been described. Even though their function is not yet fully understood, it is reported that CD8⁺ T_{regs} are strongly immunosuppressive and can promote cancer progression.⁹⁰⁻⁹²

During the process of activation, proliferation and differentiation, T cells traffic from lymphoid organs to the place of inflammation and interact with cells that present their specific MHC:peptide complex. At each stage of the immune response, T cells are accurately regulated by a large network of co-activating and co-inhibiting signals.^{93,94} A well-balanced system of these molecules is crucial for maintaining T cell homeostasis. Particularly inhibitory signals that are provided by so-called immune checkpoints have the function to ensure self-tolerance and thereby protect healthy tissues from an excessive immune response.⁹³⁻⁹⁶ Many regulatory molecules have been identified over the last years. They share similarity to the superfamily of tumor necrosis factor receptors (TNFR), such

INTRODUCTION

as the co-stimulatory receptors CD27 or 4-1BB, or can be assigned to the CD28 superfamily, such as the inducible co-stimulator (ICOS) or the inhibitory cytotoxic T lymphocyte-associated protein-4 (CTLA-4) and programmed death-1 (PD-1).^{16,97} CTLA-4 and PD-1 are inhibitory immunoreceptors that are predominantly addressed with current immunotherapies. Both checkpoints play a role at different stages of T cell immunity. While CTLA-4 stimulation by B7 on APCs regulates naïve T cells during the priming phase in the lymph node, PD-1 curtails effector functions of activated T cells in the peripheral tissue.⁹⁸

1.2.2. Cancer immunoediting and immune escape

Cancer immunosurveillance is crucial for preventing (and limiting) tumor growth and metastasis. However, in a process designated as “immunoediting”, cancerous cells may disrupt the natural immune response and become resistant to elimination.⁹⁹ In general, the depletion of these cells is a concerted process of the innate and adaptive part of the immune system, which can be subdivided into four phases:^{8,99} In phase one, the immune response is initiated. Tumor cells are recognized by innate immune cells such as natural killer (NK), NKT and $\gamma\delta$ T cells that infiltrate the tumor mass once it reaches a certain threshold and start to release IFN- γ .^{8,99-101} Phase two includes effects triggered by IFN- γ such as the production of various chemokines that inhibit neoangiogenesis and proliferation of the tumor cells and promote apoptosis.^{8,99,102,103} Additionally, NK cells, macrophages, DCs and other immune cells are attracted by the cytokine milieu and induce cancer cell death. Cell debris are ingested by DCs, which migrate to the tumor-draining lymph node (TDLN) and cross-prime resting T cells.^{8,99} In phase three, the tumor cells are kept at bay by the destructive activity of NK cells and macrophages, whereas TAA-specific naïve T cells are activated in TDLNs and differentiate into CD4⁺ and CD8⁺ effector T cells.^{8,99} In phase four, these T cells traffic to the cancer site along a chemokine gradient, where they specifically eradicate tumor cells presenting their cognate MHC:peptide antigen.^{8,99} The following process is a dynamic equilibrium of continuous tumor cell depletion and reproduction. However, the induced selection pressure and the high mutagenesis rate of tumor cells can promote the emergence of cells with reduced immunogenicity. This equilibrium process and the concomitant selection for non-immunogenic cancer cells may last several years and result in the outgrowth of tumor cell variants that escape from immune recognition.^{8,99}

One crucial mechanism of cancer immune escape is the upregulation of inhibitory immune checkpoints in the microenvironment. Although these regulatory axes are inevitable during

INTRODUCTION

inflammation to dampen the immune response, an upregulation of inhibitory ligands on tumor cells disrupts cancer immunity and promotes tumor growth.^{94,96} T cell activity, can be inhibited at different stages of the cancer immunity cycle. Aside from failure of TAA recognition in lymphoid organs or unsuccessful migration into the tumor tissue, effector T cells can be directly inhibited at the tumor site. Moreover, infiltrating T lymphocytes might differentiate into T_{regs} rather than CTLs and thus promote an immunosuppressive microenvironment.^{94,104}

For the upregulation of PD-L1 on cancer cells two general mechanisms are postulated, innate immune resistance and adaptive immune resistance.^{93,105} The first mechanism describes PD-L1 overexpression as a result of constitutive oncogenic signaling, as reported for glioblastoma, some lymphomas and prostate cancer.^{93,106} Contrarily, the acquisition of adaptive immune resistance results from a reactive upregulation of checkpoint molecules in response to a proinflammatory microenvironment.⁹³ Especially IFN- γ was shown to induce PD-L1 expression on both cancer as well as various other tissues.^{93,96,107} The paradigm of adaptive immune resistance suggests that immunogenic neoepitopes might be present in advanced cancers but that cancer immunity is inhibited by this mechanism.^{93,108} The blockade of immune checkpoints by monoclonal antibodies is thus a highly promising strategy to reactivate T cells and favor a beneficial outcome in various tumors.^{93,108}

1.2.3. The PD-1/PD-L1 immune checkpoint

Programmed death-1 (PD-1) is a 288 amino acid (aa) type I transmembrane glycoprotein with a molecular weight of 50-55 kDa that is predominantly found on activated T cells.^{96,109,110} It consists of an N-terminal extracellular IgV domain, a ~20 aa stalk, a transmembrane region and a ~95 aa intracellular part containing both an immunoreceptor tyrosine-based inhibitory motif (ITIM) and an immunoreceptor tyrosine-based switch motif (ITSM).^{96,110} Splice variants of PD-1 have been reported in activated human T cells.¹¹¹ Although PD-1 is a member of the CD28 superfamily, it shares a low sequence identity with CD28 and CTLA-4.^{110,112} In contrast to other family members, it lacks the proline-rich MYPPPY motif in its extracellular region, which is involved in CD28 ligand binding, as well as a cysteine residue responsible for dimerization.⁹⁷ Programmed death-ligand 1 (PD-L1, also known as B7-H1) and programmed death-ligand 2 (PD-L2, also known as B7-DC) have been described as PD-1 ligands.^{113,114} Both proteins contain two extracellular Ig domains. The N-terminal domain adopts an IgV fold and is responsible for PD-1 binding.¹¹⁵ PD-1 interacts with its ligands PD-L1 and PD-L2 in a 1:1 stoichiometry.^{112,116} For the PD-1/PD-L1

INTRODUCTION

interaction, a K_D value of 8.2 μM is reported, whereas the PD-1/PD-L2 interaction revealed a slightly stronger binding with $K_D = 2.3 \mu\text{M}$.¹¹⁵⁻¹¹⁷ PD-1 and PD-L1 bind to each other via the large hydrophobic surfaces at the sides of their IgV domains. By this, the loops of both IgV domains are positioned on the same side of the complex, which significantly resembles the antigen binding site of antibodies and TCRs.¹¹⁶

In contrast to other CD28 protein family members, PD-1 cannot only be found on T cells but also on activated B cells and myeloid cells such as DCs.^{109,118,119} PD-1 is not expressed by naïve T cells, but upregulated on CD4⁺ and CD8⁺ T cells upon activation.^{109,120} Rapid antigen elimination induces a decrease in PD-1 levels, whereas high levels remain on the cell surface in case of antigen persistence such as during chronic inflammation or cancer.¹²⁰⁻¹²³ T_{regs} reveal a sustained PD-1 expression and it has been shown that in the presence of CD3 and transforming growth factor (TGF)- β , PD-1⁺ T_{regs} directly promote the conversion of CD4⁺ T cells into a T_{reg} phenotype and thereby amplify the T_{reg} population at the tumor site.^{105,124} The two PD-1 ligands differ significantly in their expression patterns. PD-L1 is broadly upregulated on T cells, B cells, DCs, and myeloid cells as well as on non-hematopoietic tissues.^{96,107,120,125} It is frequently upregulated in the presence of proinflammatory cytokines, of which IFN- γ is the most potent.^{96,107} PD-L1 plays a crucial role in the acquisition of adaptive immune resistance by cancer cells.⁹³ Contrarily, PD-L2 expression is restricted to a small subset of immune cells, including DCs, macrophages and some B cell subpopulations.^{96,120,125} Under healthy conditions, PD-L2 is not expressed, but similar to PD-L1 it can be upregulated in the presence of proinflammatory cytokines.^{96,120} Although both PD-L1 and PD-L2 can be found on cancer cells, PD-L1 overexpression is more frequently observed. The expression levels, however, demonstrate a high intra- and inter-tumor variability.^{108,120,126} High surface density of PD-L1 often correlates with a decrease in overall survival (OS), thereby establishing PD-L1 as valuable prognostic biomarker.¹²⁷⁻¹³¹

By interaction of PD-1 on the T cell with its ligands, an inhibitory signaling cascade is initiated that decreases T cell activity. More precisely, PD-1 ligation with PD-L1 or PD-L2 antagonizes the activating signaling cascades of the TCR/CD3 complex and CD28 (Figure 3).¹²⁰ After PD-1 stimulation, phosphatases such as src homology 2-domain-containing tyrosine phosphatase (SHP)-2 associate with the intracellular ITSM motif of PD-1.^{120,132,133} Thereby, they interfere with phosphoinositide 3-kinase (PI3K)/AKT and rat sarcoma (RAS) pathways, resulting in reduced levels of activating transcription factors such as activator protein-1 (AP-1), nuclear factor of

INTRODUCTION

activated T cells (NFAT) and nuclear factor- κ B (NF- κ B). This leads to inhibition of T cell effector functions, growth arrest, and anergy.^{120,133,134} Recently, chemokine-like factor-like MARVEL transmembrane domain-containing protein (CMTM) 4 and 6 have been identified to contribute to immunoresistance by stabilizing PD-L1 at the cell surface via reduction of its ubiquitination.¹³⁵ Moreover, oncogenic RAS signaling leads to stabilization of PD-L1 mRNA and thus enhances antigen levels.¹³⁶

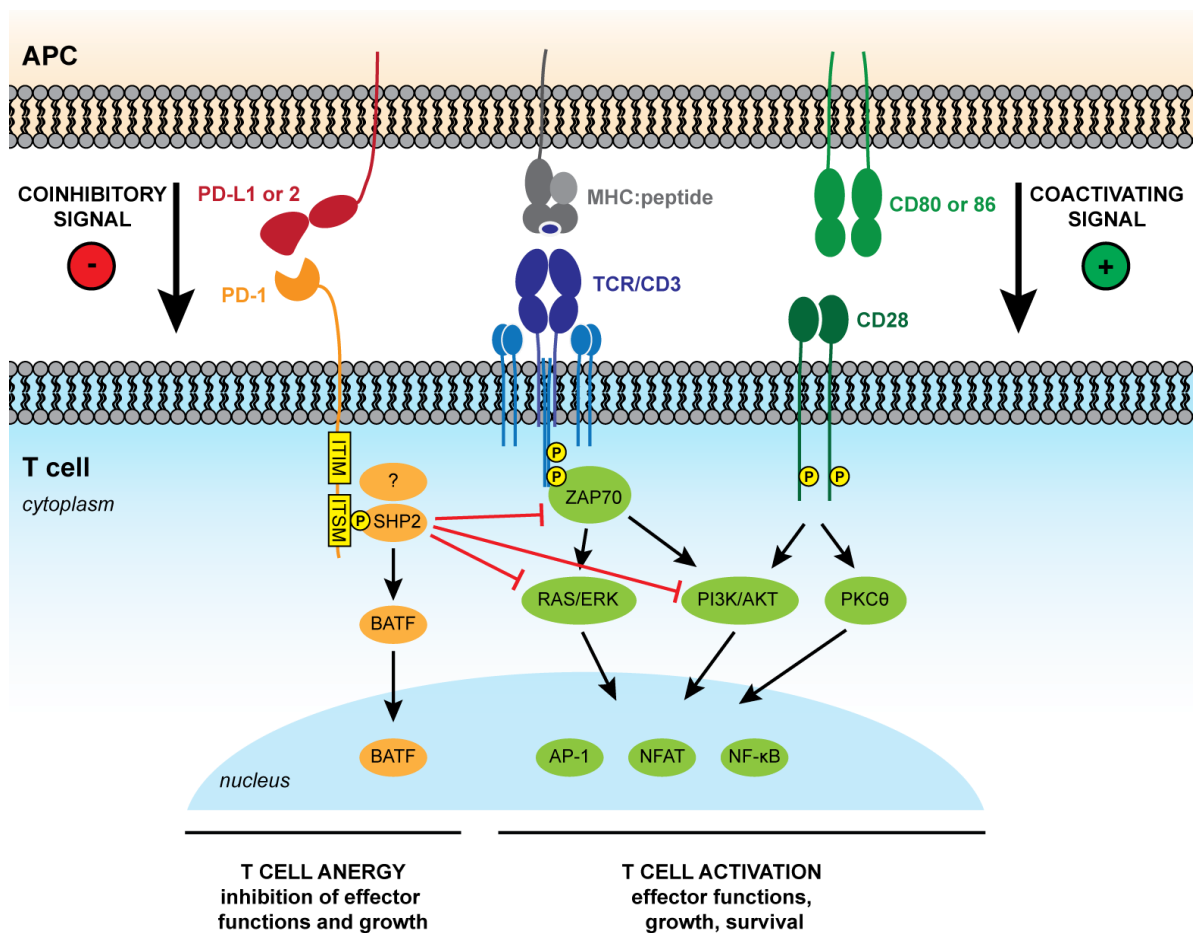


Figure 3: PD-1 signaling in the T cell.

PD-1 stimulation with PD-L1 or PD-L2 counteracts the activating TCR/CD3 and CD28 signaling cascades. Phosphatases such as SHP2 are recruited to the ITSM motif of the cytoplasmic PD-1 tail. These interfere with ZAP70, RAS and PI3K/AKT pathways and thus decrease activating and inhibiting transcription factors. Collectively, this leads to inhibition of T cell activation, growth, effector functions and survival and promotes a T cell anergy phenotype.^{120,132-134,137} ITIM, immunoreceptor tyrosine-based inhibitory motif; ITSM, immunoreceptor tyrosine-based switch motif; SHP2, src homology 2-domain-containing tyrosine phosphatase-2; ZAP70, zeta-chain-associated protein kinase 70; RAS, rat sarcoma; ERK, extracellular signal-regulated kinase; PI3K, phosphoinositide 3-kinase; AP-1 activating transcription factors such as activator protein-1; NFAT, nuclear factor of activated T cells; NF- κ B, nuclear factor- κ B; BATF, basic leucine zipper transcriptional factor ATF-like; PKC θ , protein kinase C θ . Adapted by permission from Springer Customer Service Centre GmbH: Springer Nature, Nature Reviews Immunology, The diverse functions of the PD1 inhibitory pathway, Arlene H. Sharpe, Kristen E. Pauken, *Copr.* 2017.¹²⁰

INTRODUCTION

The actual complexity of PD-1/PD-L1/2 pathway regulation, however, remains to be elucidated in detail, as it is not only dependent on the expression of PD-L1 and PD-L2. For instance, PD-L1 can additionally interact with CD80 (i.e. B7-1) and PD-L2 was shown to bind to repulsive guidance molecule B (RGMB), which both also seem to provide inhibitory signals.^{120,138,139}

1.2.4. Success and drawbacks of PD-1/PD-L1 blockade

The expression of PD-1 and its ligands has a strong influence on the inhibition of T cell-mediated anti-tumor activity.^{93,120} It is well established that the blockade of the PD-1/PD-L1 axis can counteract peripheral tolerance and reactivate anergic T cells.^{93,107} Since PD-1 is not only expressed on T cells but also on other immune cells, the interference with this pathway might furthermore result in an increased activity of NK cells as well as elevated levels of antibody production by PD-1⁺ B cells.^{93,140} Clinical investigation of mABs that interfere with the PD-1/PD-L1 pathway provided persistent and durable responses in a variety of tumors, including cancers at advanced stages such as non-small-cell lung cancer (NSCLC), kidney cancer and melanoma.^{131,141} This broad clinical success is reflected in market approval of pembrolizumab (KEYTRUDA[®]; Merck) and nivolumab (OPDIVO[®]; BMS) in 2014 as the pioneering therapeutics for PD-1 blockade, as well as the three PD-L1 mABs atezolizumab (TECENTRIQ[®]; Genentech), avelumab (BAVENCIO[®]; Merck/ Pfizer) and durvalumab (IMFINZI[™]; AstraZeneca), which are currently applied for the treatment of numerous cancers.^{120,142-146} More than a thousand clinical trials with PD-1/PD-L1 blocking agents are ongoing to evaluate these molecules in different tumor types as mono- or combination therapy.¹⁰⁵ However, there is a heterogeneity in responsiveness to PD-1/PD-L1 blockade between different cancer types and individual patients. While many patients can be treated successfully, others respond only temporally or do not show a beneficial effect at all.¹⁴⁷ Moreover, some cancer types can be efficiently treated, whereas others are refractory to PD-1/PD-L1 inhibition.¹²⁰ There are even cases in which PD-1 blockade might promote tumor growth. Wartewig and colleagues could, for example, recently show that the interference with the PD-1 pathway can lead to the acceleration of disease progression in T cell non-Hodgkin's lymphoma (NHL).¹⁴⁸

The combination with other therapeutic agents provides the possibility to overcome the unresponsiveness of patients, to extend checkpoint inhibition to tumors that are insensitive to monotherapy and to enhance therapeutic efficiency.^{93,105} Selected agents can either directly address cancer cells or components of the immune system. It is therefore inevitable to understand the

INTRODUCTION

intracellular signal integration of engaged pathways to obtain synergistic effects.¹²⁰ One therapeutic strategy is to combine PD-1/PD-L1 inhibition with direct targeting of a second immunologic pathway.¹²⁰ Highly promising clinical responses were evoked by the simultaneous blockade of CTLA-4 and PD-1 with ipilimumab and nivolumab. In a phase III clinical trial in advanced melanoma patients, this combination proved to increase the 3-year OS rate to 58% compared to 34% and 52% for ipilimumab or nivolumab monotherapy, respectively, and resulted in marketing approval of this combination in 2015.^{149,150} Other approaches address costimulatory checkpoints such as ICOS or CD40, block inhibiting cytokines such as IL-10 or are based on the co-administration of proinflammatory cytokines such as IL-2.¹²⁰ Another strategy is to combine PD-1/PD-L1 blockade with radio- or chemotherapy or with mABs that directly target the tumor. These therapies induce an immunogenic cell death resulting in the release of tumor antigens and so-called “danger signals”, which are subsequently engulfed by APCs. The presentation of cancer antigens is thus increased and cancer immunogenicity is elevated.^{120,150} A third strategy is to modulate epigenetic or metabolic pathways.¹²⁰ Especially the combination of PD-1 blockers and agents that modulate T cell metabolism seems to be highly relevant.^{151,152} Clinically applied agents include methotrexate or dichloroacetate as metabolic drugs, and DNA methyltransferase inhibitors (such as 5-azacitidine and decitabine) as well as histone deacetylase inhibitors (such as vorinostat) as epigenetic drugs.¹²⁰ Further therapeutic approaches are vaccination, the interference with T_{regs} and myeloid-derived suppressor cells (MDSCs), inhibition of angiogenesis, or direct stimulation of effector cell cytotoxicity in combination with checkpoint blockade.¹⁵⁰

Although the number of responding patients can be raised with a well-adjusted therapy, it is important to identify reliable biomarkers that allow tailoring of individualized therapies.^{150,153} Several attempts have already been made to predict clinical responsiveness, including the approach of Hugo and colleagues, who identified a transcriptional signature that characterizes resistance to PD-1 blockade (i.e. Innate PD-1 RESistance; IPRES).^{154,155} However, there is no consensus regarding reliable criteria that can be implemented in clinical practice at present.

Despite the dramatic success of PD-1/PD-L1 inhibitors, their application is frequently correlated with immune-related adverse events (irAEs).¹²⁰ These result from the systemic interference with the immune checkpoint, which leads to autoimmune toxicity against self.⁹⁸ Since PD-L1 can be expressed in almost every tissue, reported irAEs cover numerous organs and include colitis, dermatitis, hepatitis, endocrinopathies, pneumonitis and myocarditis.^{98,156-161} Adverse events can

INTRODUCTION

range from weak to severe or even fatal toxicity and often require medical intervention with corticosteroids or other immunosuppressive agents and a discontinuation of the treatment.^{158-160,162} It is not surprising that a systemic dysfunction in PD-1 signaling is correlated with autoimmune events since this was already described in preclinical models. In C57BL/6 mice, PD-1 deficiency causes chronic lupus-like autoimmune disease, and NOD-Pdcd1^{-/-} mice develop type I diabetes.^{163,164} In 129S4/SvJae mice, a PD-L1 knockout results in susceptibility to autoimmune encephalomyelitis.¹⁶⁵ In humans, impaired PD-1 functionality caused by single-nucleotide polymorphisms (SNPs) in the *PDCDI* gene was identified to promote different autoimmune diseases including systemic lupus erythematosus and rheumatoid arthritis.^{166,167} Therefore, limiting immune checkpoint blockade to the tumor site and sustaining a functional crosstalk between immune cells and healthy tissue is a promising therapeutic strategy. The design of bispecific antibodies is one way to increase tumor specificity. Molecules have been developed that simultaneously bind to two immune checkpoints such as a PD-1 and T-cell immunoglobulin and mucin-domain containing (TIM)-3, as well as formats that address PD-1 and a TAA as for instance cellular-mesenchymal to epithelial transition factor (c-Met).^{168,169} Another strategy is to combine PD-L1 blockade with high-affinity targeting of extracellular matrix proteins in the tumor stroma, thereby increasing the retention time at the tumor site.¹⁷⁰ Although multiple approaches are currently evaluated, none of them has been approved by regulatory authorities yet.

1.3. Acute myeloid leukemia

1.3.1. AML pathogenesis and conventional therapy

Acute myeloid leukemia (AML) originates from malignantly transformed cells of the myeloid lineage with abnormal differentiation and proliferation properties.^{16,171} Leukemic blasts expand clonally and accumulate in bone marrow, blood and infrequently in different extramedullary tissues. This hampers normal hematopoiesis and consequently results in anemia, granulocytopenia and thrombocytopenia.^{172,173} AML cells reveal a high level of heterogeneity at both cellular and molecular levels, and different leukemic clones can be detected at the time of diagnosis.¹⁷² Based on cytomorphologic and cytochemical characteristics, the French-American-British (FAB) classification distinguishes between eleven subtypes.^{171,174} To integrate genetic alterations as well as clinical criteria, an additional classification is provided by the World Health Organization (WHO) and was last revised in 2016.^{171,175,176} Categorizing patients according to these criteria

INTRODUCTION

improves the risk-stratification and identification of the best therapeutic options.¹⁷⁷ However, AML therapy has not significantly improved over the last 30 years.¹⁷² Conventional treatment consists of induction therapy, in which the high burden of cancer cells is reduced by intensive chemotherapy with cytarabine and an anthracycline to achieve complete remission.^{172,178} Subsequently, patients undergo a consolidation or postremission therapy to prevent a potential relapse. This mostly includes two to four cycles of intermediate-dose cytarabine chemotherapy or, depending on the genetic risk profile, allogeneic hematopoietic stem cell transplantation (HSCT).^{172,178} With standard therapy, AML can be cured in 35 to 40% of adult patients who are 60 years old or younger.^{172,177} However, in older patients, who cannot endure intensive chemotherapies, median OS is less than one year.¹⁷² Although many patients initially respond to chemotherapy, relapse rates are high and succeeding treatment is challenging.¹⁷² Remaining leukemic cells in the bone marrow are of high prognostic value to assess the risk of relapse as well as long-term survival.¹⁷⁹ Presumably, this so-called minimal residual disease (MRD) originates from chemoresistant leukemic stem cells (LSCs) that bear the potential for self-renewal and asymmetric cell division and thus have the ability to reinitiate and sustain the disease.¹⁸⁰⁻¹⁸² A high mortality rate after relapse indicates that LSCs are not efficiently eradicated by chemotherapy, and that alternative strategies are needed to specifically address this cell population.^{180,183} To date, HSCT represents the only curative option, but a matching donor is often lacking and the therapy itself goes along with a high rate of morbidity and mortality due to infections or graft-versus-host disease.¹⁸⁴

1.3.2. The immunosuppressive microenvironment in AML

In the last years, it became evident that one reason for the failure of conventional chemotherapy is the induction of immune escape pathways that lead to immunologic tolerance.¹⁸⁵⁻¹⁸⁷ These mechanisms are expected to impede the efficient eradication of leukemic cells by endogenous anti-leukemia immune responses as well as AML therapies.¹⁸⁶⁻¹⁸⁸ It has been suggested that the expression of inhibitory immune ligands such as PD-L1 is due to adaptive immune resistance mechanisms.⁹³ Similar to the healthy state, in which PD-L1 is upregulated in the presence of proinflammatory cytokines as protective mechanism against an excessive immune response, PD-L1 expression can be induced on AML cells in an inflamed microenvironment and hence protect the tumor from eradication by the immune system.^{120,189-191} Accordingly, the finding that at primary diagnosis PD-L1 is only expressed in a subset of cases might be an indication for a non-

INTRODUCTION

inflamed, immunosuppressive state.¹⁹²⁻¹⁹⁴ Upon initial treatment or relapse after HSCT, PD-L1 levels are detected more frequently.^{189,190,194-197} Preclinical studies in mice reveal that after injection of the PD-L1⁺ AML cell line C1498, PD-1 was significantly upregulated at leukemic sites and the number of T_{regs} increased.¹⁸⁶ Furthermore, PD-1 knockout as well as the administration of a PD-L1 blocking mAb were able to decelerate disease progression and prolong survival.¹⁸⁶ The combination of PD-1/PD-L1 blockade and depletion of T_{regs} even enhanced the therapeutic success.¹⁸⁶ Thus, PD-L1 expression not only directly inhibits the cytolytic activity of CTLs but also acts by increasing the frequency of T_{regs}.¹⁸⁶

In addition to the PD-1/PD-L1 axis, the upregulation of CTLA-4 and CD200 are described to substantially contribute to immune tolerance in AML.^{198,199} However, the tolerogenic environment is not only mediated by the upregulation of inhibitory ligands but rather shaped by a complex interplay of leukemia, stroma and immune cells that collectively lead to a dysregulated immune response (Figure 4).¹⁸⁵

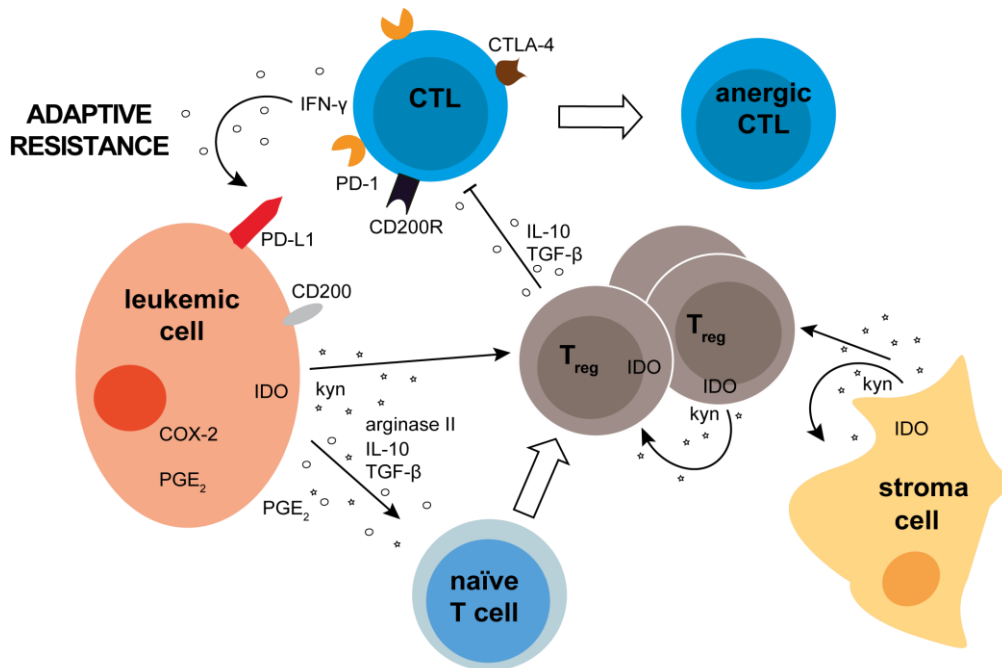


Figure 4: Immunosuppressive microenvironment in AML.

In the AML microenvironment, T cells can be inhibited by the secretion of immunosuppressive molecules such as TGF- β , arginase II, IL-10 or kynurenine (kyn), or by direct stimulation of inhibitory receptors such as PD-1, CTLA-4 or CD200R. By the secretion of proinflammatory cytokines (e.g. IFN- γ), cytotoxic T lymphocytes (CTLs) contribute to the upregulation of inhibitory ligands on AML cells and thus to the acquisition of adaptive immune resistance.^{185,200} COX-2, cyclooxygenase-2; IDO, indoleamine 2,3-dioxygenase; PGE₂, prostaglandine E₂. Adapted from Alessandro Isidori *et al.* (2016), originally published in Cancer Research Frontiers, Copr. Isidori *et al.* 2016, licensed by CC BY 4.0 (<http://creativecommons.org>).²⁰⁰

INTRODUCTION

AML and stroma cells are shown to express molecules that inhibit T cell activation and proliferation as well as T_H1 cytokine production.¹⁸⁸ *In vitro* studies indicate that these include the release of arginase II, TGF- β and IL-10.^{188,193} Furthermore, AML cells reveal high levels of cyclooxygenase-2 (COX-2) and thus an increased production of prostaglandine E₂ (PGE₂), which further promote immunosuppression.^{201,202} Additionally, they upregulate indoleamine 2,3-dioxygenase (IDO) in the presence of IFN- γ .^{192,201,202} Moreover, the increased abundance of T_{regs} and MDSCs significantly contributes to immune suppression.^{203,204} Elevated T_{reg} levels can be detected at different stages of therapy, and high levels often correlate with poor prognosis.^{204,205} It has been shown in mice that the frequency of T_{regs} is increased at leukemic sites and that adoptively transferred CTLs are compromised in their proliferation capacity, IFN- γ release and their ability to deplete AML cells.²⁰⁶ This suppressive effect could be abrogated by T_{reg} elimination with IL-2 diphtheria toxin, resulting in increased CTL-mediated reduction of the tumor burden.²⁰⁶

1.3.3. Immunotherapeutic approaches in AML

In general, AML is susceptible to immunotherapy. One established approach that is based on a functional immune response is the graft-versus-leukemia (GvL) effect of allogeneic HSCT, which is mediated by TCR recognition of foreign antigens.^{202,207} Also in autologous settings, the detection of leukemic cells by T cells is essential for a successful immune response.²⁰² Several leukemia-associated antigens (LAAs) have been identified, including gene fusions such as *DEK-CAN* and neoantigens that evolved from genetic aberrations such as internal tandem duplications (ITD) in the gene of FSM-like tyrosine kinase 3 (*Flt3*) as well as mutations in the gene of nucleophosmin 1 (*NPM1*).^{202,208-211} In addition, antigens have been identified that are overexpressed on the surface of leukemic blasts compared to healthy tissue. Of these, the most established targets are myeloid differentiation antigen CD33 (i.e. sialic acid-binding immunoglobulin-like lectin-3; Siglec-3) and the α -subunit of the IL-3 receptor, CD123.²¹² These are present on the majority of myeloid blasts but absent or detected at lower levels on hematopoietic stem cells (HSCs), which qualifies them as promising targets to eliminate leukemic cells while maintaining the capacity for hematopoietic reconstitution.^{79,213-215} Furthermore, they are expressed on LSCs, which makes them good target antigens to eradicate MRD and to counteract relapse.^{79,213,216}

Since it was discovered that the depletion of CD33⁺ cells still allows the reconstitution of normal hematopoiesis *in vitro*, CD33 moved into focus of AML immunotherapy.²¹⁷ Amongst others, Krupka and coworkers were able to validate CD33 as specific AML target by screening 621 AML

INTRODUCTION

patients. They reported overexpression in >99% of samples and confirmed CD33 presence on bulk AML cells as well as on CD34⁺CD38⁻ LSCs. Notably, CD34⁺CD38⁻ bone marrow (BM) cells from healthy donors demonstrated a comparably lower expression of CD33.⁷⁹ Several immunotherapeutic approaches have been tailored to address CD33, including naked mABs and derivatives, ADCs and chimeric antigen receptor (CAR) T cells.^{75,217-221} The first CD33-targeting mAB was already evaluated in a phase I clinical trial more than 20 years ago.²²² Since then, mABs have continuously improved. The most advanced unconjugated mAB, lintuzumab (SGN-CD33), was investigated in a phase III clinical trial before it was discontinued due to lack of efficiency.^{219,223} This might be partially due to the fact that CD33 internalizes upon crosslinking.²²⁴ ADCs, however, take advantage of this targeted endocytosis to release their cytotoxic payload within the cell. Thus, the only CD33-targeting agent that hitherto gained market access is gemtuzumab ozogamicin (GO; Mylotarg[®]), which is a humanized IgG4 mAB conjugated to the cytotoxic agent N-acetyl- γ -calicheamicin dimethyl hydrazide (CalichDMH) via a bifunctional linker.²²⁵⁻²²⁷ Upon internalization, CalichDMH is released in the cell to induce DNA double-strand breaks and trigger tumor cell apoptosis.²²⁸ Due to its intriguing success in treating relapsed AML patients, GO gained accelerated approval by the U.S. FDA in the year 2000.^{225,229} Ten years later, it was voluntarily withdrawn by Pfizer due to frequent reports of high toxicity and lack of efficiency in post-marketing studies.^{225,230} However, after careful investigation it was most recently reapproved to treat adults with newly diagnosed as well as r/r AML.^{226,231,232} Aside from therapeutic molecules that are based on the conventional IgG format, the CD33xCD3 BiTE[®] antibody AMG 330 is currently evaluated in a clinical phase I trial (NCT02520427).^{75,221} In contrast to mABs, AMG 330 is not internalized and has no influence on CD33 surface antigen density.²²¹ It reveals efficient cytolytic activity on AML cell lines and is able to activate T cells *ex vivo* in an autologous setting of cynomolgus monkey bone marrow aspirates and human patient samples.^{75,79} Further, in a murine xenograft model, it induces AML regression and prolonged survival.⁷⁵

Notably, not all patients respond to CD33-targeted therapies.²²⁹ One reason is the upregulation of inhibitory immune checkpoints in the tumor microenvironment, including PD-1 and PD-L1.¹⁹⁵⁻¹⁹⁷ Expression levels can be particularly increased in response to proinflammatory cytokines, which are released upon immune stimulation by tumor neoantigens or therapeutics such as T cell engagers.^{189-191,194} In this regard, recent *ex vivo* studies indicated that AMG 330 treatment leads to upregulation of PD-1 on T cells and PD-L1 on AML cells.¹⁹⁴ The coexpression of CD33 and PD-L1 or PD-L2 on AML cell lines decreased the AMG 330-mediated cytolytic activity of T cells, which

INTRODUCTION

could be reversed by the addition of PD-L1 or PD-L2 blocking mABs.²³³ Further, it could be shown that the depletion of primary AML samples was enhanced by the combined application of AMG 330 and PD-1/PD-L1 blocking agents.¹⁹⁴ As preclinical investigations of PD-1/PD-L1 blockade in AML revealed a beneficial effect on disease progression, PD-1 and PD-L1 blocking mABs are currently evaluated in clinical phase I and II trials.²³⁴ This includes the administration as monotherapy or the combination with chemotherapy and/or other checkpoint blocking mABs such as ipilimumab.²³⁴⁻²³⁶ The aforementioned findings, however, provide a strong rationale for combining PD-1/PD-L1 checkpoint blockade with targeted antibody therapy as well. The efficacy of simultaneous CD33-targeting and PD-1/PD-L1 checkpoint blockade, though successful *in vitro*, has yet to be shown *in vivo* in preclinical animal models and in clinical trials.¹⁹⁴ In the future, the combination of two different immunotherapeutic strategies might be a highly potent strategy for the treatment of AML.

2. Objectives

In AML, novel therapeutic approaches are urgently needed. Although most patients initially respond to conventional chemotherapy, relapse rates are high. This is presumably due to the persistence of chemoresistant LSCs and the upregulation of inhibitory immune checkpoints. One approach to prevent reoccurrence of disease is targeted immunotherapy against AML antigens that are expressed on both bulk AML cells and LSCs. Moreover, the inhibition of the PD-1/PD-L1 checkpoint is clinically investigated in AML at present. Five PD-1/PD-L1 monoclonal blocking antibodies have already been approved by regulatory authorities for different types of cancer, and more than a thousand trials are ongoing that evaluate these agents as mono- and combination therapies. However, the intriguing clinical response rates are accompanied by irAEs that result from systemic checkpoint inhibition. Since PD-L1 can be upregulated by almost every cell of the body as natural reaction to inflammation, reported side effects are distributed across various organs and can develop into a severe or fatal state.

The aim of this thesis was to develop a novel molecular format that locally restricts immune checkpoint blockade to the cytolytic synapse between T cell and leukemic cell and thus maintains the crosstalk between T cells and healthy tissue. This was accomplished by synergizing PD-1/PD-L1 blockade with specific T cell redirection. Our new molecule is designated “Checkpoint inhibitory T cell Engager” (CiTE) and its unique functionality is conferred by three distinct modules: (1) the extracellular domain of human PD-1 (PD-1_{ex}) for local immune checkpoint blockade, (2) a CD3 ϵ -specific scFv for T cell redirection and (3) a high-affinity CD33-specific single-chain variable fragment (scFv) for AML targeting. PD-1_{ex} holds a naturally occurring low affinity to PD-L1 and was therefore expected to only interact with its ligand in conjunction with a high-affinity tumor-targeting module. The CiTE was compared to a single-chain triplebody (sctb) format in which the checkpoint blocking module is represented by a high-affinity PD-L1 scFv, and to a BiTE[®]-like molecule lacking this module. The present work consisted of the design, the expression and purification of CiTE, sctb and respective control molecules as well as their biochemical and biophysical evaluation. The biological functionality was evaluated *in vitro* on different cell lines. In collaboration with Christina Krupka and Katrin Deiser ^a, they were further investigated on primary AML patient samples and *in vivo* in a murine xenograft model.

^a Laboratory of Marion Subklewe, Gene Center Munich, LMU München, Germany

3. Materials and methods

3.1. Materials

All chemicals utilized in this thesis were purchased from Carl Roth, Merck, or Sigma-Aldrich, if not otherwise stated. Restriction enzymes for microbiological applications were obtained from New England Biolabs or Fermentas. Cell culture media were obtained from Thermo Fisher Scientific and cell culture supplies from Sarstedt unless indicated otherwise.

3.1.1. *E. coli* strains and cell lines

Table 1: *E. coli* strains used for cloning and expression of recombinant proteins.

strain	genotype	company
XL1-Blue	<i>recA1 endA1 gyrA96 thi-1 hsdR17 supE44 relA1 lac</i> [F' <i>proAB lacI^qZΔM15 Tn10</i> (TetR)]	Stratagene
BL-21 (DE3)	<i>fhuA2 [lon] ompT gal (λ DE3) [dcm] ΔhsdS</i> <i>λ DE3 = λ sBamH1o ΔEcoRI-B</i> <i>int::(lacI::PlacUV5::T7 gene1) i21 Δnin5</i>	New England Biolabs

Table 2: Mammalian cell lines.

cell line	company
FreeStyle™ 293-F	Thermo Fisher Scientific
Expi293F™	Thermo Fisher Scientific
Flp-In™ T-REx™ 293	Thermo Fisher Scientific
HEK293:PD-L1	created during the present work
HEK293:CD33	created during the present work
HEK293:CD33:PD-L1	created during the present work
Jurkat	DSMZ
MOLM-13	DSMZ
MOLM-13:PD-L1	created during the present work
OCI-AML3	kindly provided by Marion Subklewe, originally purchased from DSMZ
OCI-AML3:PD-L1	created during the present work
Panc02OVA:mPD-L1	kindly provided by Sebastian Kobold

MATERIALS

3.1.2. Plasmids

Table 3: Vector backbones used for protein expression and generation of stable cell lines.

vector	company
pSecTag2/Hygro C	Life Technologies
pAK400	generated in the laboratory of Andreas Plückthun ²³⁷
pMXs	kindly provided by Sebastian Kobold
pcDNA5/FRT/TO	Thermo Fisher Scientific

Table 4: Expression vectors.

name	encoded sequence	tag
pSecTag2 - PD-1 _{ex} .αCD3.αCD33	hPD-1 _{ex} / hCD3ε-specific scFv/ hCD33-specific scFv	N-His ₆
pSecTag2 - αPD-L1.αCD3.αCD33	hPD-L1-specific scFv/ hCD3ε-specific scFv/ hCD33-specific scFv	N-His ₆
pSecTag2 - αCD3.αCD33	hCD3ε-specific scFv/ hCD33-specific scFv	N-His ₆
pSecTag2 - PD-1 _{ex} .αCD3	hPD-1 _{ex} / hCD3ε-specific scFv	N-His ₆
pSecTag2 - αPD-L1.αCD3	hPD-L1-specific scFv/ hCD3ε-specific scFv	N-His ₆
pSecTag2 - αHer2.αCD3.αCD33	hHer2-specific scFv /hCD3ε-specific scFv/ hCD33-specific scFv	N-His ₆
pSecTag2 - αHer2.αCD3.αHer2	hHer2-specific scFv/ hCD3ε-specific scFv	N-His ₆
pAK400 - PD-L1scFv	hPD-L1-specific scFv	C-His ₆
pSecTag2 - PD-1 _{ex} -Fc	hPD-1 _{ex}	C-His ₆ / IgG1 Fc
pMXs - hPD-L1	hPD-L1	-
pcDNA5 - hPD-L1	hPD-L1	-
pcDNA5 - hCD33	hCD33	-
pcDNA5 - hCD33/ hPD-L1	hCD33/ hPD-L1	-

3.1.3. Oligonucleotides

All oligonucleotide primers were purchased from Metabion international AG.

MATERIALS

Table 5: Primers designed for cloning.

name	5'→3' sequence
PD-1 N33 for SfiI	TTTAAGGCCAGCCGGCCAACCCCCCACCTTCTCCCCAG
PD-1 A149 rev SfiI	TTTAAGGCCCGAGGCCGATGCCCTTCTCTCTGTCACCCTG AG
PD-L1 A18 for SfiI	TTTAAGGCCAGCCGGCCGCATTTACTGTCACGGTTCCCAA G
PD-L1 R238 rev SfiI	TTTAAGGCCCGAGGCCGACCTTTCATTTGGAGGATGTGC CAG
CD3scFv for NotI	TTTAAGCGGCCGCGGACATCAAACCTGCAGCAGTCAG
CD3scFv rev XhoI	TTTAACTCGAGCTTTCAGCTCCAGCTTGGTCCCAGC
CD3scFv stop rev EcoRV	TTAAAGATATCCTACGCTTTCAGCTCCAGCTTGGTCCCAGCA CCGAACG
CD3scFv for G4S KasI	CTCGAGGGTGGCGGAGGTTCTGGCGCCGACATCAAACCTGCA GCAGTCAG
PD-L1 VL for NheI	GATCTGCTAGCCACCATGAGGATATTTGCTGTCTTTATATTC ATG
PD-L1 VL rev EcoRV	AGATCGATATCTTACGTCTCCTCCAAATGTGTATCACTTTG
PD-1 _{ex} rev G4S XhoI	GCCAGAACCTCCGCCACCCTCGAGTGCCCTTCTCTCTGTCAC CCTGAG
pAK400 rev EcoRI SfiI	CTAGAGAATTCTAATGATGGTGATGATGGTGATCGGCCCC CGAGGCCGA
PD-L1scFv for SfiI	CATGGCTTCGAAAAAGCGGCCAGCCGGCCATG
PD-L1scFv rev XhoI	CCACCCTCGAGAGCAGACACGGTCACGAGGGTTCC
PD-1 _{ex} rev EcoRV	AGTCAGATATCTTATGCCCTTCTCTCTGTCACC
PD-L1 VL for EcoRV	CTGCAGATATCATGAGGATATTTGCTGTCTTTATATTCATGA
PD-L1 VL rev XhoI	CTAGACTCGAGCTATTACGTCTCCTCCAAATGTGTATC
CD33 VL for EcoRV	CTGCAGATATCATGCCACTCCTCCTGCTG
CD33 VL rev XhoI	CTAGACTCGAGCTATTATCATTGAGTCCGCACTTCG
PD-L1 VL rev linker	GGAGCCTCTCTTGGCCCAGTCTCCTCCAAATGTGTATCAC
CD33 VL for linker	GTGATACACATTTGGAGGAGACGCGGGCCAAGAGAGGCTC C
PD-L1 VL for PacI	GCTAGTTAATTAATGAGGATATTTGCTGTCTTTATATTCAT GACC
PD-L1 VL rev NotI	GTGCTGGCGGCCGCTTACGTCTCCTCCAAATGTGTATCACTT TGC

MATERIALS

Table 6: Primers designed for DNA sequencing.

name	5'→3' sequence
MHsq01 ahCD33 rev	CCTGATACCATAGTTATCGAGAG
MHsq02 ahCD33 for	CTCTCGATAACTATGGTATCAGG
MHsq03 hPD1ex for	CTCAGGGTGACAGAGAGAAG
MHsq05 hPDL1VL for	GAACTGACATGTCAGGCTGAGG
MHsq06 pAK400 for	CACAGGAAACAGCTATGAC
MHsq07 pAK400 rev	GACGCAGTAGCGGTAAAC
MHsq08 ahCD3 for	CATACTCTCTCACAATCAGC
MHsq09 ahPDL1 for	CTACCTACTACGCCGACA
MHsq10 ahPDL1 for2	GACACCAGCAAGAACAC
MHsq12 ahHer2 for	GCGTGCAGAAGATACCG
MHsq13 ahHer2 for	TATCCATTGGGTTCGTCAGG
MHsq17 pMXs for	GAC GGC ATC GCA GCT TGG ATA CAC
MHsq18 ahCD3 rev	CTGGAGGATTTGTCTGTAGTC

3.1.4. Amino acid sequences

Table 7: Amino acid sequences of binding modules and ligands.

name	sequence
extracellular domain of human PD-1 (PD-1 _{ex})	NPPTFSPALLVVTEGDNATFTCSFSNTSESFVLNWyRMSP SNQTDKLAAPEDRSQPGQDCRFRVTQLPNGRDFHMSVVR ARRNDSGTYLCGAISLAPKAQIKESLRAELRVTERRA
full-length human PD-L1	MRIFAVFIFMTYWHLNNAFTVTVPKDLYVVEYGSNMTIEC KFPVEKQLDLAALIVYWEMEDKNIIQFVHGEEDLKVQHSS YRQRARLLKDQLSLGNAALQITDVKLQDAGVYRCMISYGG ADYKRITVKVNAPYNKINQRILVVDVPTSEHELTCQAEGY PKAEVIWTSSDHQVLSGKTTTTNSKREEKLFNVSTLRIN TTTNEIFYCTFRRLDPEENHTAELVIPELPLAHPPNERTH LVILGAILLCLGVALTFIFRLRKGRMMDVKKCGIQDTNSK KQSDTHLEE
full-length human CD33	MPLLLLLPLWAGALAMDPNFWLQVQESVTVQEGLCVLVP CTFFHPIPYDYKNSPVHGYWFREGAIISRDSPVATNKLDQ EVQEETQGRFRLGDP SRNNCSLSIVDARRRDNGSYFFRM ERGSTKYSYKSPQLSVHVTDLTHRPKILIPGTLEPGHSKN LTCSVSWACEQGTPIIFSWLSAAPTSLGPRTTHSSVLIIT

MATERIALS

	<p>PRPQDHGTNLTCQVKFAGAGVTTERTIQLNVTYVPQNPTT GIFPGDGSQKQETRAGVVHGAIGGAGVTALLALCLCLIFF IVKTHRRKAARTAVGRNDTHPTTGSASPKHQKSKLHGPT ETSSCSGAAPT VEMDEELHYASLNFGHMNPSKDTSTEYSE VRTQ</p>
<p>PD-L1 scFv (YW243.55.S70- derived)²³⁸</p>	<p>DIQMTQSPSSLSASVGDRVITICRASQDVSTAVAWYQQ KPGKAPKLLIYSASFLYSGVPSRFSGSGSGTDFTLTISSL QPEDFATYYCQQYLYHPATFGQGTKVEIKRGGGGSGGGGS GGGSGGGGSEVQLVESGGGLVQPGGSLRLSCAASGFTFS DSWIHWRQAPGKGLEWVAWISPYGGSTYYADSVKGRFTI SADTSKNTAYLQMNSLRAEDTAVYYCARRHWPGGFDYWGQ GTLVTVSA</p>
<p>CD3ε scFv (OKT3-derived)^{86,239}</p>	<p>DIKLQQSGAELARPGASVKMSCKTSGYTFTRYTMHWVKQR PGQGLEWIGYINPSRGYTNYNQKFKDKATLTTDKSSSTAY MQLSSLTSEDSAVYYCARYYDDHYCLDYWGQGTTLTVSSV EGGSGSGGGSGGGVDDIQLTQSPAIMSASPGKVTMTC RASSVSYMNWYQKSGTSPKRWIYDTSKVASGVPYRFSG SSGGTSYSLTISSMEAEDAATYYCQQWSSNPLTFGAGTKL ELK</p>
<p>CD33 scFv (hP67.6-derived)²⁴⁰</p>	<p>DIQLTQSPSTLSASVGDRVITICRASESLDNYGIRFLTWF QQKPGKAPKLLMYAASNQSGVPSRFSGSGSGTEFTLTIS SLQPDDFATYYCQQTKEVPWSFGQGTKVEVKGGGGSGGGG SGGGGSGGGGSEVQLVQSGAEVKKPGSSVKVSKKASGYTI TDSNIHWVRQAPGQSLEWIGYIYPYNGGTDYNQKFKNRAT LTVDNPTNTAYMELSSLRSEDFAFYCVNGNPWLAYWGQ TLVTVS</p>
<p>Her2 scFv (4D5-8-derived, kindly provided by Matthias Peipp)^{86,241}</p>	<p>DIQMTQSPSSLSASVGDRVITICRASQDVNTAVAWYQQKP GKAPKLLIYSASFLYSGVPSRFSGSRSGTDFTLTISSLQP EDFATYYCQQHYTTPPTFGQGTKVEIKRGGGGSGGGGSGG GSGGGGSEVQLVESGGGLVQPGGSLRLSCAASGFNIKDT YIHWVRQAPGKGLEWVARIYPTNGYTRYADSVKGRFTISA DTSKNTAYLQMNSLRAEDTAVYYCSRWGGDGFYAMDYWGQ GTLVTVS</p>
<p>human IgG1 Fc</p>	<p>DKTHTCPPCPAPELLGGPSVFLFPPKPKDTLMISRTPEVT CVVVDVSHEDPEVKFNWYVDGVEVHNAKTKPREEQYNSTY RVVSVLTVLHQDWLNGKEYKCKVSNKALPAPIEKTISKAK GQPREPQVYTLPPSREEMTKNQVSLTCLVKGFYPSDIAVE WESNGQPENNYKTTTPVLDSDGSFFLYSKLTVDKSRWQQG NVFSCSVMHREALHNHYTQKSLSLSPGK</p>

MATERIALS

3.1.5. Commercial antibodies

Table 8: Commercial antibodies for flow cytometry and western blot analysis.

antigen	fluorophore	reactivity	isotype	clone	company
CD2	PE, FITC, APC, PE/Cy5	human	mouse IgG1, K	RPA-2.10	BioLegend
CD3	PE	human	hamster IgG	145-2C11	BioLegend
	FITC, PE/Cy5, unconjugated	human	mouse IgG2a, K	HIT3a	BioLegend
	BV421	human	mouse IgG1, K	UCHT1	Biolegend
CD4	APC-H7	human	mouse IgG1, K	RPA-T4	BD Pharmingen
CD16	PE	human	mouse IgG1, K	3G8	BioLegend
CD25	PerCP/Cy5.5	human	mouse IgG1, K	M-A251	BioLegend
PD-1	PE, APC, PerCP, unconjugated	human	mouse IgG1, K	EH12.2H7	BioLegend
PD-L1	PE, PECy7	human	mouse IgG1, K	MIH1	BD Pharmingen
	APC, unconjugated	human	mouse IgG2b, K	29E.2A3	BioLegend
	APC	mouse	rat IgG2b, K	10F.9G2	BioLegend
PD-L2	APC	human	mouse IgG2a, K	24F.10C12	BioLegend
CD33	FITC	human	mouse IgG1, K	HIM3-4	BD Pharmingen
	PE, APC, unconjugated	human	mouse IgG1, K	WM53	BioLegend
	unconjugated	human	mouse IgG1, K	P67.6	BioLegend
CD45	FITC	human	mouse IgG1, K	2D1	BioLegend
CD56	APC	human	mouse IgG1, K	HCD56	BioLegend
CD69	APC	human	mouse IgG1, K	FN50	BioLegend
penta-His	Alexa Fluor 488	human	mouse IgG1		Qiagen
IgG	FITC	mouse	rat polyclonal IgG	polyclonal	BioLegend
His	HRP	human	mouse IgG2b	GG11-6F4.3.2	Miltenyi

MATERIALS

3.1.6. Buffers and media

Table 9: List of standard buffers used for biochemical and cell culture methods.

buffer	components
10 x PBS (1 l)	80 g NaCl, 2 g KCl, 14.4 g Na ₂ HPO ₄ x 2 H ₂ O, 2 g KH ₂ PO ₄ (pH 7.4)
1 x PBS-T (1 l)	100 ml 10 x PBS, 0.1% (v/v) Tween-20
10 x transfer buffer (1 l)	30.3 g tris base, 144 g glycine
1 x transfer buffer (1 l)	100 ml 10 x transfer buffer, 20% (v/v) ethanol
4 x Laemmli buffer	0.11 M tris base (pH 6.8), 16% (v/v) glycerol, 4% (w/v) SDS, 5% (v/v) β-mercaptoethanol, 0.05% (w/v) bromophenol blue
Coomassie stain	50% (v/v) ethanol, 7% (v/v) acetic acid, 0.2% (w/v), Coomassie Brilliant Blue R250
20 x ECL solution	2 M tris base (pH 8.5)
1 x ECL staining solution (10 ml)	10 ml 20x ECL solution, 3 μl H ₂ O ₂ , 25 μl cumaric acid (90 mM), 50 μl luminol (250 mM)
FACS buffer	1% (v/v) FBS in 1x PBS

Table 10: List of media and buffers for *E. coli*.

medium	components
LB medium (1 l)	10 g bacto tryptone, 5 g yeast extract, 5 g NaCl, 1.3 ml NaOH
LB agar (1 l)	LB medium + 15 g agar
TSS buffer	LB medium with 10% (w/v) PEG 6000, 5% (v/v) DMSO, 50 mM MgSO ₄ (pH 6.5-6.8), frozen at -20°C

3.1.7. Technical equipment

Aekta Purifier 10, Explorer, Basic, FPLC	GE Healthcare
Agarose gel electrophoresis system	Bio-Rad
Amersham™ Imager 600	GE Healthcare
BD FACS Calibur	BD Biosciences
Cell culture laminar-flow	BDK Luft- und Reinraumtechnik GmbH
Countess, automated cell counter	Thermo Fisher Scientific

MATERIALS

Guava easyCyte 6HT	Merck Millipore
Hemocytometer Neubauer improved	Brand GmbH and Co KG
HeraCell CO ₂ incubator	Thermo Scientific
Innova 44 Shaker	New Brunswick Scientific
Inverted laboratory microscope Leica DM IL LED	Leica
Microplate reader Infinite M1000 Pro	Tecan
Mini-Trans Blot® electrophoretic transfer cell	Bio-Rad
Mr. Frosty freezing container	Thermo Fisher Scientific
Model 200 / 2.0 power supply	Bio-Rad
Multitron Cell incubator	Infors HT
Nanodrop ND-1000	Peqlab Biotechnologies GmbH
Novex® NuPAGE® SDS-PAGE Gel System	Thermo Fisher Scientific
pH-meter 766	Knick
Realtime system CFX96	Bio-Rad
Rotanta 460 RT centrifuge	Hettich
Sartorius scale LE 22025	Sartorius AG
Sorvall RC6+ centrifuge	Thermo Scientific
T personal thermocycler	Biometra
Tabletop centrifuges	Eppendorf
Thermomixer comfort	Eppendorf
Vi-Cell™ XR cell viability analyzer	Beckman Coulter
X-Omat M35	Kodak

3.1.8. Software

Adobe Illustrator CS6 version 16.0.3	Adobe Systems Inc.
Ape - A plasmid Editor version 2.0.36	M. Wayne Davis
Graph Pad Prism version 6	GraphPad Software Inc.
InCyte Software version 3.1.1	Merck Millipore
PyMOL Molecular Graphics System version 2.0	Schrödinger, LLC

3.2. Molecular biology methods

3.2.1. Molecular cloning

CiTE antibody, sctb and control molecules were generated using conventional molecular biology methods. The CD33 scFv originates from antibody clone hP67.6, it is composed of V_L connected to V_H by a (G₄S₄)₄-linker and it has a humanized backbone.²⁴⁰ The CD3ε scFv is derived from antibody clone OKT3, comprising a murine backbone and V_H connected to V_L by a (G₂S)₄G₂ linker.^{86,239} The PD-L1 scFv was generated based on published sequences.²³⁸ This scFv has a humanized backbone and V_L and V_H are connected by a (G₄S₄)₄ linker.²³⁸

General molecular cloning techniques such as site-specific cleavage of DNA with restriction enzymes, dephosphorylation and ligation as well as size-dependent separation of DNA fragments by agarose gel electrophoresis were conducted according to standard protocols.²⁴² Commercially available enzymes and ready-made kits were used following manufacturer's instructions. Plasmid DNA was isolated from *E. coli* XL-1 blue using NucleoSpin[®] Plasmid EasyPure kit (MACHEREY-NAGEL) or QIAfilter Plasmid Maxi Kit (QIAGEN). The NucleoSpin[®] Gel and PCR clean-up kit (MACHEREY-NAGEL) was used to purify DNA from agarose gels or PCR reactions. The correct DNA sequence was assured by the sequencing of all generated DNA vectors at Eurofins Genomics. DNA sequences of scFvs were ordered from GeneArt and inserted into a pAK400 vector containing a pelB leader sequence and a C-terminal His₆ tag via SfiI restriction sites. For recombinant protein expression in HEK293-based expression systems, the respective DNA sequences were subcloned into a pSecTag2/Hygro C vector including an Igk leader sequence and an N-terminal hexahistidine (His₆) tag. The N-terminal module of trispecific molecules was inserted via SfiI, the central module via NotI and XhoI and the C-terminal module via KasI and EcoRV. For generation of stable cell lines, full-length cDNA sequences of CD33 and PD-L1 were either cloned into the vector pcDNA5/FRT/TO via EcoRV and XhoI or into pMXs via PacI and NotI restriction sites.

3.2.2. PCR and site-directed mutagenesis

The cDNA sequences of the extracellular domain of human PD-1 (PD-1_{ex}) and human full-length PD-L1 were obtained by PCR from isolated human muscle cDNA. PCR was also utilized to amplify scFvs from plasmid DNA. If necessary, primer sequences contained restriction sites or

METHODS

included sequences encoding affinity tags or leader sequences. PCR reactions for amplification of coding sequences were performed using Phusion Flash High-Fidelity PCR Master Mix (Thermo Fisher Scientific). Correct assembly of DNA sequences after molecular cloning was assured by colony PCR with GoTaq[®] DNA polymerase (Promega). For this purpose, bacteria from a single colony were picked with an inoculation loop and used as template.

A common PCR reaction with Phusion Flash Master Mix contained 10-100 ng DNA template and 0.5 μ M of each primer. It was run as follows:

Table 11: Conventional PCR program for Phusion Flash Master Mix.

step	temperature	time
initial denaturation	98°C	30 sec
20-30 cycles amplification	98°C annealing temperature of primers 72°C	10- 30 sec 30 sec 30 sec / kb
final extension	72°C	5 – 10 min
hold	16°C	

For common PCR reactions using Taq polymerase the following protocol was used:

Table 12: Conventional PCR protocol for Taq polymerase.

step	temperature	time
initial denaturation	95°C	30 sec
20-30 cycles amplification	95°C annealing temperature of primers 68°C	30 sec 60 sec 60 sec / kb
final extension	68°C	5 – 10 min
hold	16°C	

Site-directed mutagenesis was used to generate point mutations or to introduce or delete parts of DNA sequences. The 5' and the 3' end of the primer pairs surrounding the mutation allowed homology pairing of at least 20 bp. In the reaction, 10-100 ng DNA template were incubated with 0.05 μ M of each primer and Phusion Flash High-Fidelity PCR Master Mix (Thermo Fisher Scientific) following the protocol in Table 11. Afterwards, the reaction product was digested with DpnI to remove maternal DNA. Subsequently, the DNA was transformed into chemically

METHODS

competent *E. coli* XL-1 blue cells and DNA isolated from single clones was verified by sequencing at Eurofins Genomics.

3.3. Microbiology methods

3.3.1. Transformation in *E. coli*

Chemically competent bacterial cells were generated.²⁴³ Briefly, 200 ml of LB medium containing the appropriate antibiotics (Table 13) were inoculated with 2 ml of an overnight culture and grown to an OD₆₀₀ of 0.3-0.5. Subsequently, the cells were centrifuged at 3,000 g for 5 min at 4°C, resuspended in ice-cold TSS buffer (Table 10), aliquoted, shock-frozen in liquid nitrogen and stored at -80°C until further usage.

The *E. coli* strains used in this work are listed in Table 1. For transformation, 10-100 ng of plasmid DNA or the complete volume of a ligation mixture or mutagenesis PCR were added to 75 µl of bacterial cells before incubation on ice for 15 min. Bacteria were heat-shocked at 42°C for 45 sec and subsequently transferred back on ice for 2 min before they were allowed to recover in 600 µl of prewarmed LB medium at 37°C for 1 h while shaking. Afterwards, the cells were centrifuged briefly, most of the supernatant was removed and the cells were resuspended in the remaining LB medium before plating them on LB agar plates supplemented with the appropriate antibiotics (Table 13).

Table 13: Concentrations of stock solutions of antibiotics and IPTG used for bacteria. Antibiotic and IPTG stock solutions were applied at 1:1000 (v/v) dilution.

ampicillin	100 mg/ml	(in water)
chloramphenicol	34 mg/ml	(in ethanol)
tetracycline	10 mg/ml	(in ethanol)
IPTG	0.5 M	(in water)

Single colonies were picked and inoculated in 5 ml of LB medium containing the appropriate antibiotics. The cells were shaken over night at 37°C and plasmid DNA was isolated.

3.3.2. Recombinant periplasmic protein expression

The scFvs were overexpressed in the periplasm of *E. coli*. Therefore, pAK400 plasmids carrying the respective coding sequences were transformed into competent *E. coli* BL21 (DE) cells (NEB)

METHODS

under chloramphenicol selection pressure. 30 ml of an overnight pre-culture were used to inoculate 3 l of LB growth medium, which was shaken at 200 rpm at 37°C until an OD₆₀₀ of 0.5-0.7 was reached. Subsequently, protein expression was induced by adding 0.5 mM IPTG while keeping the cells shaking at 25°C. After 5 h, the cells were pelleted by centrifugation at 5,000 rpm for 10 min at 4°C using a SLC 6000 rotor (Sorvall). Cell pellets were directly placed on ice, subsequently proceeding with cell disruption and protein purification (section 3.5.1.).

3.4. Cell culture methods

3.4.1. Cell lines

All cell lines used in this project were purchased from the “Deutsche Sammlung von Mikroorganismen und Zellkulturen” (DSMZ) or Thermo Fisher Scientific, or they were adapted by transfection or transduction and selection of stable cell clones (Table 2). Cell lines were routinely tested for mycoplasma contaminations.

The T cell leukemia cell line Jurkat (DSMZ) grows in suspension and is maintained in RPMI1640/ GlutaMAX medium supplemented with 10% FBS at a density of 0.5-2x10⁶ cells/ml. MOLM-13 and OCI-AML3 cell lines (DSMZ) originate from AML patients and are kept in suspension in RPMI1640/ GlutaMAX medium supplemented with 10% FBS at a density of 0.4-2x10⁶ cells/ml. To provide stable PD-L1 expression levels, these two cell lines were modified by retroviral transduction of a pMXs vector containing the full-length human PD-L1 cDNA sequence to generate MOLM-13:PD-L1 and OCI-AML3:PD-L1 cells, respectively (section 3.4.6.). Flp-In™ T-REx™ 293 cells (Thermo Fisher Scientific) are adherent cells derived from the HEK293 cell line, and they were utilized to generate HEK293:PD-L1, HEK293:CD33 and HEK293:CD33:PD-L1 cell lines (section 3.4.5.). These cells carry one stably integrated FRT site (pFRT/lacZeo) at a transcriptionally active locus to allow stable expression of the gene of interest. Additionally, they contain a tetracycline inducible system (pcDNA™6/TR) derived from the *E. coli* Tn10 -encoded (Tet) resistance operon, which represses protein expression in the basal state.²⁴⁴ Parental cells are maintained in DMEM/ GlutaMAX medium supplemented with 10% FBS, 100 µg/ml zeocin and 15 µg/ml blasticidin. Modified Flp-In™ T-REx™ 293 cell lines are kept under selection pressure of 15 µg/ml blasticidin and 50 µg/ml hygromycin B gold (InvivoGen). Antigen expression can be increased by the addition of 1 µg/ml tetracycline 24 h prior to the

METHODS

experiment. FreeStyle™ 293-F and Expi293™ cells (Thermo Fisher Scientific) are derived from HEK293 cells and adapted to suspension culture in their corresponding expression media (FreeStyle™ 293 or Expi293™ Expression Medium). Both cell lines were maintained in 125 ml Erlenmeyer flasks (Corning) and shaken at 125 rpm. FreeStyle™ 293-F cell grow at a density of $0.5-2 \times 10^6$ cells/ml, whereas Expi293™ cells are kept at $0.5-6 \times 10^6$ cells/ml. Panc02OVA:mPD-L1 cells were kindly provided by Sebastian Kobold and maintained in DMEM/ GlutaMAX medium supplemented with 10% FBS. These cells originate from a mouse pancreatic ductal adenocarcinoma cell line and were modified to additionally express ovalbumin and murine PD-L1.²⁴⁵

3.4.2. Cell line maintenance

Human cell lines were maintained at 37°C/ 5% CO₂ in shaking or standing incubators, respectively. Cells were split twice per week, and live cell numbers were determined using a Countess automated cell counter (Thermo Fisher Scientific) and trypan blue exclusion stain (0.4%) (Thermo Fisher Scientific). Suspension cells were resuspended, counted and the respective amount of cells was transferred back into the culture dish before adding fresh medium. In case of adherent cells, the medium was carefully aspirated and the cells were washed with 1x DPBS. Afterwards, 0.05% trypsin-EDTA (1x) was added and the cells were placed in the incubator for 2-3 minutes. Cells were detached by repeatedly tapping the culture dish. The tryptic digest was arrested by addition of an equal volume of cell culture medium containing 10% FBS. After cell counting, the respective amount of cells was centrifuged at 1,400 rpm for 4 min, the supernatant was discarded, the pellet resuspended in fresh medium and transferred to a new plate.

For freezing of cell lines, cells were centrifuged at 1,400 rpm for 4 min, the supernatant was discarded and the cell pellet was resuspended in culture medium without antibiotics containing 10% DMSO. Cells were distributed to cryovials and quickly placed in a freezing container, which was transferred to -80°C. After 24 h, the cell vials were transferred to a liquid nitrogen container.

3.4.3. Recombinant protein expression in HEK293-based expression systems

Protein expression in human cells was conducted in FreeStyle™ 293-F cells or Expi293F™ cells. In both cases, pSecTag2/Hygro C vectors containing an N-terminal Igk leader sequence, an N- or C-terminal His₆ tag and the desired ORF were transfected into the cells using lipid-based

METHODS

transfection reagents according to manufacturer's instructions. The protein was expressed in the supernatant for 5-7 days.

Briefly, for the expression in 30 ml of FreeStyle™ 293-F cells, cells were adjusted to a density of 0.5×10^6 cells/ml one day prior to transfection. The following day, 30 µg of plasmid were mixed with 60 µl of TransIT-LT1 transfection reagent (Mirus Bio LLC) and 3 ml of Opti-MEM™ reduced serum medium. The transfection mix was incubated at room temperature for 20 min and afterwards added dropwise to the cells, which were further maintained at 37°C/ 5% CO₂ in a shaking incubator. To avoid cell clumping, 6-12 h later anti-clumping agent (Gibco) was added in a dilution of 1:750. For the expression in 30 ml of Expi293F™ cells, one day prior to transfection the cells were adjusted to a density of 2×10^6 cells/ml in a total volume of 25.5 ml. The following day, two times 1.5 ml Opti-MEM™ reduced serum medium were mixed with either 30 µg DNA or 80 µl ExpiFectamine™ and separately incubated at RT for 5 min. Afterwards both mixtures were combined and again incubated for 20 min. Subsequently, the transfection mix was added dropwise to the cells, which were kept at 37°C/ 5% CO₂ in a shaking incubator. 16-18 h post transfection, 150 µl of “Enhancer 1” and 1.5 ml of “Enhancer 2” were added.

For expression in stable cell lines, FreeStyle™ 293-F or Expi293F™ cells expressing the respective protein were adjusted to a density of 1×10^6 cells/ml or 2×10^6 cells/ml, respectively, and the supernatant was harvested 5-7 days later.

3.4.4. Generation of stable Expi293F™ and FreeStyle™ 293 expression cell lines

To generate higher amounts of protein than obtained by transient expression in Expi293F™ or FreeStyle™ 293 cells, stable cell lines were generated. Therefore, one day after transfection, 100-300 µl of FreeStyle™ 293-F cells or Expi293F™ cells were transferred to 3 ml DMEM/ GlutaMAX medium supplemented with 10% FBS and 50 µg/ml hygromycin B gold (InvivoGen) in a 6-well plate. Cells that stably integrated the plasmid were allowed to become adherent and grow out in clones while frequently changing the medium to remove dead cells. After 3-6 weeks, protein expression in stable cell pools was evaluated by western blot detecting the His₆ tag and the highest protein expressing pools were expanded.

METHODS

3.4.5. Generation of stable Flp-In™ T-REx™ 293 cell lines

HEK293:PD-L1, HEK293:CD33 and HEK293:CD33:PD-L1 cells were generated from Flp-In™ T-REx™ 293 cells (Thermo Fisher Scientific) by transfecting the eukaryotic expression vector pcDNA5/FRT/TO containing either the full-length cDNA sequence of human PD-L1, human CD33 or the full-length cDNA sequence of human CD33 fused to the cDNA sequence of human PD-L1 by a P2A site. In order to allow site-directed integration at the FRT site, the plasmid comprising the gene of interest was co-transfected with the pOG44 Flp recombinase expression plasmid (Thermo Fisher Scientific) at a ratio of 1:9 (w/w) using TransIT-LT1 transfection reagent (Mirus Bio LLC). Briefly, one day prior to transfection 1×10^6 cells in 2.5 ml culture medium were seeded per well of a 6-well plate. The following day, 0.5 µg expression vector and 4.5 µg pOG44 vector were mixed with 15 µl of transfection reagent and 500 µl Opti-MEM™. After 20 min incubation at room temperature, the mixture was added dropwise to two wells. Two days later, the selection process was initiated by adding 50 µg/ml hygromycin B gold (InvivoGen) and 15 µg/ml blasticidin (Invitrogen). The following 3-4 weeks, the outgrowth of polyclonal cell lines was frequently monitored under the microscope and the medium was regularly changed to remove cell debris. After 4 weeks, the newly generated cell lines were transferred to a 10 cm dish and antigen expression was evaluated by flow cytometry.

3.4.6. Generation of stable PD-L1⁺ AML cell lines

MOLM-13:PD-L1 and OCI-AML3:PD-L1 cell lines were generated from parental MOLM-13 and OCI-AML3 cell lines through retroviral transduction by Felicitas Rataj and Constanze Heise^b. Therefore, the retroviral packaging cell line Platinum-A (Plat-A) (CellBiolabs) was cultivated in DMEM/ GlutaMAX medium supplemented with 10% FBS, 1% penicillin/streptomycin (P/S) and 1% L-Gln. At day 1, cells were plated at a density of 1.2×10^6 cells per well of a 6-well plate and 24 h later transfected with pMX vector containing the full-length cDNA of human PD-L1 by calcium phosphate transfection. 15 µl CaCl₂ solution (2.5 M) were mixed with 18 µg of pMXs-hPD-L1 and the solution was filled up to 150 µl with ddH₂O. While vortexing, 150 µl of Plat-A transfection buffer (280 mM NaCl, 10 mM KCl, 1.5 mM Na₂HPO₄, 50 mM HEPES (pH 6.8)) was added dropwise. The transfection mix was incubated for 30 min at room temperature before

^b Laboratory of Sebastian Kobold, Clinical Pharmacology, Department of Internal Medicine IV, Klinikum der LMU München, Germany

METHODS

transferring it to the Plat-A cells. After 6 h incubation at 37°C/ 5% CO₂, the medium was carefully replaced and the cells were cultivated for 42 h. During the incubation period, 24-well plates were coated with 400 µl of DPBS and 5 µl RetroNectin (0.5 mg/ml) (TaKaRa) over night at 4°C. Afterwards, wells were blocked with 500 µl of 2% BSA for 30 min followed by a washing step with DPBS. At day 4, virus supernatant of the Plat-A cells was harvested on ice and filtered through a 0.45 µm filter. 1 ml of virus supernatant was transferred to each well of the RetroNectin-coated plate and immobilized by centrifugation at 3,000 g for 90 min at 32°C. After removing the liquid, 0.5x10⁶ MOLM-13 or OCI-AML3 cells were added to the wells in a total volume of 1 ml and spun down at 800 g for 30 min at 32°C before incubation over night at 37°C. Plat-A cells were resuspended in 3 ml fresh medium and cultivated at 37°C/ 5% CO₂ for further 24 h. At day 5, the virus supernatant was again harvested as described, the virus was added to MOLM-13 or OCI-AML3 cells and again centrifuged for 90 min and 800 g at 32°C, before 24 h of cultivation at 37°C/ 5% CO₂. At day 6, the transduced MOLM-13 or OCI-AML3 cells were placed in fresh medium and subsequently expanded. At day 10, the transduction efficiency was determined by flow cytometry and at day 18, the PD-L1⁺ cells were separated by FACS. Sorted cells were seeded into 96-well plates by dilution cloning, single-cell clones were raised and expression levels were characterized by flow cytometry.

3.4.7. Patient and healthy donor (HD) material

Human samples were collected in accordance to the declaration of Helsinki and in agreement with the Institutional Review board of the Ludwig-Maximilians-Universität München.²⁴⁶ Donor material included peripheral blood (PB) from healthy donors (HDs) as well as PB and BM from patients after initial diagnosis or upon relapse. HD samples were cryoconserved in 90% FBS and 10% DMSO at -80°C, patient samples in liquid nitrogen. AML diagnosis based on the FAB (French-American-British) classification and was done by the Laboratory of Leukemia Diagnostics of the Department of Internal Medicine III of the Klinikum der Universität München.^{171,174} Work on patient samples was performed by Christina Krupka^c.

3.4.8. Isolation of peripheral blood mononuclear cells (PBMCs) and T cells

PBMCs were isolated from whole blood of HDs by density gradient centrifugation using Biocoll separating solution (Biochrom). Briefly, heparinized blood was mixed 1:1 with 1x DPBS and

^c Laboratory of Marion Subklewe, Gene Center Munich, LMU München, Germany

METHODS

gently pipetted into a 50 ml falcon tube on top of 25 ml Biocoll separating solution. After centrifugation at 818 g for 30 min at room temperature and deceleration without brakes, the PBMC fraction was carefully removed with a pipette and washed twice in RPMI1640/ GlutaMAX supplemented with 10% FBS. The pan T cell population was isolated from PBMCs by negative selection using the Pan T cell isolation kit (Miltenyi Biotec) according to manufacturer's instructions. The cellular composition was determined by flow cytometric analysis. Staining was performed with antibodies against CD3 (clone HIT3a, FITC), CD16 (clone 3G8, PE) and CD56 (clone HCD56, APC) (all purchased from BioLegend) and T cells were identified as CD3⁺ population. T cells and PBMCs were either cryoconserved in FBS/ 10% DMSO or used for T cell expansion.

3.4.9. T cell expansion

PBMCs or Pan T cells were plated at a density of 0.5×10^6 cells/ml in 20-50 ml of RPMI1640/ GlutaMAX medium supplemented with 5% human serum, 500 units/ml IL-2 and 10 ng/ml CD3 antibody OKT3 (BioLegend). At day 5, the antibody was removed by washing with 1x DPBS, and cells were resuspended in medium without OKT3 at a density of 0.5×10^6 cells/ml. Cells were counted every second day and adjusted to 0.5×10^6 cells/ml. At day 5, 9, 14, and the day of cell harvest, the cellular composition was monitored by flow cytometry as described in 3.4.8., and T cell effector functions were confirmed by redirected lysis assay (section 3.7.1.). At day 18-20, the cells were harvested by centrifugation and cryoconserved in FBS and 10% DMSO.

3.5. Protein biochemistry methods

3.5.1. Purification of poly-Histidine tagged proteins from *E. coli* periplasm

A bacterial cell pellet from 3 l *E. coli* culture (section 3.3.2.) expressing scFvs was resuspended in 100 ml periplasm lysis buffer (30 mM Tris pH 8, 1 mM EDTA, 20% (w/v) sucrose) and incubated on ice for 10 min. Afterwards, the suspension was centrifuged at 4,500 rpm for 20 min at 4°C, the supernatant was separated and stored on ice. The pellet was resuspended in 50 ml of 5 mM MgSO₄ and after 10 min incubation on ice it was again centrifuged at 4,500 rpm for 20 min at 4°C. Both supernatants were combined and centrifuged at 15,000 g for 20 min at 4°C using an SS-34 rotor (Thermo Scientific) to remove remaining cell debris. After overnight dialysis against 100 volumes

METHODS

of dialysis buffer (20 mM Tris pH 7, 300 mM NaCl), the His₆ tagged scFvs were enriched by nickel affinity chromatography. 1 ml of Ni-NTA agarose beads (Qiagen) were added to the supernatant and imidazole was adjusted to a final concentration of 10 mM to hamper unspecific binding. After rotation at 4°C over night, the beads were collected by centrifugation at 3,500 rpm at 4°C for 10 min and applied to a Spin[®] chromatography column (Bio-Rad). Bead-bound impurities were removed by washing with one column volume of wash buffer (20 mM His (pH 6.5), 300 mM NaCl, 10 mM imidazole) and the protein was eluted in 5 elution steps of one column volume at a time using elution buffer (20 mM His (pH 6.5), 300 mM NaCl, 200 mM imidazole). All wash and elution fractions were collected and analyzed by denaturing polyacrylamide gel electrophoresis (SDS-PAGE, section 3.5.4.). Protein bands were visualized by Coomassie Brilliant Blue staining, which enabled the determination of the fractions containing the desired protein. These were pooled and further purified by analytical size exclusion chromatography (SEC) using a Superdex 75 10/300 column (GE Healthcare) in 20 mM His (pH 6.5), 300 mM NaCl (i.e. SEC buffer). Afterwards, the chromatography fractions were evaluated by SDS-PAGE and pure monomeric fractions were pooled and concentrated using an Amicon spin concentrator (Millipore, cutoff 10 kDa). Protein concentration was measured as absorption at 280 nm by Nanodrop ND-1000 (PepLab Biotechnologies), proteins were shock-frozen in liquid nitrogen and stored at -80°C.

3.5.2. Purification of poly-Histidine tagged proteins from cell culture supernatant

All proteins expressed in HEK293-based expression systems were designed to carry an N- or C-terminal His₆ tag and were secreted into the medium. Cell culture supernatants were harvested 5-7 days after transfection (section 3.4.3.) by centrifugation at 1,500 rpm. Afterwards, remaining cell fragments were removed in a second centrifugation step at 15,000 g using a SS-34 rotor (Thermo Scientific). Ni-NTA agarose beads (Qiagen) and 10 mM imidazole were added and the supernatant was incubated at 4°C for at least 2 h meanwhile rotating. Afterwards, nickel affinity chromatography was performed as described in 3.5.1. and protein fractions were analyzed by SDS-PAGE. Fractions containing the protein of interest in high purity were pooled and dialyzed over night against SEC buffer. The following day, the protein was concentrated and further purified using a Superdex 200 10/300 GL column (GE Healthcare), which was run in SEC buffer. The peak fractions were again evaluated by SDS-PAGE and the fractions containing the correct monomeric protein at high purity were pooled, concentrated, shock-frozen in liquid nitrogen and stored at -80°C until further use. Stability of the proteins after freezing was confirmed by analytical SEC

METHODS

using a Superdex 200 5/150 GL column (GE Healthcare) in SEC buffer. Prior to functional assays, all proteins were thawed on ice and centrifuged at 15,000 g for 10 min at 4°C.

3.5.3. Protein purification for analysis in murine NSG xenograft model

Proteins designated for injection into a murine non-obese diabetic (NOD) severe combined immunodeficiency (scid) (NSG) xenograft model were expressed and purified under endotoxin-free conditions. For this purpose, the proteins were expressed in HEK293-based suspension cells as described in 3.4.3. and purified according to 3.5.2. However, special attention was paid to obtain low endotoxin levels in the sample. Thus fresh, endotoxin-free Ni-NTA agarose beads, chromatography columns and plasticware were used. SEC columns as well as Äkta systems including tubings and adaptors were preincubated with 0.5 M NaOH for at least 4 h and rinsed with 3 column volumes of ddH₂O. After nickel affinity chromatography, the protein was dialyzed against 1x DPBS, which was also used as running buffer for gel filtration chromatography. Before freezing in liquid nitrogen, the protein was sterile filtered using a 0.45 µm filter (Ultrafree-MC HV Centrifugal Filter units, Merck Millipore) and aliquoted under a laminar airflow cabinet. Low endotoxin levels were confirmed with the Pierce™ LAL Chromogenic Endotoxin Quantitation Kit (Thermo Fisher Scientific) which was used according to manufacturer's instructions.

3.5.4. Denaturing polyacrylamide gel electrophoresis (SDS-PAGE)

The purity of protein samples was evaluated by denaturing polyacrylamide gel electrophoresis (sodium dodecyl sulfate polyacrylamide gel electrophoresis, SDS-PAGE) using precast 4-20% Bis-Tris gels of the RunBlue® SDS-PAGE Gel System (Expedeon).²⁴⁷ Before loading the gel, protein samples were mixed with Laemmli buffer and denatured at 95°C for 5 min. Protein separation was achieved by running the gels at 120 V in 1x RunBlue SDS Run TEO-Tricine buffer. Afterwards, proteins were either stained 30 min using Coomassie Brilliant Blue staining solution followed by destaining in water, or the gel was used for western blot analysis. PageRuler™ Unstained Protein Ladder or PageRuler™ Prestained Protein Ladder (both Thermo Fisher Scientific) served as size standards.

3.5.5. Western blot analysis

Protein samples of interest were separated according to their size by SDS-PAGE (section 3.5.4.) and transferred to a PVDF membrane by wet transfer using a Mini-Trans Blot® electrophoretic

METHODS

transfer cell (Bio-Rad). The PVDF membrane was activated in >99% EtOH, and all other components were presoaked in 1x transfer buffer. The gel and the PVDF membrane were sandwiched between a foam pad and two Whatman papers on each side, clamped tightly and transferred to the blotting chamber, which was filled with 1x transfer buffer and run at 100 V for 50 min. Afterwards, the membrane was washed in PBS-T for 5 min and subsequently incubated with a 1:10,000 dilution of His-HRP antibody (Miltenyi) in 3% milk powder/ PBS-T for 1 h at room temperature while agitating. The membrane was washed with 1x PBS-T three times for 20 min. For protein detection, it was incubated in 10 ml of 1x ECL solution for 1 min and subsequently placed in an exposure cassette. Either a light sensitive Hyperfilm™ ECL™ (GE Healthcare) was exposed for varying time intervals followed by film development in a Kodak X-Omat M35 developing machine, or the chemiluminescence was directly measured in a digital film developer (Amersham™ Imager 600, GE Healthcare). The buffer compositions are listed in Table 9.

3.5.6. Fluorescence-based thermal shift (ThermoFluor) assay

The thermal stability of proteins was determined in a fluorescence-based thermal shift (ThermoFluor) assay.²⁴⁸ Briefly, the proteins were diluted to a concentration of 100 ng/μl and mixed with a 1:500 dilution of CYPRO® Orange (Thermo Fisher Scientific). Protein unfolding over a temperature gradient from 10°C to 95°C was recorded using a CFX96 Touch Real-Time PCR Detection System (Bio- Rad, Munich, Germany) with a stepwise temperature increase of 0.5°C/ 10 sec and one scan after each cycle using FAM and SYBR Green I filter pairs.

3.6. Flow cytometry methods

3.6.1. Detection of cell surface antigens

To analyze the expression of cell surface antigens, 1×10^5 cells per well were transferred to a v-bottom 96-well plate (Costar). Cells were centrifuged at 1,400 rpm for 4 min and the pellets were resuspended in FACS buffer containing the diluted FACS antibody of choice (Table 8). To ensure the specificity of staining, isotype controls were included. Additionally, for compensation of the dyes, controls were performed where cells were stained with each FACS antibody individually. Cells were incubated for 30 min at 4°C in the dark, washed with 200 μl 1x PBS and resuspended

METHODS

in 200 μ l FACS buffer. Afterwards measurements were conducted on a Guava easyCyte 6HT instrument (Merck, Millipore). Mean fluorescence intensity (MFI) ratios were calculated as median of expression intensities normalized to the median of isotype control staining.

3.6.2. Determination of surface antigen density

Surface antigen density of cell lines was evaluated using the commercial QIFIKIT (Dako) following manufacturer's instructions. Briefly, cell lines were incubated with saturating concentrations of unconjugated primary murine antibody directed against human CD33, PD-L1 or CD3 (clone P67.6, clone 29E.2A3 and clone HIT3a, respectively, BioLegend) followed by secondary staining with a FITC labeled detection antibody that was provided by the kit. QIFIKIT calibration beads served as calibration standard for the determination of the amount of apparent surface antigens.²⁴⁹

3.6.3. Binding studies and determination of dissociation constants (K_D)

Binding analysis of CiTE, sctb and controls to cell surface antigens was assessed by incubating cells with the respective protein at saturating concentration, followed by secondary staining with α Penta·His Alexa Fluor 488 Conjugate (Qiagen). Briefly, 1×10^5 cells were stained with 30 μ l of 15 μ g/ml CiTE, sctb or controls diluted in FACS buffer, if not otherwise stated. After 30 min of incubation at 4°C, cells were washed in 200 μ l 1x PBS and the pellet was resuspended in 30 μ l α Penta·His Alexa Fluor 488 Conjugate (Qiagen) at a dilution of 1:200. The cells were again incubated for 30 min at 4°C in the dark, subsequently washed in 1x PBS, resuspended in FACS buffer and measured on a Guava easyCyte 6HT instrument (Merck, Millipore).

K_D values were determined by calibrated flow cytometry similar to a described method.²⁵⁰ Briefly, CiTE, sctb or control molecules were titrated to target cells in a concentration range between 0.01-15 μ g/ml and detected by the secondary α Penta·His Alexa Fluor 488 Conjugate (Qiagen). As calibration control, 3.0–3.4 μ m Rainbow Calibration particles of 8 peaks (BioLegend) were included. Data points were normalized to the maximum MFI and fitted to a one-site specific binding model.

METHODS

3.6.4. Internalization assay

Internalization of bi- and trispecific molecules was evaluated on MOLM-13:PD-L1 target cells. Briefly, 0.5×10^6 cells were transferred into a 96-well v-bottom plate and incubated with or without 15 ng/ μ l of the molecules in FACS buffer in a total volume of 50 μ l for 30, 60 or 120 min at 37°C or on ice for 2 h as control. Additionally, the CD33 mAB clone P67.6 (BioLegend) was included as positive control. Afterwards, the cells were washed with 200 μ l ice-cold FACS buffer and centrifuged at 1,600 rpm for 4 min. Following removal of the supernatant, 50 μ l of the secondary α Penta-His Alexa Fluor 488 Conjugate (Qiagen) was added at a 1:200 dilution and incubated at 4°C in the dark for 30 min. The CD33 mAB was detected by adding a FITC-coupled antibody targeting mouse IgG Fc (BioLegend) at a dilution of 1:100. After another washing step with 200 μ l FACS buffer and centrifugation of cells, the pellet was resuspended in 200 μ l FACS buffer. The internalization was monitored on a Guava easyCyte 6HT instrument (Merck Millipore) recording 5,000 events per well. Internalization was quantified as follows:

$$\text{internalization [\%]} = \frac{(\text{MFI}_{4^{\circ}\text{C}} - \text{MFI}_{\text{background}}) - (\text{MFI}_{37^{\circ}\text{C}} - \text{MFI}_{\text{background}})}{(\text{MFI}_{4^{\circ}\text{C}} - \text{MFI}_{\text{background}})} \times 100$$

3.7. Biological assays

3.7.1. Redirected lysis assay with pre-activated T cells

Redirected lysis of target cells by pre-activated T cells was investigated in analogy to a published protocol.²⁵¹ 18-21 days IL-2 expanded and cryopreserved T cells were used as effector cells and thawed one day prior to the experiment in RPMI 1640/ GlutaMAX medium supplemented with 10% FBS. MOLM-13:PD-L1 target cells were split to a density of 0.6×10^6 cells/ml. The next day, 2×10^6 target cells were labeled with 15 μ M Calcein AM (Thermo Fisher Scientific). Redirected lysis assays were performed in 96-well u-bottom plates in a total volume of 200 μ l RPMI1640/ GlutaMAX medium supplemented with 10% FBS per well. T cells and target cells were applied at an effector to target (E:T) ratio of 5:1 (10,000 target cells and 50,000 T cells) and the molecules were added at concentrations ranging from 10 fM to 100 nM. As positive control, target cells were lysed with 2.5% Triton X-100 (denoted as max lysis). Background lysis without effector molecules was monitored by including a control with target cells only (BG) and a control with a mixture of target and T cells (BG+T). After incubation at 37°C/ 5% CO₂ for 4 h and centrifugation at

METHODS

1,600 rpm for 4 min, 100 μ l of the supernatant was transferred to a black 96-well polystyrene plate (Nunc) and cytolysis was monitored by reading out the emitted fluorescence of released Calcein at 485 nm with an Infinite[®] M100 plate reader instrument (TECAN). Specific lysis was calculated as follows:

$$\text{specific lysis [\%]} = \frac{(\text{fluorescence}_{\text{sample}} - \text{fluorescence}_{\text{BG+T}})}{(\text{fluorescence}_{\text{max lysis}} - \text{fluorescence}_{\text{BG}})} \times 100$$

In a dose-response curve, the averaged specific lysis was plotted against the concentration of molecules and analyzed with Prism software (Graph Pad Software Inc.) using the integrated four parameter non-linear fit model to determine concentrations of half-maximal target cell lysis (EC₅₀ values).

3.7.2. Preferential lysis assay with pre-activated T cells

The preferential lysis assay was performed according to 3.7.1. HEK293:PD-L1 and HEK293:CD33:PD-L1 cells were used as target cells and labeled with 15 μ M Calcein AM. Pre-activated T cells were incubated with a 1:1 mixture of unlabeled HEK293:PD-L1 and labeled HEK293:CD33:PD-L1 cells and vice versa at a total E:T ratio of 2:1. CiTE, scTb and control molecules were added as described and compared to the maximum unspecific lysis induced by 2.5% Triton X-100. After 4 h, fluorescence intensity in the supernatant was measured by an Infinite[®] M100 plate reader (TECAN) and specific lysis was calculated.

3.7.3. Redirected lysis assay with non-stimulated T cells

3.7.3.1. Redirected lysis assay with non-stimulated T cells and CD33^{bright} cells

Frozen, isolated HD T cells were taken into culture in RPMI1640/ GlutaMAX medium supplemented with 10% FBS (T cell medium) one day prior to the experiment. In parallel, CD33^{bright} MOLM-13 and MOLM-13:PD-L1 cells were split to a density of 0.6x10⁶ cells/ml. The next day, the assay was set up in T cell medium in 96-well flat bottom cell culture plates in a total volume of 200 μ l per well. T cells were mixed with MOLM-13 or MOLM-13:PD-L1 cells at an E:T ratio of 2:1 and a total cell density of 3x10⁵ cells/ml, and CiTE, scTb and controls were added (500 fM to 50 nM). 3x10⁵ α CD3/ α CD28 coupled beads (Thermo Fisher Scientific) served as positive control and a negative control without molecules was included. After incubation at 37°C/ 5% CO₂ for 72 h, the cell mixture was resuspended carefully and transferred to a 96-well v-bottom

METHODS

plate. The supernatant was removed and the cell pellets were resuspended in 30 μ l of premixed FACS antibodies against CD2, CD33 and LIVE/DEAD stain, as further specified in Table 14. Additionally, control stainings with the respective isotypes were performed as well as stainings with the single FACS antibodies as compensation controls.

Table 14: Antibodies used for flow cytometric readout of redirected lysis assay.

antigen / stain	dye	clone	applied concentration	dilution	company
CD2	PE	RPA2.10	0.05 μ g/ml	1:500	BioLegend
CD33	FITC	HIM3-4	n.a.	1:10	BD Pharmingen
LIVE/DEAD [®] Fixable Dead Cell Stain				1:1000	Thermo Fisher Scientific

Cells were stained for 60 min at 4°C in the dark, subsequently washed with 1x PBS and resuspended in 200 μ l FACS buffer. The total number of live target cells was assessed by flow cytometry within a fixed time frame of 60 sec. Due to the positive displacement syringe pump and the precise microfluidic system it was possible to quantify the absolute number of events without the addition of counting beads on the Guava easyCyte 6HT instrument (Merck Millipore). The number of remaining target cells was normalized to the negative control and plotted against the concentration of molecules. Data was evaluated using Prism software (Graph Pad Software Inc.) and fitted with an integrated four-parameter non-linear fit model to determine concentrations of half-maximal target cell lysis (EC_{50} values).

3.7.3.2. Redirected lysis assay with non-stimulated T cells and CD33^{dim} cells

Redirected lysis assays with CD33^{dim} OCI-AML3 and OCI-AML3:PD-L1 target cells were performed similarly to 3.7.3.1. The two cell lines were split to a density of 0.6×10^6 cells/ml one day prior to the experiment. At the day of the assay, the cells were labeled with 2 μ M PKH67 dye (Sigma-Aldrich) according to manufacturer's instructions. Briefly, 4×10^6 cells of each cell line were placed in a 15 ml falcon tube and washed twice in RPMI1640/ GlutaMAX medium. A 2x solution of the PKH67 dye was prepared by mixing 400 μ l of Diluent C buffer with 1.6 μ l of dye. The cells were resuspended in 400 μ l of Diluent C buffer and mixed with 400 μ l of the dye solution. After 5 min incubation at room temperature and frequent mixing, the staining was stopped by addition of 400 μ l FBS and 1 min incubation. The cells were centrifuged at 1,400 rpm for 4 min, the supernatant was discarded and the pellet was washed twice in RPMI1640/ GlutaMAX medium. Subsequently, the assay was set up as described (section 3.7.3.1.) using molecules at concentrations

METHODS

from 5 fM to 50 nM. Readout was conducted by staining with a FACS antibody against CD2 and LIVE/DEAD stain (Table 14) and measurement of total events within a fixed time frame of 60 sec on a Guava easyCyte 6HT instrument (Merck Millipore).

3.7.4. T cell proliferation assay

Freeze-downs of HD T cells were thawed one day prior to the experiment and recovered in T cell medium. Additionally, target cells were split to a density of 0.6×10^6 cells/ml. The following day, T cells were stained with CFSE (Thermo Fisher Scientific). Briefly, T cells were centrifuged at 1,600 rpm for 5 min and the pellet was resuspended in 1 ml of a prewarmed solution of 2 μ M CFSE in 1x DPBS supplemented with 0.5% FBS. The cells were incubated for 12 min at 37°C/ 5% CO₂, centrifuged, and the pellet was resuspended in 10 ml of fresh T cell medium followed by 30 min of incubation to ensure complete CFSE acetate hydrolysis. Afterwards, the cells were spun down and the pellet was washed with fresh T cell medium. Subsequently, the assay was set up in 96-well flat bottom cell culture plates in a total volume of 200 μ l per well and a total cell density of 3×10^5 cells/ml. The labeled T cells were mixed with target cells in T cell medium at an E:T ratio of 2:1 and CiTE, sctb and controls (5 fM to 50 nM). A positive control with 3×10^5 α CD3/ α CD28 coupled beads (Thermo Fisher Scientific) and a negative control without molecules was included. Additionally, unlabeled T cells were used as control. The assay was incubated at 37°C/ 5% CO₂ for 96 h. Subsequently, the cells were carefully resuspended and transferred to a 96-well v-bottom plate. After centrifugation and discarding the supernatant, the cells were labeled with a FACS antibody against CD2 and LIVE/DEAD stain, as further specified in Table 15, at a total volume of 30 μ l for 60 min. Control stainings with isotype as well as single stainings for compensation were performed.

Table 15: Antibodies used for flow cytometric readout of T cell proliferation assay.

antigen / stain	dye	clone	applied concentration	dilution	company
CD2	PE/Cy5	RPA2.10	0.5 μ g/ml	1:50	BioLegend
LIVE/DEAD [®]	Fixable Dead Cell Stain			1:1000	Thermo Fisher Scientific

After washing, 2,000 live/CD2⁺ events were recorded on a Guava easyCyte 6HT instrument (Merck Millipore). Data was evaluated using Prism software (Graph Pad Software Inc.). In

METHODS

particular, the percentage of divided T cells was plotted against the concentration of molecules and fitted with an integrated four-parameter non-linear fit model.

3.7.5. T cell activation assay

T cell activation assays were set up as described in 3.7.3.1., except that CiTE, sctb and control molecules were applied at 5 nM concentration. After 96 h, the cell mixtures were transferred to a 96-well v-bottom plate for FACS staining. They were centrifuged and the pellets were resuspended in antibody dilutions directed against CD2, PD-1, CD25 and CD69 in FACS buffer, as further specified in Table 16. Control stainings were included. All stainings were performed at 4°C protected from light for 30 min, and after washing with 1x PBS and resuspending the pellet in 200 µl of FACS buffer, 5,000 events in the FSC/SSC lymphocyte gate were recorded on a Guava easyCyte 6HT instrument (Merck Millipore).

Table 16: Antibodies used for flow cytometric readout of T cell activation assay.

antigen	dye	clone	applied concentration	dilution	company
CD2	FITC	RPA2.10	1 µg/ml	1:100	BioLegend
PD-1	PE	EH12.2H7	1.25 µg/ml	1:40	BioLegend
CD25	PerCP/Cy5.5	M-A251	2.5 µg/ml	1:40	BioLegend
CD69	APC	FN50	5 µg/ml	1:100	BioLegend

3.7.6. *Ex vivo* redirected lysis assay of primary AML patient samples

Ex vivo redirected lysis assays of AML patient samples were performed by Christina Krupka^d in α -MEM medium (PAN Biotech) supplemented with 12.5% FBS, 12.5% horse serum (Gibco) and 1% P/S/L-Gln (Invitrogen). Similar to a method previously described, recombinant human granulocyte-colony stimulating factor (rhG-CSF), rhu interleukin (IL)-3 and rhu thrombopoietin (TPO) (Peprotech, Germany) were added to the medium at a final concentration of 20 ng/ml.²⁵² Irradiated MS-5 cells were used as feeder layer (irradiation at 60 Gy for 2 h) in 12-well flat-bottom cell culture plates, and AML patient cells and HD T cells were added at an E:T ratio of 1:5.²⁵³⁻²⁵⁵ CiTE, sctb and controls were applied at a concentration of 10 nM and the PD-L1 blocking mAb at

^d Laboratory of Marion Subklewe, Gene Center Munich, LMU München, Germany

METHODS

10 µg/ml. The percentage of lysis as well as PD-1 and PD-L1 expression were monitored after 3-4 days.

3.7.7. Determination of cytokine levels

Cytokine levels were determined in cell culture supernatants by Cytometric Bead Array (CBA) (Human IFN- γ Flex Set, Human IL-2 Flex Set, BD Biosciences) according to manufacturer's instructions. Specifically, the supernatants from redirected lysis assays with non-stimulated T cells and MOLM-13 or MOLM-13:PD-L1 target cells (section 3.7.3.1.) and 5 nM or 0.5 nM CiTE, scfb or control molecules were analyzed. Additionally, the BiTE[®]-like molecule was evaluated in combination with PD-L1 scFv, PD-1_{ex}-Fc, and commercial PD-1 (EH12.2H7, BioLegend) or PD-L1 (NIH1, eBioscience) blocking antibodies at 5 nM or 250 nM concentration. After 72 h, 15 µl of assay supernatant were transferred into a 96-well v-bottom plate and mixed with 15 µl of 1:50 diluted capture beads. After incubation for 60 min at room temperature, 15 µl of 1:50 diluted PE detection reagent was added, the components were mixed and incubated for another 120 min at room temperature in the dark. Afterwards, the beads were washed with 180 µl wash buffer, centrifuged at 1,400 rpm for 4 min and the pellets resuspended in 200 µl wash buffer. Subsequently, 600-2,000 beads were measured on a Guava easyCyte 6HT instrument (Merck Millipore). Absolute IFN- γ and IL-2 levels were calculated from standard curves derived from a serial dilution of cytokine standards provided by the manufacturer, which were fitted with a four parameter logistic regression using Prism software (Graph Pad Software Inc.).

3.8. Mouse studies

All mouse work was performed in cooperation with Katrin Deiser [°].

3.8.1. Study design

The effects of CiTE, scfb and BiTE[®]-like molecule were evaluated in a murine AML xenograft model on NSG background. All mice were female, 170-265 days old and they were housed under pathogen-free conditions at the research animal facility of the Helmholtz Zentrum München, Munich, Germany. Animal experiments were approved by the Bavarian government (no. 55.2-1-54-2532-226-2013). Based on a published experimental design, mice were inoculated with 2×10^4

[°] Laboratory of Marion Subklewe, Gene Center Munich, LMU München, Germany

METHODS

MOLM-13:PD-L1 cells intravenously (i.v.) on day 0.²⁵⁶ On day 3, 1×10^7 *in vitro* pre-activated T cells were transferred intraperitoneally (i.p.) and mice were randomized into 5 groups: 3 groups for treatment with either CiTE, sctb or BiTE[®]-like molecule containing 6 mice each, a specificity control group of 4 mice and a 1x DPBS control group of 5 mice. On day 4, 50 pmol of therapeutic proteins, specificity control or 1x DPBS were injected i.v., which was repeated for 9 days. The body weight of the mice was monitored every second day. On day 13, the mice were sacrificed by CO₂ asphyxiation. Murine whole blood, femurs of hind legs and spleens were collected and mice were macroscopically examined for bowel inflammation.

3.8.2. Cell isolation from murine organs and extraction of murine whole blood

For bone marrow isolation, femurs of hind legs were removed and subsequently placed on ice. The femurs were opened at both ends and the bone marrow was washed out with 1x PBS using a 27G needle. The spleens were disrupted mechanically and filtered through a moistened 70 μ m cell strainer. Both cell suspensions were centrifuged at 550 g for 5 min and washed with 1x PBS. Afterwards, they were incubated with ACK buffer (150 mM NH₄Cl, 10 mM KHCO₃, pH 7.2-7.4) for 90 sec to lyse erythrocytes and the reaction was stopped by the addition of 7 ml PBS. After centrifugation at 550 g for 5 min, the cells were resuspended in 1x PBS and prepared for flow cytometry analysis. Murine whole blood was drawn from the heart immediately after sacrificing the mice. For this purpose, the heart was punctured with a 27G needle containing 20 μ l of 0.5 M EDTA and blood was transferred to a 1.5 ml Eppendorf tube on ice. Plasma was isolated by centrifugation of whole blood at 500 g for 10 min at 4°C. The supernatant was carefully transferred to a new tube and again centrifuged. Subsequently, the plasma was transferred, frozen in liquid nitrogen and stored at -80°C until further usage.

3.8.3. Flow cytometry analysis of murine cells

For flow cytometric analysis, 50 μ l of murine whole blood, 1×10^6 cells from spleen or 0.5×10^6 cells from bone marrow were preincubated with 3 μ l Fc blocking reagent (Miltenyi Biotech) for 15 min, subsequently washed and incubated with FACS antibodies that were diluted in FACS buffer in a total volume of 50 μ l. Human T cells and AML cells were separated from murine cells by CD45 staining (clone 2D1, BioLegend) and further discriminated by staining for CD3 (clone UCHT1, BioLegend), CD33 (clone WM3, BioLegend), CD4 (clone RPA-T4, BD Biosciences) and PD-1 (clone EH12.2H7, BioLegend).

METHODS

3.9. Plotting and statistical analysis

For curve fitting and statistical evaluation, GraphPad Prism Software (GraphPad Software Inc.) was used. Unpaired Student's t-test with Welch correction was applied for samples following Gaussian distribution and Mann-Whitney U test was used for data with unknown distribution. The result was considered to be statistically significant if $p < 0.05$. * corresponds to $p = 0.01-0.05$, ** to $p = 0.001-0.01$ and *** to $p \leq 0.001$.

4. Results

4.1. Design of CiTE antibody format

The blockade of the PD-1/PD-L1 axis to counteract adaptive immune escape is a highly efficient strategy in the treatment of various cancers. However, all high-affinity PD-1 and PD-L1 blocking agents share the risk to induce broadly distributed adverse events since almost every tissue is able to upregulate PD-L1 in response to proinflammatory cytokines.⁹⁸ We developed the “Checkpoint inhibitory T cell Engager” (CiTE) format to restrict immune checkpoint blockade to the surface of tumor cells and to thereby avoid systemic on-target off-leukemia events. The CiTE described in this thesis consists of three distinct modules: (1) The N-terminal extracellular domain of human PD-1 (PD-1_{ex}) as checkpoint blocking module, (2) a central CD3ε scFv for the polyclonal redirection of T cells, and (3) a C-terminal CD33 scFv for high-affinity targeting of AML cells (Figure 5).

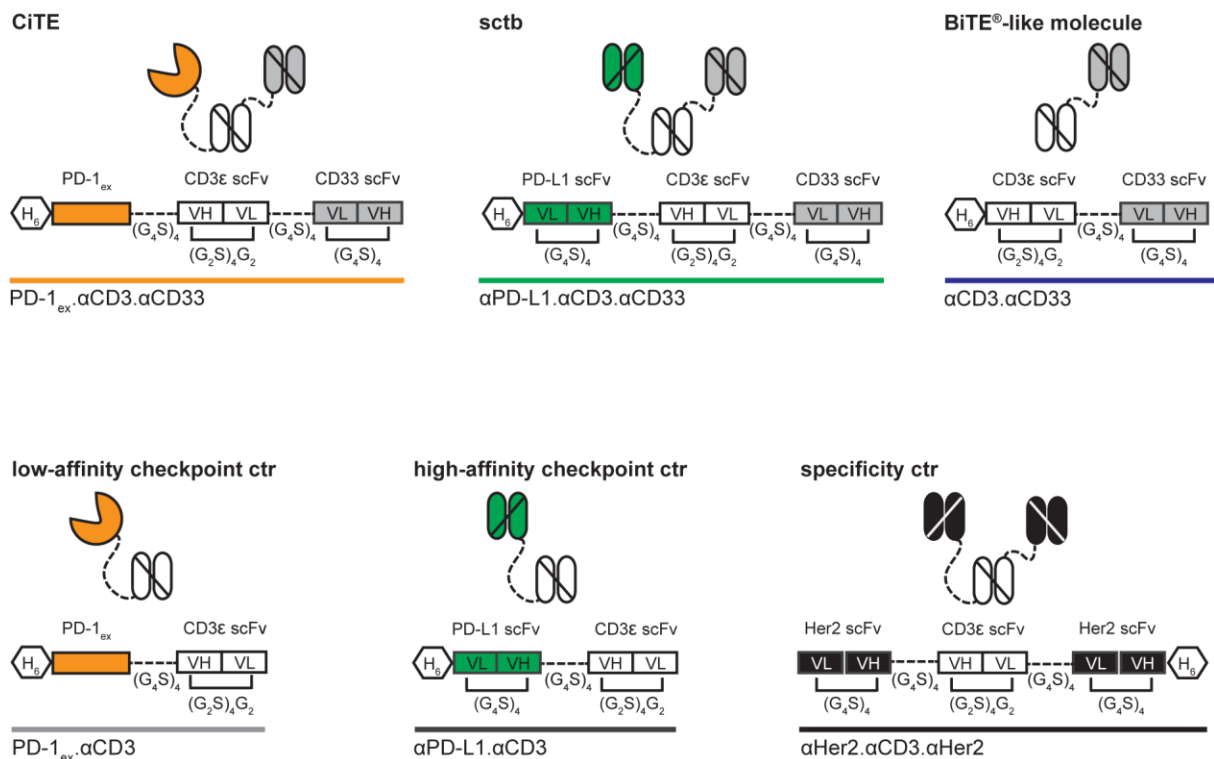


Figure 5: Schematic representation of CiTE, sctb and control molecules.

Modular composition of CiTE, sctb, BiTE[®]-like molecule, low- and high-affinity checkpoint controls PD-1_{ex}.αCD3 and αPD-L1.αCD3 as well as specificity control. The checkpoint blocking modules (orange and green) were cloned N-terminally of a central CD3ε scFv (white) and a C-terminal CD33 leukemia-targeting scFv (grey).

RESULTS

The utilized CD33 scFv originates from antibody clone hP67.6 and an OKT3-derived CD3 ϵ scFv served as T cell engaging module.^{86,239,240} Both scFvs were already described in previous studies.^{86,87,257} The PD-L1 scFv was generated based on published sequences.²³⁸ To ensure flexibility of the binding arms, the respective binding modules were connected to each other by 4-times poly-Gly-Ser linkers (G₄S)₄. The CiTE was compared to a single-chain triplebody (sctb), in which checkpoint blockade is mediated by a high-affinity PD-L1 scFv.⁸⁶ Due to the low affinity of PD-1_{ex}, the CiTE is not expected to induce targeting of PD-L1⁺ cells, whereas in analogy to high-affinity blocking agents, the sctb is intended to systemically address PD-L1⁺ cells. As control molecules, the BiTE[®]-like molecule, a low-affinity PD-1_{ex}. α CD3 and a high-affinity α PD-L1. α CD3 checkpoint control were generated. The previously published α Her2. α CD3. α Her2 molecule served as non-targeting specificity control.⁸⁶

4.2. Generation and stability of CiTE antibody and sctb

4.2.1. Expression and purification of CiTE antibody and sctb

All molecules were expressed in stable FreeStyle[™] 293-F or Expi293F[™] cell pools and purified in a two-step purification procedure. Exemplarily, Figure 6 displays the purification of CiTE antibody and sctb. The proteins were captured in the cell culture supernatant using Ni²⁺-NTA agarose beads. Two washing steps were performed to remove bead-bound impurities and the protein was eluted in five steps (Figure 6 A, B). Under reducing conditions of SDS-PAGE, the CiTE antibody revealed a higher apparent molecular weight than the theoretical value of 71.4 kDa, which was presumably due to PD-1_{ex} glycosylation.¹⁰⁹ The sctb indicated the expected molecular weight of 84.2 kDa. As can be concluded from visible bands at the respective molecular weights in the flow through fractions, at high protein levels a single capture step was not sufficient to achieve a full protein recovery. Thus, the flow through was reapplied to Ni²⁺-NTA affinity chromatography (data not shown). Analysis of the separate chromatography fractions demonstrated that CiTE antibody and sctb were mainly enriched in the first elution fractions (i.e. E1-E2 and E1-E3, respectively). Chromatograms of the subsequent SEC with a Superdex 200 increase 10/300 GL column revealed three elution peaks for both proteins (I-III) (Figure 6 C, D). However, the higher-molecular weight peaks I and II were less pronounced for the sctb. SDS-PAGE analysis confirmed that all peaks accounted for the expressed proteins, therefore I and II were considered to be multimers (Figure 6 E, F). Accordingly, the fractions of monomer peak III

RESULTS

were pooled for further analysis. Protein yields were determined to be 1-4.3 mg/l for the CiTE antibody and 10.8-19.7 mg/l for the sctb.

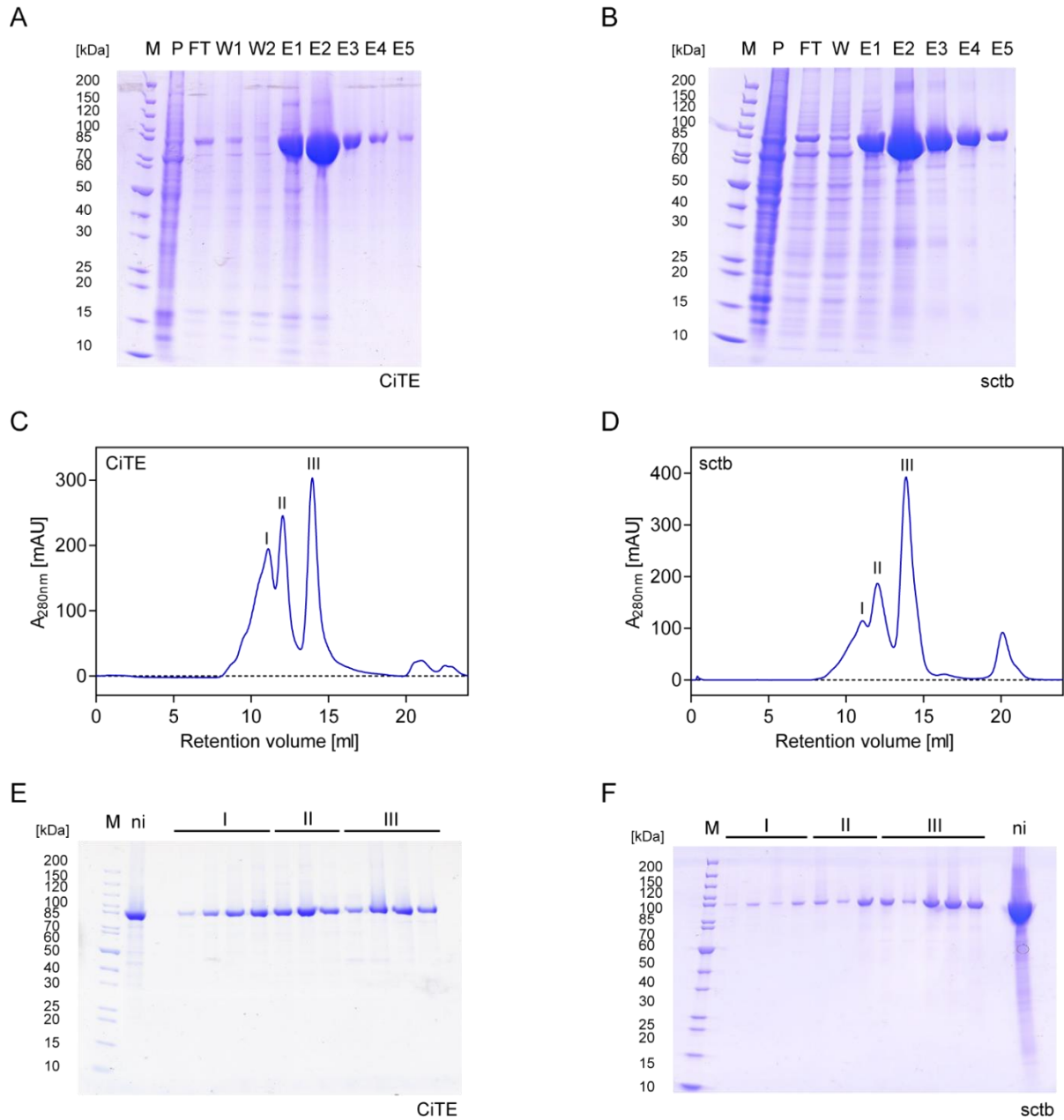


Figure 6: Expression and purification of CiTE antibody and sctb.

SDS-PAGE analysis of Ni^{2+} -NTA affinity chromatography fractions of (A) CiTE and (B) sctb purified from supernatants of stable FreeStyle™ 293-F cell pools. (C), (D) SEC chromatograms of CiTE and sctb with Superdex 200 increase 10/300 GL column with three main peaks (I, II, III). (E), (F) Evaluation of SEC fractions by SDS-PAGE. M, marker; P, pellet; FT, flow through; W1-W2, wash fractions; E1-E5, elution fractions; ni, protein after Ni^{2+} -NTA affinity chromatography.

RESULTS

An overview of the proteins is depicted in Figure 7, in which single bands confirm their purity. On the polyacrylamide gel, the bands of sctb and the BiTE[®]-like molecule, α PD-L1. α CD3 and specificity control correlated with the calculated molecular weights of 84.2 kDa, 57.7 kDa, 55.2 kDa and 87.2 kDa, respectively. With 71.4 kDa and 42.3 kDa, CiTE and PD-1_{ex}. α CD3 demonstrated a higher apparent molecular weight than calculated, which is presumably due to glycosylation.¹⁰⁹

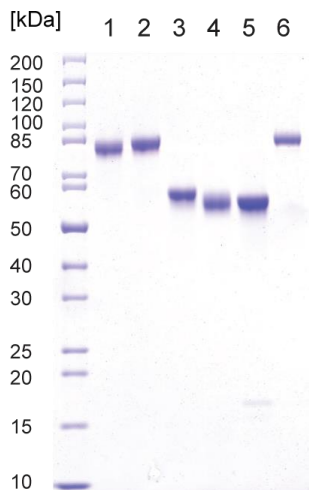


Figure 7: SDS-PAGE analysis of purified CiTE antibody, sctb and control molecules.

SDS-PAGE analysis of (1) CiTE antibody, (2) sctb, (3) BiTE[®]-like molecule, (4) PD-1_{ex}. α CD3, (5) α PD-L1. α CD3 and (6) specificity control after purification by Ni²⁺-NTA affinity chromatography and SEC.

4.2.2. Protein stability of CiTE antibody, sctb and BiTE[®]-like molecule

After two-step purification, the proteins could be obtained in a pure, monomeric state. However, storage conditions as well as assay incubation at 37°C can significantly influence protein quality and lead to degradation or aggregation. To evaluate whether the molecules tolerate storage at -80°C and are suitable for the application *in vitro* and *in vivo* over several days, the stability of CiTE antibody, sctb and BiTE[®]-like molecule was determined. After one-time freezing at -80°C, the proportion of monomeric protein was monitored by SEC using a Superdex 200 increase 5/150 column. The elution profile displayed one main peak for each molecule (Figure 8 A). No significant high- or low-molecular weight peaks were observed, indicating the absence of aggregation or degradation products. Further, the thermal stability of the three molecules was investigated by ThermoFluor assay (Figure 8 B). Analysis of thermal unfolding resulted in a melting temperature of 54°C for the CiTE, a 3-step unfolding of the sctb with the lowest melting temperature at 52.5°C

RESULTS

and a 2-step unfolding of the BiTE[®]-like molecule starting at 51.5°C. Further, the proteins were incubated at 37°C for 14 days, large aggregates were separated by centrifugation and supernatant as well as pellet were subsequently evaluated by SDS-PAGE. As shown exemplarily for the CiTE in Figure 8 C, no significant degradation bands could be noted and no considerable aggregation was detected in the pellet fraction after 14 days. This confirms that the proteins can be stored at -80°C and they are sufficiently stable at physiological temperatures.

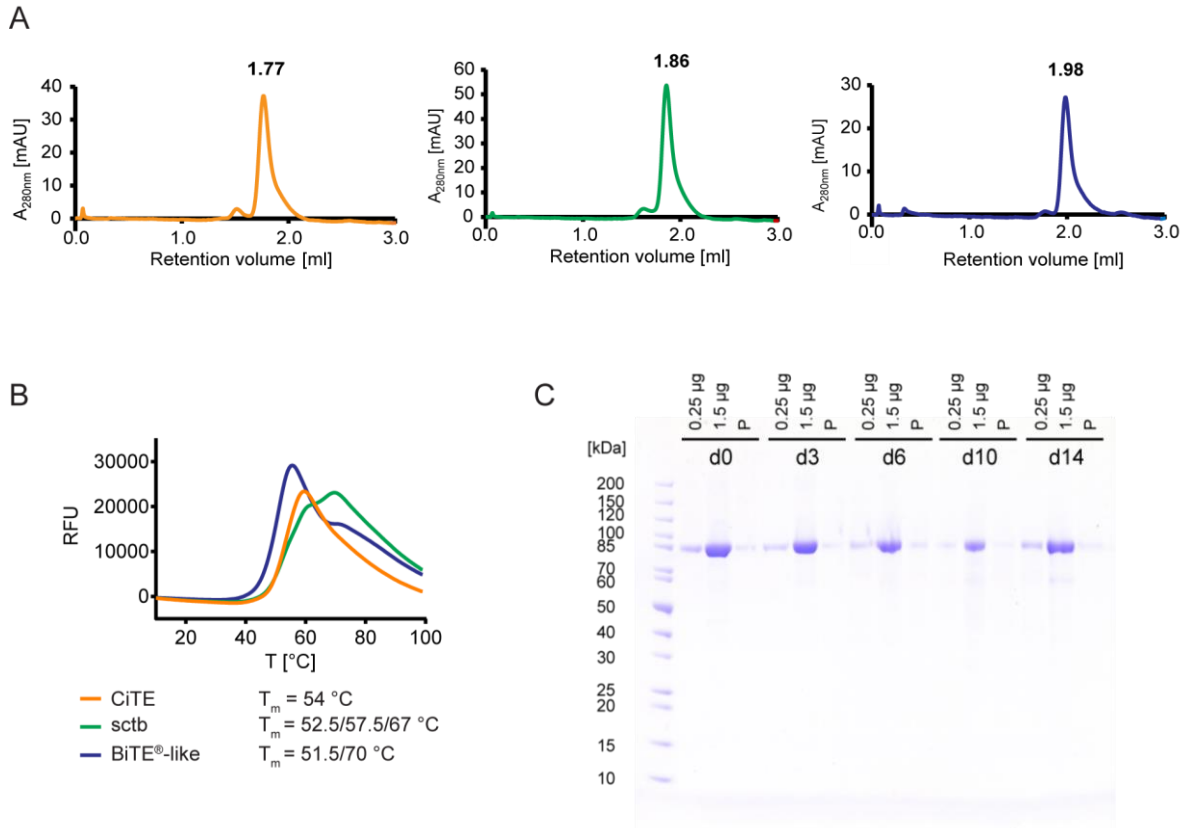


Figure 8: Biochemical and biophysical evaluation of protein stability.

(A) SEC chromatograms of proteins after 1x freezing using a Superdex 200 increase 5/150 GL column. (B) Melting curves as determined by ThermoFluor assay with calculated melting temperatures indicated. (C) SDS-PAGE of CiTE antibody after incubation at 37°C for indicated days in 20 mM His (pH 6.5), 300 mM NaCl. P, pellet.

4.3. Characterization of target cell lines

4.3.1. Generation of PD-L1⁺ AML target cell lines

Screenings of CD33 expression levels in AML patient samples report a significant but heterogeneous upregulation of the myeloid differentiation antigen with high variation between

RESULTS

patients and leukemic subpopulations.⁷⁹ Thus, two AML cell lines with different CD33 expression levels were selected as target cell lines. MOLM-13 cells were identified to express high (CD33^{bright}) and OCI-AML3 low (CD33^{dim}) CD33 levels, however, both of them lack PD-L1 on the cell surface (Figure 9). The second known ligand of PD-1, i.e. PD-L2, was not detected on MOLM-13 but on OCI-AML3 cells.

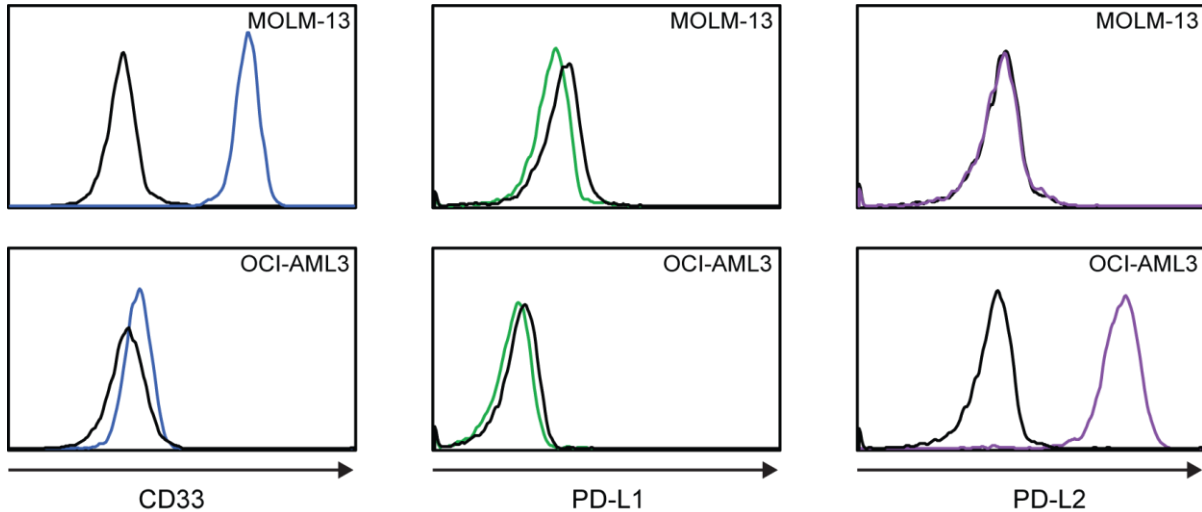


Figure 9: Antigen expression by selected AML cell lines.

Flow cytometric evaluation of CD33, PD-L1 and PD-L2 expression on parental MOLM-13 and OCI-AML3 cells. The black line indicates unspecific staining by the isotype control.

It is reported *in vitro* and *in vivo* that IFN- γ induces the upregulation of PD-L1 on AML cells.¹⁸⁹⁻¹⁹¹ Thus, MOLM-13 and OCI-AML3 cells were incubated with 100 ng/ μ l IFN- γ and after 24 h PD-L1 expression was analyzed by flow cytometry. However, with this strategy, no significant PD-L1 induction could be triggered (data not shown). Thus, stable PD-L1 expression on MOLM-13 and OCI-AML3 cells was ensured by retroviral transduction of the parental cell lines^f. This strategy guaranteed the maintenance of a stable cell background for functional assays and enabled the selection of cell lines with distinct PD-L1 expression levels. MOLM-13 cells were transduced with a pMXs vector containing the full-length human PD-L1 cDNA sequence, which yielded a transduction efficiency of 11% (Figure 10). Subsequently, PD-L1⁺ cells were separated by FACS sorting, and by dilution cloning homogeneous cell lines were raised from single cells. In total, the PD-L1 expression level of 78 clones was assessed by flow cytometry, and the five shown

^f Retroviral transduction and FACS sorting were performed by Felicitas Rataj and Constanze Heise, Laboratory of Sebastian Kobold, Clinical Pharmacology, Department of Internal Medicine IV, Klinikum der LMU München, Germany

RESULTS

in Figure 10 B were cryoconserved for further analysis. Clone 56 was selected for the present study since it exhibited similar expression levels for PD-L1 and CD33. It is hereafter referred to as MOLM-13:PD-L1 cell line. Characterization of MOLM-13 and MOLM-13:PD-L1 cells confirmed similar CD33 levels and homogeneous PD-L1 expression on MOLM-13:PD-L1 cells (Figure 10 C). According to the same procedure, OCI-AML3:PD-L1 cells were generated.

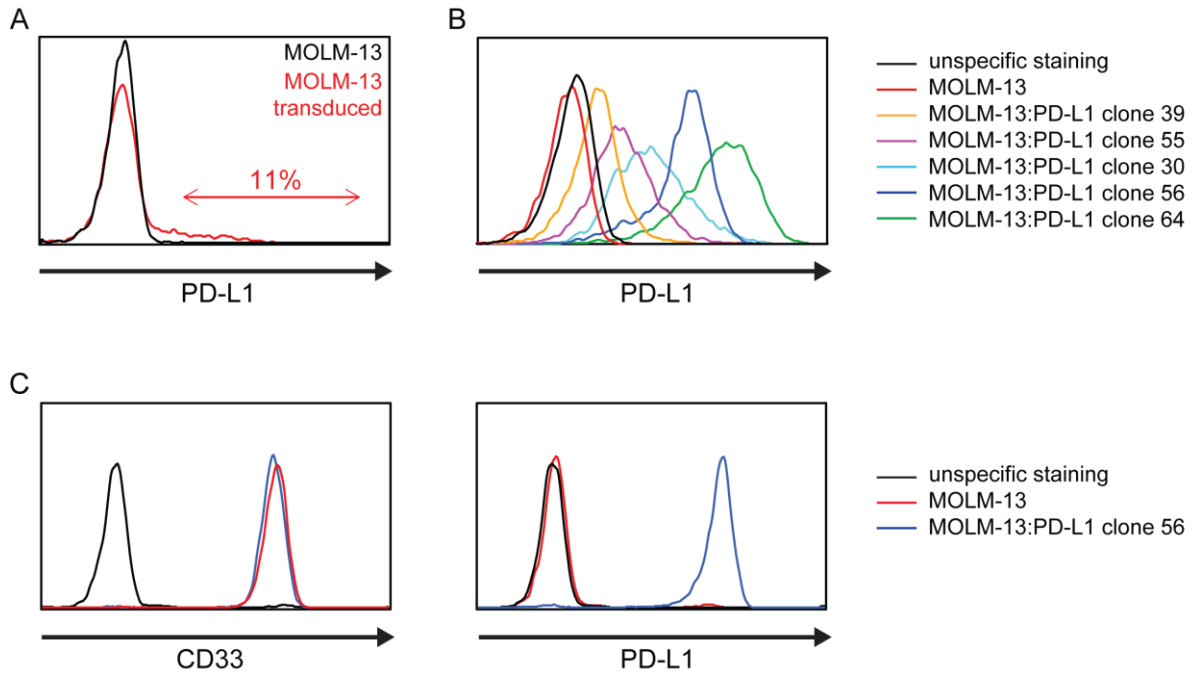


Figure 10: Generation of PD-L1⁺ MOLM-13 cells by transduction and single-cell cloning.

(A) Flow cytometric analysis of PD-L1-transduced bulk MOLM-13 cells in comparison to parental MOLM-13 cells. (B) PD-L1⁺ single cell clones with different PD-L1 expression levels. (C) CD33 and PD-L1 expression of selected MOLM13:PD-L1 clone 56 in comparison to parental MOLM-13 cells. The black line indicates unspecific staining.

All cell lines were quantified regarding their surface antigen density (Table 17). Notably, CD33 and PD-L1 expression levels were in a similar range on MOLM-13:PD-L1 cells, whereas OCI-AML3:PD-L1 cells displayed a significantly higher density of PD-L1 compared to CD33.

RESULTS

Table 17: Surface antigen density of AML target cell lines as determined by QIFIKIT.

Table summarizes mean values of surface antigen density calculated from 3-4 experiments. Errors indicate SEM.

	CD33	PD-L1
MOLM-13	$69.2 \times 10^3 \pm 8.2 \times 10^3$	-
MOLM-13:PD-L1	$78.3 \times 10^3 \pm 4.5 \times 10^3$	$99.3 \times 10^3 \pm 9.7 \times 10^3$
OCI-AML3	$3.0 \times 10^3 \pm 0.6 \times 10^3$	-
OCI-AML3:PD-L1	$3.3 \times 10^3 \pm 1.3 \times 10^3$	$121.9 \times 10^3 \pm 7.9 \times 10^3$

4.3.2. Generation of stable PD-L1⁺, CD33⁺ and CD33⁺PD-L1⁺ target cell lines

Since PD-L1 can be ubiquitously upregulated on cells in the presence of proinflammatory cytokines, for the evaluation of potential on-target off-leukemia effects of CiTE and scfb a target cell system was required that represents this cell population of the body.¹⁰⁷ To this end, the Flp-In™ 293 T-Rex system was used to raise PD-L1⁺, CD33⁺ as well as CD33⁺PD-L1⁺ cell lines of the same cell background. Stable cell lines were grown under hygromycin selection pressure within several weeks. The resulting HEK293:PD-L1, HEK293:CD33 and HEK293:CD33:PD-L1 cell lines were confirmed to homogeneously express the integrated antigens and PD-L1 and CD33 levels were quantified (Table 18). Notably, PD-L1 expression on HEK293:PD-L1 cells was determined to be similar to HEK293:CD33:PD-L1 cells. Basal antigen expression of all three cell lines could be increased by the addition of tetracycline. Yet, induced cell lines were exclusively applied for binding studies, whereas cell lines with antigen expression in a physiologically more relevant range were utilized for functional assays.

Table 18: Surface antigen density of Flp-In™ T-Rex-derived cell lines as determined by QIFIKIT.

Table summarizes mean values of surface antigen density calculated from 3-4 experiments. Errors indicate SEM.

	CD33	PD-L1
HEK293:PD-L1	-	$8.8 \times 10^3 \pm 1.8 \times 10^3$
HEK293:PD-L1_ind.	-	$348.2 \times 10^3 \pm 13.8 \times 10^3$
HEK293:CD33	$22.5 \times 10^3 \pm 7.8 \times 10^3$	-
HEK293:CD33_ind.	$235.7 \times 10^3 \pm 3.4 \times 10^3$	-
HEK293:CD33:PD-L1	$15.4 \times 10^3 \pm 0.6 \times 10^3$	$8.5 \times 10^3 \pm 0.9 \times 10^3$

RESULTS

4.4. Binding and internalization of CiTE antibody

4.4.1. Binding of CiTE antibody to target and effector cells

The CiTE antibody is designed to bind to CD33⁺ AML cells and T cells but to spare PD-L1⁺ non-AML cells. This binding selectivity is conferred by the PD-1_{ex} module, which is described to interact with PD-L1 with low affinity and a K_D value of 8.2 μM .¹¹⁵⁻¹¹⁷ To evaluate the binding properties of CiTE antibody and scfb, the interaction of the molecules to MOLM-13:PD-L1 target cells and healthy donor T cells was investigated (Figure 11 A). Both bound comparably to target and effector cells, which was independent of the affinity of the checkpoint blocking module. As the unique functionality of the CiTE antibody is its weak affinity to PD-L1, the binding properties of the two checkpoint blocking modules PD-1_{ex} and PD-L1 scFv were analyzed. To sustain the direct molecular environment of the modules, they were not investigated as single modules but incorporated into bispecific checkpoint controls where they are connected to a C-terminal CD3 ϵ scFv (i.e. PD-1_{ex}. αCD3 and $\alpha\text{PD-L1}$. αCD3). Cell lines with low (HEK293:PD-L1), intermediate (MOLM-13:PD-L1) and high PD-L1 levels (HEK293:PD-L1_ind.) served as target cells (Figure 11 B).

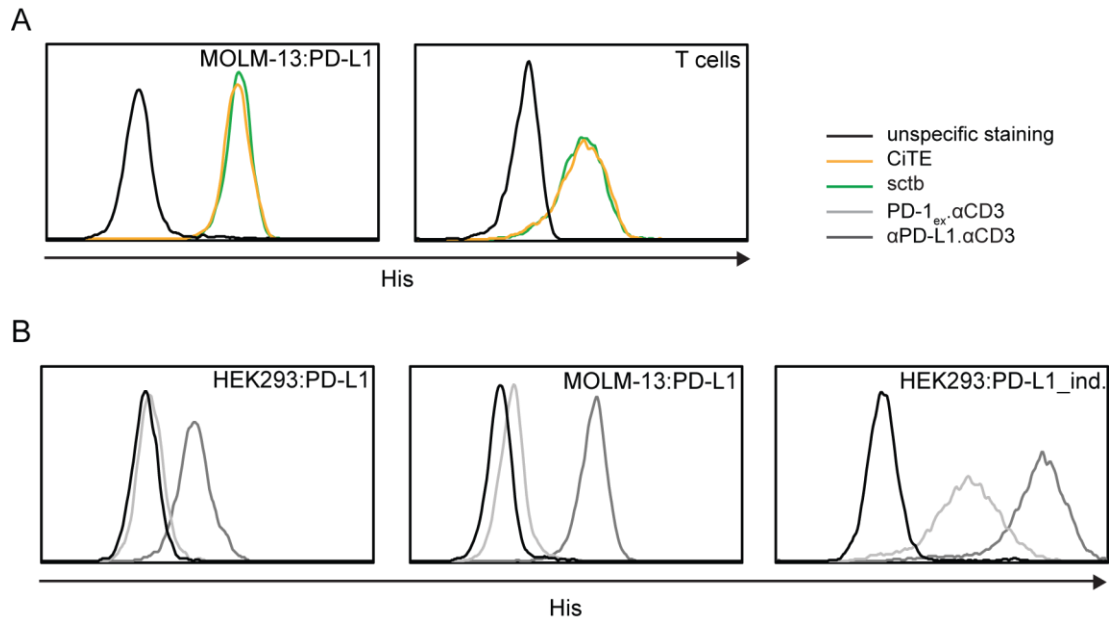


Figure 11: Binding properties of CiTE antibody and scfb.

(A) Binding studies of CiTE antibody and scfb at saturating conditions of 15 ng/ μl to MOLM-13:PD-L1 target cells and HD T cells as determined by flow cytometry. (B) Binding analysis of PD-1_{ex} in PD-1_{ex}. αCD3 and PD-L1 scFv in $\alpha\text{PD-L1}$. αCD3 to cell lines with different PD-L1 expression levels at a protein concentration of 1.5 ng/ μl . Molecules were detected by a secondary antibody (His). The black line shows unspecific staining. Histograms display one out of three independent experiments with similar results.

RESULTS

Flow cytometry analysis of PD-1_{ex} binding revealed a much lower MFI shift than binding of the PD-L1 scFv, indicating a comparably weaker affinity. Binding of both modules directly correlated with the number of PD-L1 molecules on the target cells, demonstrating the lowest MFI shift on HEK293:PD-L1, an intermediate shift on MOLM-13:PD-L1 and the highest shift on HEK293:PD-L1_{ind.} cells.

4.4.2. K_D determination of scFv modules in CiTE antibody and scfb

Binding of the scFv modules within CiTE antibody, scfb and bispecific molecules was quantified by calibrated flow cytometry analysis and dissociation constants (K_D) were determined (Figure 12).

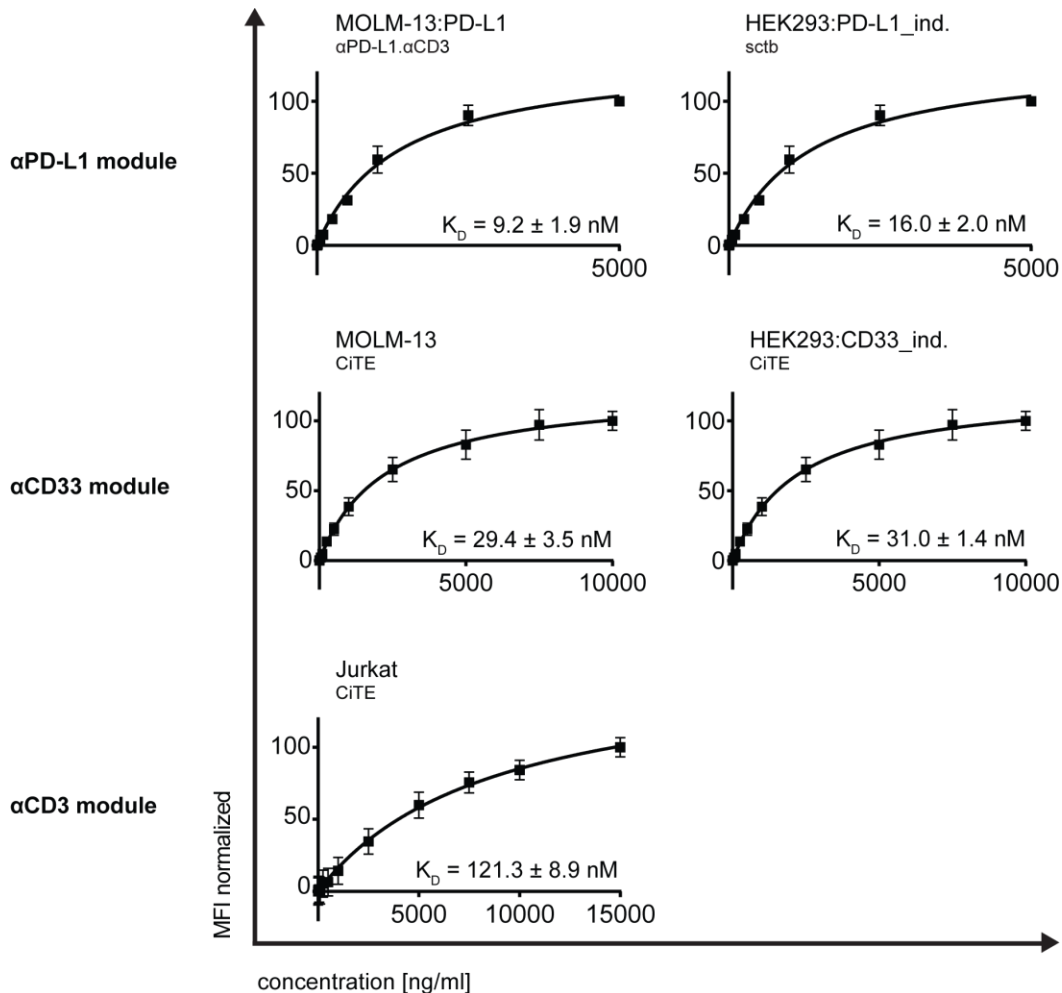


Figure 12: K_D measurements of scFv binding modules.

Concentration-dependent binding of the PD-L1 scFv (in α PD-L1. α CD3) to PD-L1 expressing MOLM-13:PD-L1 and HEK293:PD-L1_{ind.} cells, CD33 scFv in the CiTE to MOLM-13 and HEK293:CD33_{ind.} cells, and CD3 ϵ scFv in the CiTE to Jurkat cells. K_D values are indicated. Graphs show mean values of three independent experiments with SEM as error bars.

RESULTS

Interaction of the cancer-targeting modules with their ligands was investigated on cell lines expressing moderate levels of PD-L1 (MOLM-13:PD-L1) and CD33 (MOLM-13) and on cell lines with high overexpression of the target antigens (HEK293:PD-L1_ind. and HEK293:CD33_ind.). Binding of the T cell recruiting module α CD3 ϵ was evaluated on the T cell leukemia cell line Jurkat. For the PD-L1 scFv, mean K_D values of $9.2 \text{ nM} \pm 1.9 \text{ nM}$ and $16.0 \pm 2.0 \text{ nM}$ were calculated. The determined K_D values of $29.4 \pm 3.5 \text{ nM}$ and $31.0 \pm 1.4 \text{ nM}$ for CD33 scFv are similar to published values for other scFv-based bispecifics.^{75,258} Furthermore, the affinity of $121.3 \pm 8.9 \text{ nM}$ for the CD3 ϵ scFv was comparable to previously developed formats.⁷⁰ The stronger binding of the tumor targeting modules in comparison to the T cell recruiting module is in accordance to the concept that the molecules bind to the target cells with higher affinity to facilitate T cell migration and serial lysis.⁶⁹

4.4.3. Internalization of CiTE antibody

CD33-targeting mABs (particularly clone P67.6) as well as mABs that address PD-L1 were reported to trigger internalization of their target antigens.^{224,259,260} Thus CiTE antibody, sctb and control molecules were investigated regarding their potency to internalize upon binding to MOLM-13:PD-L1 cells. As readout after incubation, remaining molecules on the target cell surface were quantified (Figure 13). The PD-1_{ex.} α CD3 control was excluded due to its low binding affinity to the target cells.

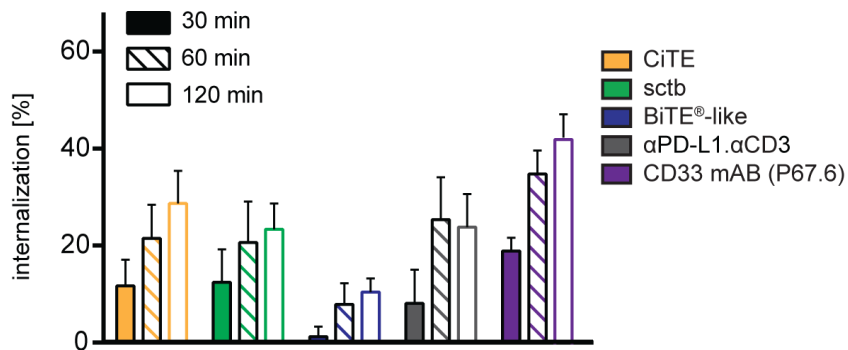


Figure 13: Internalization of CiTE antibody and sctb on PD-L1⁺ AML cells.

Internalization of CiTE antibody, sctb and controls on MOLM-13:PD-L1 cells at 15 ng/ μ l concentration as determined by flow cytometry. Graphs show mean values of five independent experiments with SEM as error bars.

CiTE and sctb revealed similar internalization rates. After 30 min of incubation, $11.7 \pm 5.4\%$ of CiTE and $12.4 \pm 6.8\%$ of sctb were internalized, after 60 min $21.5 \pm 6.9\%$ and $20.7 \pm 8.5\%$, and

RESULTS

after 120 min $28.7 \pm 6.7\%$ and $23.4 \pm 5.3\%$, respectively. In comparison, the bivalent CD33 mAB showed $42.3 \pm 4.8\%$ of internalization after 120 min, which is in the range of published data.²⁶¹ Interestingly, CiTE antibody and sctb but also α PD-L1. α CD3 revealed higher internalization rates than the BiTE[®]-like molecule that lacks the checkpoint blocking module. This leads to the conclusion that in CiTE and sctb, PD-L1 binding might increase internalization compared to CD33 monotargeting.

4.4.4. CiTE-mediated PD-L1 blockade on AML cells

CiTE antibody and sctb binding to AML cells was expected to block the interaction of PD-1 with PD-L1 and thus to interfere with PD-1 signaling in the T cell. The CiTE molecule was intended to target AML cells by its high-affinity CD33 scFv, which leads to an avidity-dependent local PD-L1 blockade by PD-1_{ex}. Due to its low affinity, we hypothesized that PD-1_{ex} is not sufficient to induce checkpoint blockade on single-positive cells. To this end, MOLM-13:PD-L1 cells were incubated with saturating concentrations of CiTE, sctb and controls. A PD-L1 mAB (clone MIH1) that competes with PD-1_{ex} and the PD-L1 scFv for their binding sites was applied and binding was determined by flow cytometry (Figure 14). The detection of cell-bound molecules revealed comparable binding of CiTE antibody, sctb, BiTE[®]-like molecule as well as α PD-L1. α CD3, whereas PD-1_{ex}. α CD3 binding was weaker due to its low affinity (Figure 14 A). The readout of the PD-L1 mAB as a measure for accessible PD-L1 binding sites demonstrated a CiTE-mediated blockade of a significant proportion of PD-L1 surface molecules, whereas the high-affinity sctb led to complete blockade (Figure 14 A, B). Investigation of the high-affinity α PD-L1. α CD3 showed that sole binding by the PD-L1 scFv is sufficient to occupy PD-L1 sites completely, whereas the low-affinity PD-1_{ex}. α CD3 was not able to interact with PD-L1 by itself. These findings suggest that PD-1_{ex}-mediated PD-L1 blockade by the CiTE antibody is strictly dependent on the avidity contribution of the high-affinity tumor-targeting arm. Thereby, the local PD-1_{ex} concentration (i.e. residence time) is increased at the target cell surface, which is necessary for efficient PD-L1 binding. However, since the binding affinity of PD-1_{ex} is weak, CiTE-mediated blockade was not as strong as the blockade induced by the sctb. Similar results were obtained for the investigation of binding competition with a low-affinity PD-1_{ex}-Fc (data not shown).

RESULTS

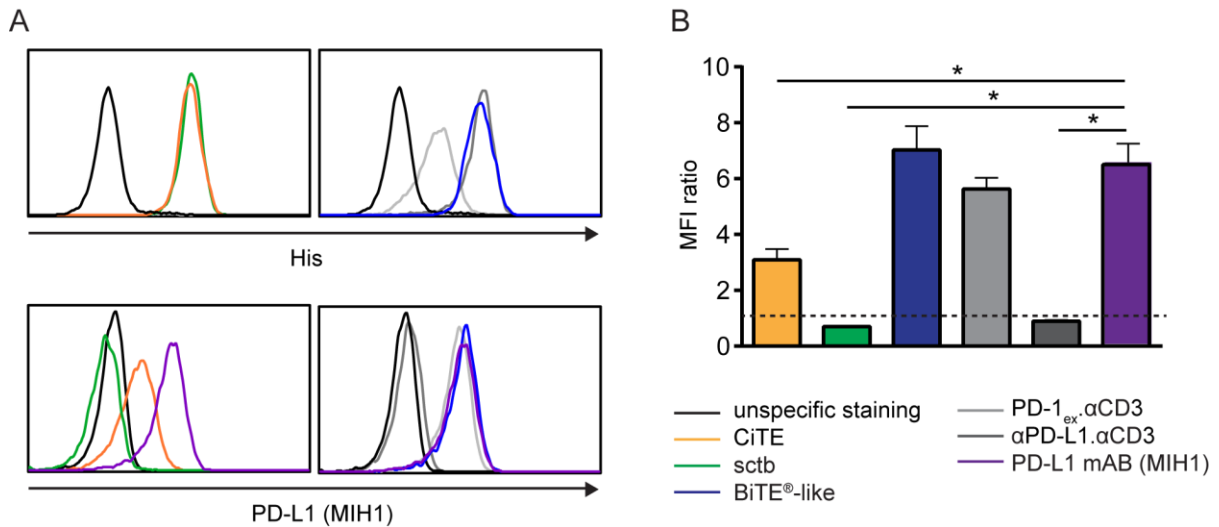


Figure 14: Blockade of PD-L1 accessibility on MOLM-13:PD-L1 cells.

Blocking assay was performed by sequential administration of 15 ng/μl CiTE antibody, sctb or controls and PD-L1 mAB (MIH1) to MOLM-13:PD-L1 cells. (A) Binding of CiTE, sctb and controls as detected by a secondary antibody (His) and binding of PD-L1 mAB. Histograms show one out of three independent experiments with similar results. (B) MFI ratios of PD-L1 mAB binding. Dashed line indicates an MFI ratio of 1. The graph shows mean values of three independent experiments with SEM as error bars.

4.5. Functional characterization of CiTE antibody on cell lines

4.5.1. Activation of resting T cells

An important requirement for T cell engagers is to activate T cells exclusively upon physical linkage to tumor cells. This is highly relevant since the CD3 mAB OKT3 (i.e. muronomab; Orthoclone OKT3[®]) leads to basal T cell activation that can cause CRS in patients.^{73,262,263} Thus, the impact of the molecules on resting T cells was investigated in the presence and absence of AML cells. For this purpose, human healthy donor T cells were incubated with MOLM-13 or MOLM-13:PD-L1 cells at saturating concentrations of the molecules. T cell activation was determined by quantifying CD69 and CD25 (i.e. IL-2 receptor α-chain) expression as well as PD-1 levels by flow cytometry (Figure 15). In the presence of target cells, CiTE antibody, sctb and BiTE[®]-like molecule induced the upregulation of CD69, CD25 and PD-1 on T cells. Due to the saturating conditions of the experimental system, measured expression levels were similar irrespective of PD-L1 expression. Even the high-affinity αPD-L1.αCD3 induced an activation on both cell lines with only slightly higher levels on MOLM-13:PD-L1 cells. As it is described that AML cell lines are able to express PD-L1 in the presence of IFN-γ, this observation is most

RESULTS

probably due basal PD-L1 expression on MOLM-13 cells.¹⁸⁹ Similar tendencies were observed for PD-1_{ex}. α CD3, however, the effects were minor due to its low affinity towards the target cells. When evaluating the sole effect of the molecules on T cells without the addition of target cells, no upregulation of CD69 and CD25 could be detected, whereas both markers were clearly expressed in the positive control. Notably, the specificity control did not affect T cells in any condition. Thus, monovalent CD3-targeting does not *per se* induce T cell activation. Instead, a physical crosslink between T cell and leukemic cell is crucial, which might prevent unwanted T cell activation and associated cytokine release in healthy tissue.

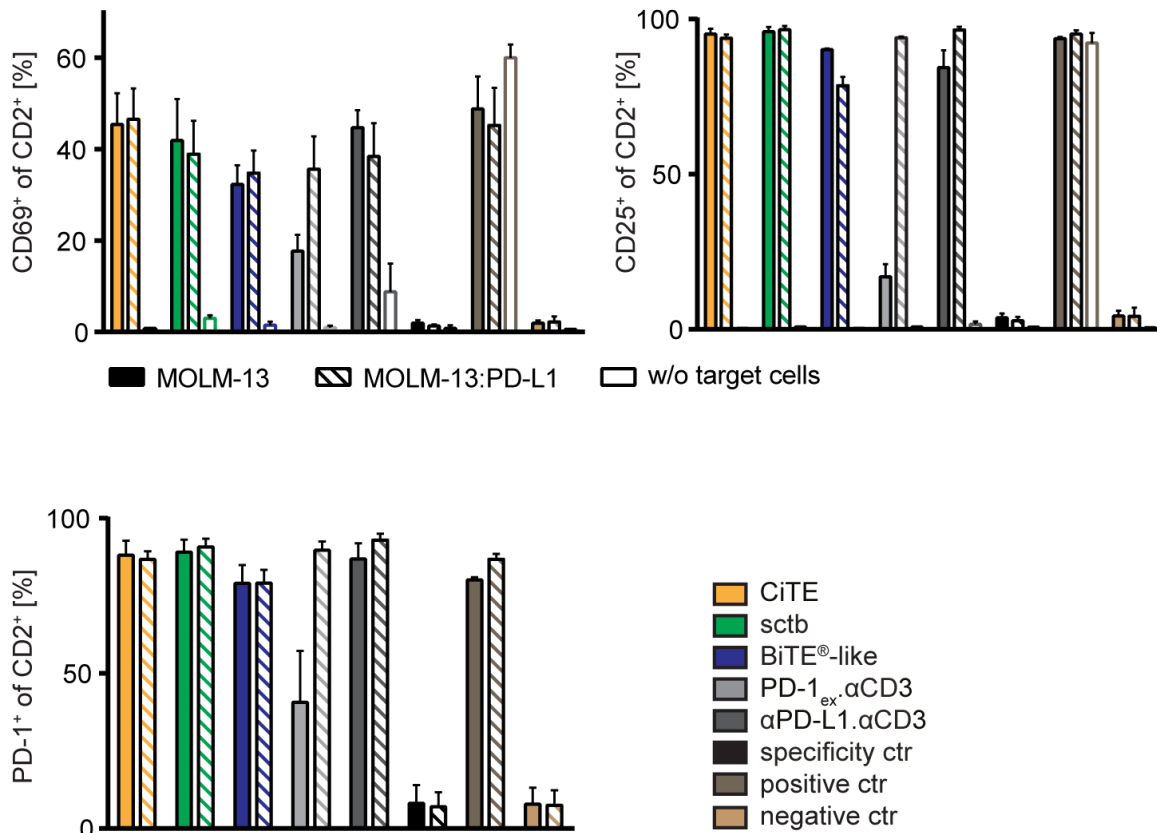


Figure 15: CiTE- and sctb-mediated activation of non-stimulated T cells.

Non-stimulated HD T cells were incubated with 5 nM of molecules in the presence or absence of MOLM-13 or MOLM-13:PD-L1 target cells at an E:T ratio of 2:1. After 96 h, activation markers were detected by flow cytometry. Bar charts show mean values of three independent experiments with SEM as error bars.

4.5.2. Induction of cytotoxic lysis of AML cells by pre-activated T cells

Similar to BiTE[®] molecules, the intended functionality of CiTE antibody and sctb is to redirect antigen-experienced T cells to AML cells irrespective of their antigen specificity.⁶⁹ Redirected

RESULTS

lysis assays with pre-stimulated T cells were chosen as initial evaluation to analyze CiTE-mediated induction of specific T cell effector functions. MOLM-13:PD-L1 target cells were Calcein AM-labeled prior to the assay and redirected lysis was determined by quantifying the released Calcein in the supernatant. Figure 16 displays the dose-dependent increase of specific lysis for all molecules besides the specificity control, indicating the requirement of binding to both target and effector cell for the exertion of T cell cytotoxicity.

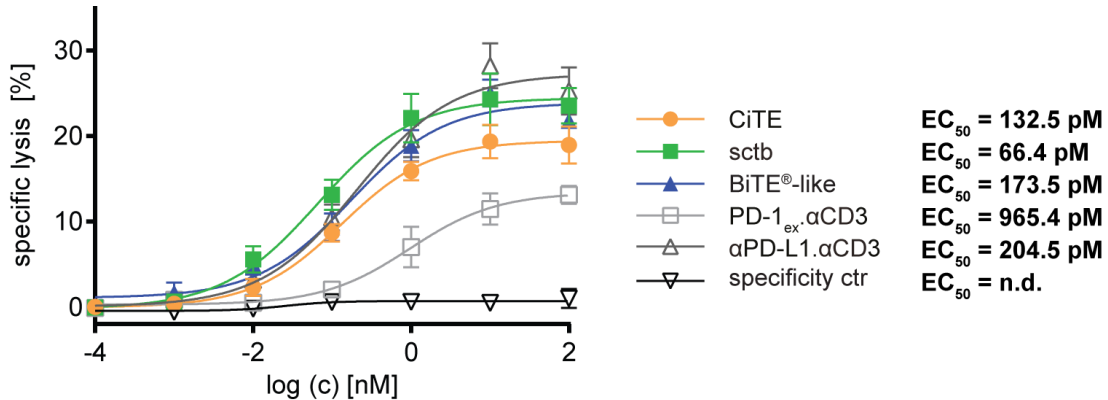


Figure 16: Cytotoxic lysis of PD-L1⁺ AML cells by CiTE antibody, sctb and control molecules.

Redirected lysis assays of MOLM-13:PD-L1 target cells were performed for 4 h at an E:T ratio of 5:1 using IL-2 pre-activated HD T cells. Graph shows mean values of three independent experiments with SEM as error bars. n.d., not determined.

For CiTE, sctb as well as BiTE[®]-like molecule and αPD-L1.αCD3, specific lysis at 100 nM concentration was determined to be rather low in this setting with a maximum of 25.3% for αPD-L1.αCD3. This is most probably due to the short incubation time and to cell line-specific characteristics and has already been described previously.^{87,261} Notably, CiTE antibody, sctb, BiTE[®]-like molecule and αPD-L1.αCD3 revealed comparable dose-response curves. Also calculated EC₅₀ values were of similar magnitude with 132.5 pM for CiTE, 66.4 pM for sctb, 173.5 pM for the BiTE[®]-like molecule and 204.5 pM for αPD-L1.αCD3. PD-1_{ex}.αCD3 showed a lower EC₅₀ value of 965.4 pM and a decreased maximum specific lysis due to its low affinity to the target cells, which has already been described in binding analyses.

These findings reflect the ability of the molecules to induce redirected lysis of AML cells. However, the use of pre-activated T cells as effectors in a time range of a few hours seems to be too insensitive to investigate effects that depend on avidity or immune checkpoint blockade.

RESULTS

4.5.3. CiTE-mediated increase in redirected lysis of PD-L1⁺ AML cell lines

In order to evaluate the ability of the molecules to engage resting T cells, in a further setting non-stimulated T cells were used as effectors and their cytolytic activity was investigated. To this end, healthy donor T cells were incubated with different AML target cell lines and increasing concentrations of CiTE antibody, sctb and control molecules and live target cells were quantified by flow cytometry. More precisely, CD33^{bright} MOLM-13 and MOLM-13:PD-L1 cells were detected as CD33⁺CD2⁻ population, whereas the CD33^{dim} OCI-AML3 and OCI-AML3:PD-L1 cells were labeled with PKH67 prior to the experiment and the number of PKH67⁺CD2⁻ cells was monitored. The gating strategy of this assay is indicated in Figure 17. In the forward scatter (FSC)/side scatter (SSC) plot, a gate was set comprising lymphocyte and target cell populations. A second gate was restricted to live cells, and in a third step, the target cells were determined as CD2⁻CD33⁺ or CD2⁻ PKH67⁺ population. To allow quantification of the events without the application of counting beads, absolute target cell numbers were measured within a restricted time frame of 60 sec and normalized to the negative control.

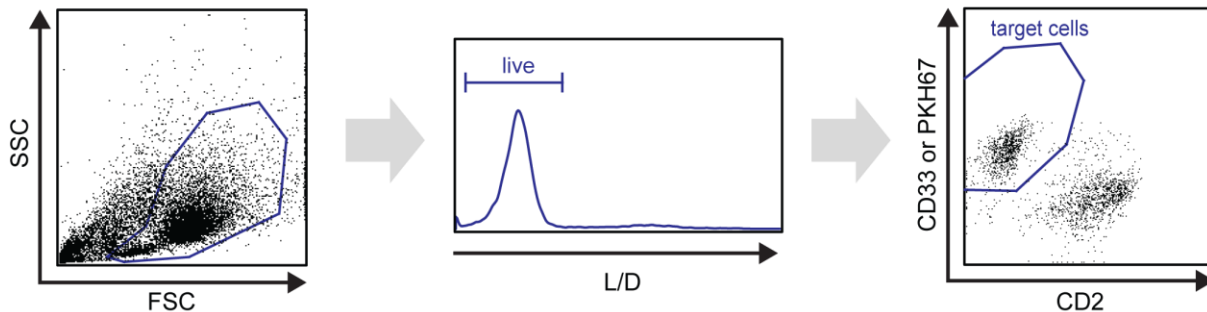


Figure 17: Gating strategy of redirected lysis assays with non-stimulated T cells.

Lymphocytes and target cells were separated in the FSC/SSC plot. Remaining target cells were gated as live CD33⁺CD2⁻ or PKH67⁺CD2⁻ population. FSC, forward scatter; SSC, side scatter; L/D, LIVE/DEAD stain.

To determine the influence of PD-L1 expression on CiTE- and sctb-induced cytotoxicity, the effects on CD33⁺ and CD33⁺PD-L1⁺ target cells were investigated in parallel. Since AML patients demonstrate a high heterogeneity in their CD33 expression levels, MOLM-13 and MOLM-13:PD-L1 as well as OCI-AML3 and OCI-AML3:PD-L1 target cells were selected to analyze the impact of differential CD33 expression (Figure 18 and Figure 19).⁷⁹ At high concentrations all molecules aside from the specificity control induced complete eradication of the target cell lines independent of PD-L1 and CD33 expression levels.

RESULTS

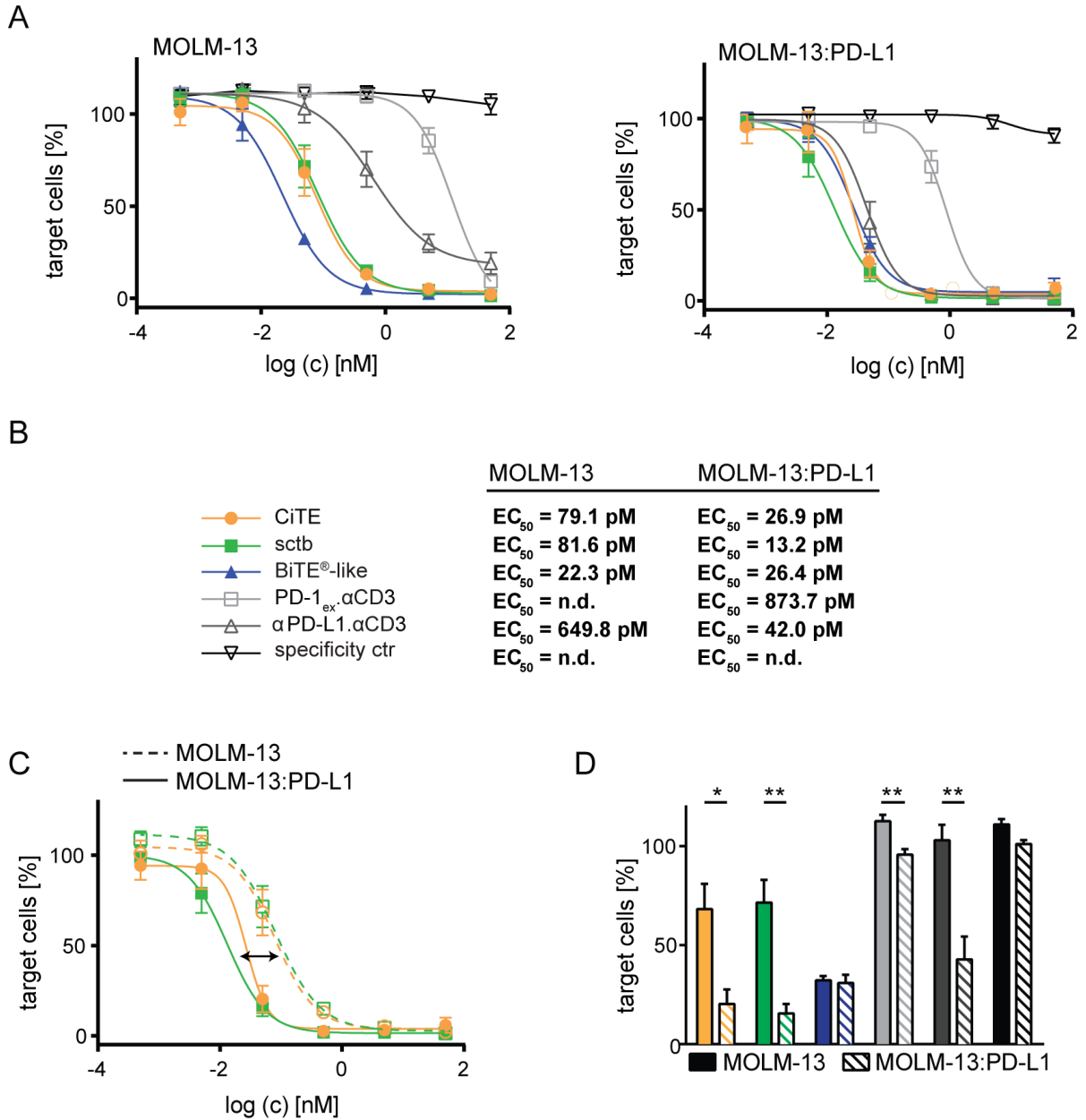


Figure 18: Redirected lysis of MOLM-13 and MOLM-13:PD-L1 cells by non-stimulated T cells.

(A) Dose-dependent redirected lysis of MOLM-13 or MOLM-13:PD-L1 cells by T cells as induced by CiTE antibody, sctb and control molecules. (B) EC_{50} values as calculated. (C) Direct comparison of CiTE- and sctb-induced redirected lysis of MOLM-13 and MOLM-13:PD-L1 target cells. (D) Cytotoxicity of the two cell lines at 50 pM concentration, Experiments were performed for 72 h at an E:T ratio of 2:1 using non-stimulated HD T cells. The graphs show mean values of five independent experiments with SEM as error bars.

The evaluation of the dose-response curves on MOLM-13 cells indicated a concentration-dependent cytolysis, at which the molecules differed in their efficiency (Figure 18 A). The BiTE[®]-like molecule indicated the highest potency to induce cytolysis, whereas CiTE antibody and sctb revealed a slightly worse performance. Also α PD-L1. α CD3 and to a lower extent PD-1_{ex}. α CD3

RESULTS

induced cytotoxicity at elevated concentrations. As previously described, this was most probably due to a presumably low PD-L1 expression on MOLM-13 cells.^{189,190} Weak effects of PD-1_{ex}. α CD3 are attributed to its low binding affinity to PD-L1.

When comparing MOLM-13 and MOLM-13:PD-L1 target cells, the BiTE[®]-like molecule demonstrated a similar effect on the two cell lines. Contrarily, the trispecific molecules as well as α PD-L1. α CD3 indicated a shift towards lower effective concentrations. Calculated EC₅₀ values (Figure 18 B) are in the picomolar range, and in the presence of PD-L1 they shift from 79.1 pM to 26.9 pM for the CiTE (5-fold decrease) and from 81.6 pM to 13.2 pM for the sctb (7-fold decrease). In the direct overlay of dose-response curves in the presence and absence of PD-L1, the same effect can be observed as shift to lower concentrations (Figure 18 C). At 50 pM, which approximately corresponds to EC₅₀ values, a significant decrease of PD-L1⁺ target cells (from 68.3 \pm 12.8% to 20.4 \pm 7.3% for the CiTE antibody and from 71.6 \pm 11.5% to 15.6 \pm 4.8% for the sctb) was monitored, whereas no such change occurred upon application of the BiTE[®]-like molecule (Figure 18 D). This effect is most probably due to avidity-dependent binding and notably it seems to be independent of the affinity of the checkpoint blocking module. Besides that, the high efficiency of α PD-L1. α CD3 indicates that the high-affinity PD-L1 scFv is sufficient to target PD-L1⁺ cells without a second binding module, whereas the low-affinity PD-1_{ex} requires a tumor-targeting arm to enable efficient binding.

Evaluation of CiTE, sctb and controls on CD33^{dim} OCI-AML3 and OCI-AML3:PD-L1 cells led to similar observations as for the CD33^{bright} target cells (Figure 19). However, there were slight differences regarding the range of EC₅₀ values, the concentration shift and the behavior of the bispecific molecules. In this system, the efficient concentrations were approximately 10-fold lower compared to MOLM-13 cells. This is reflected in the EC₅₀ values, which are determined to be 20.8 pM on OCI-AML3 and 2.3 pM on OCI-AML3:PD-L1 cells for the CiTE (15-fold decrease), and 27.4 pM and 1.9 pM for the sctb, respectively, (20-fold decrease) (Figure 19 B). In the absence of PD-L1, the BiTE[®]-like molecule showed a similar dose-response curve as the trispecific molecules, whereas it was clearly outpaced by CiTE antibody and sctb upon PD-L1 expression (Figure 19 A, B). Taken together, CiTE antibody and sctb induced a decrease of EC₅₀ values upon PD-L1 expression on both CD33^{dim} and CD33^{bright} cells. Since PD-L1 expression does not have an impact on the performance of the BiTE[®]-like molecule, this effect is most probably due to avidity-dependent binding.

RESULTS

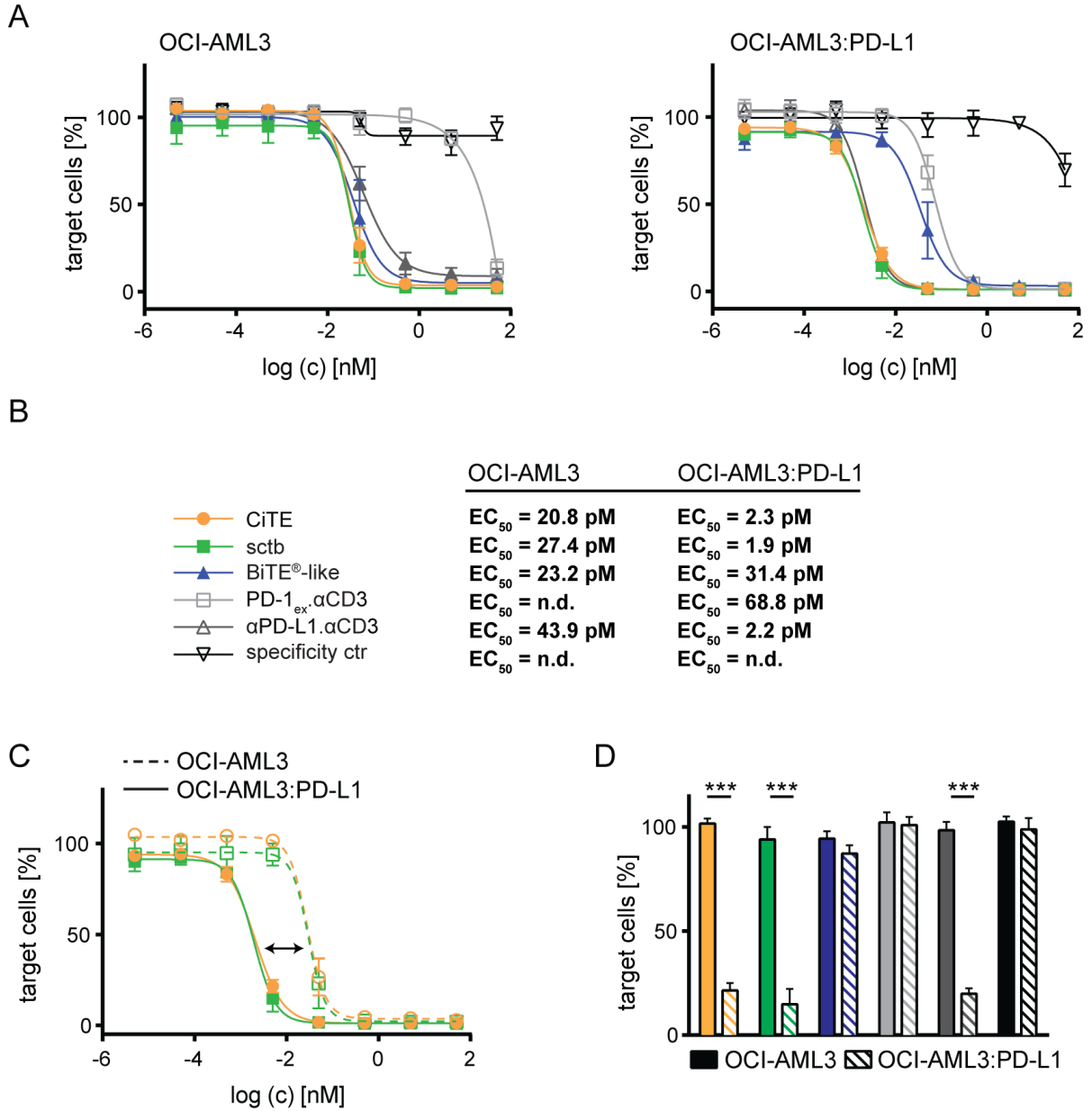


Figure 19: Redirected lysis of OCI-AML3 and OCI-AML3:PD-L1 cells by non-stimulated T cells.

(A) Dose-dependent redirected lysis of OCI-AML3 or OCI-AML3:PD-L1 cells by T cells as induced by CiTE antibody, sctb and control molecules. (B) EC₅₀ values as calculated. (C) Direct comparison of CiTE- and sctb-induced redirected lysis of OCI-AML3 and OCI-AML3:PD-L1 target cells. (D) Cytotoxicity of the two cell lines at 5 pM concentration, Experiments were performed for 72 h at an E:T ratio of 2:1 using non-stimulated HD T cells. The graphs show mean values of four independent experiments with SEM as error bars.

Sterical differences between the molecular scaffolds may be responsible for the more efficient cytolysis of MOLM-13 cells by the BiTE[®]-like molecule than the trispecific molecules. These might be particularly advantageous at high CD33 expression levels, since on OCI-AML3 cells such differences were not observed. We hypothesized that, depending on the targeted tumor, a BiTE[®]

RESULTS

format might be beneficial for the formation of a cytolytic synapse due to more favorable steric properties. Another possibility is, that the influence of an N-terminal domain attached to the CD3 ϵ scFv per se affects its functionality. To address this question, a trispecific control molecule was generated and evaluated in comparison to the BiTE[®]-like molecule (section 4.5.5).

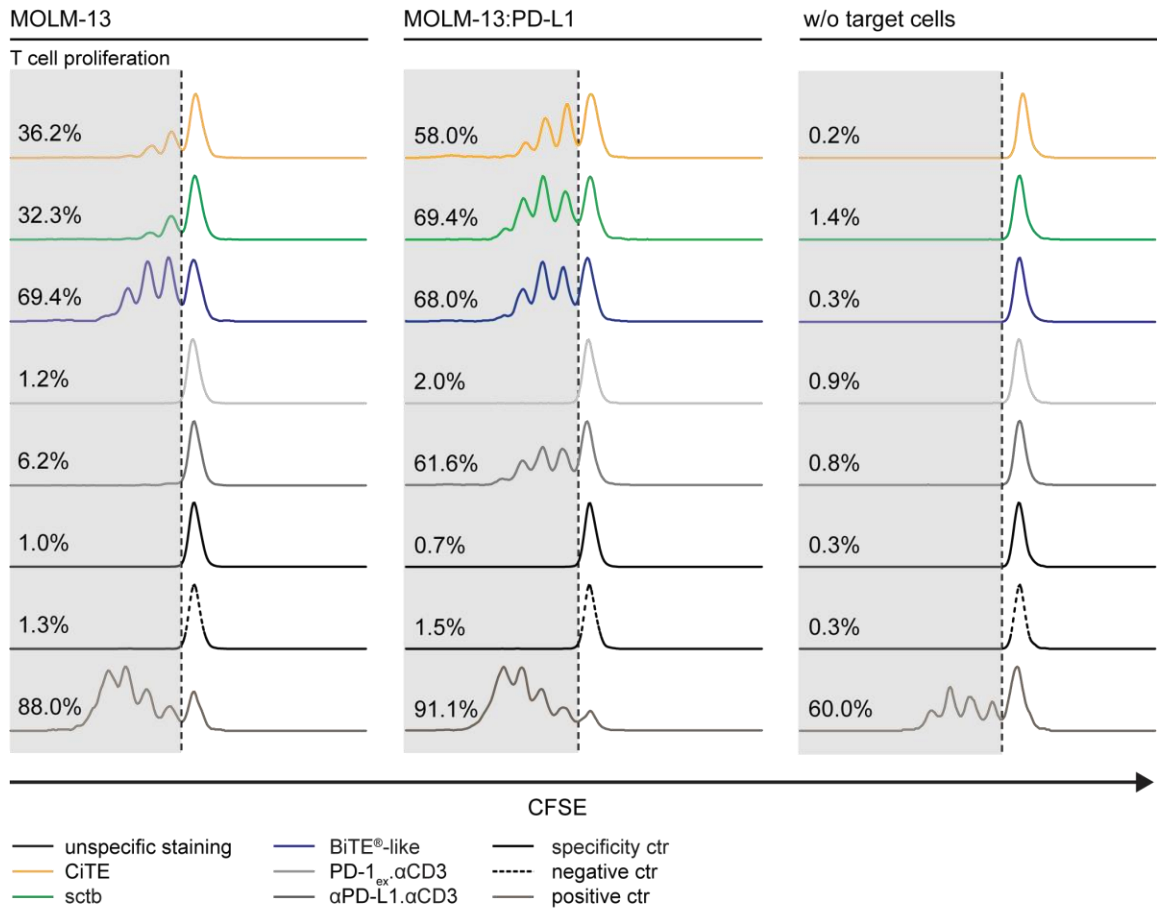
4.5.4. CiTE-mediated increase in T cell proliferation

Another important prerequisite for a T cell engager is the induction of T cell proliferation to expand the available T cell effector pool and multiply the effector cell population as well as the immune response as a whole. Therefore, CFSE-labeled non-stimulated healthy donor T cells were incubated with either MOLM-13 vs. MOLM-13:PD-L1 cells or OCI-AML3 vs. OCI-AML3:PD-L1 cells and increasing concentrations of CiTE antibody, sctb and controls (Figure 20). Additionally, the impact of the molecules on proliferation without target cells was analyzed. Figure 20 A shows that CiTE antibody, sctb and BiTE[®]-like molecule already induced T cell proliferation of 36.2%, 32.3% and 69.4%, respectively, at a low concentration of 5 pM and in the presence of MOLM-13 target cells. PD-1_{ex}. α CD3 and α PD-L1. α CD3 did not reveal an effect in the absence of PD-L1 expression. In the presence of MOLM-13:PD-L1 cells, however, CiTE and sctb treatment increased T cell proliferation and reached levels of 58.0% and 69.4%, whereas the BiTE[®]-like molecule displayed an almost unchanged level of 68.0%. The high-affinity α PD-L1. α CD3 induced 61.6% proliferated T cells in the presence of MOLM-13:PD-L1 target cells. PD-1_{ex}. α CD3 did not have an effect at the displayed concentration, which is likely due to its weak binding affinity to PD-L1. All of the indicated molecules led to at least three generations of T cells. When analyzing T cells without target cells, none of the molecules was able to induce T cell proliferation by the sole interaction with CD3. These findings support the previous observations that CiTE antibody and sctb exclusively activate T cells upon crosslinking to target cells.

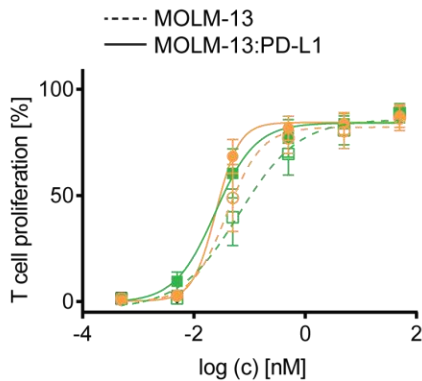
As already observed for cytotoxicity induction, CiTE- and sctb- induced T cell proliferation was also increased on AML cell lines that additionally expressed PD-L1, which we attribute to avidity-dependent binding (Figure 20 B, C). Notably, this effect was more pronounced at low CD33 levels. Since the performance of CiTE and sctb was similar, the potency to induce T cell proliferation seems to be independent of the affinity of the checkpoint blocking modules.

RESULTS

A



B



C

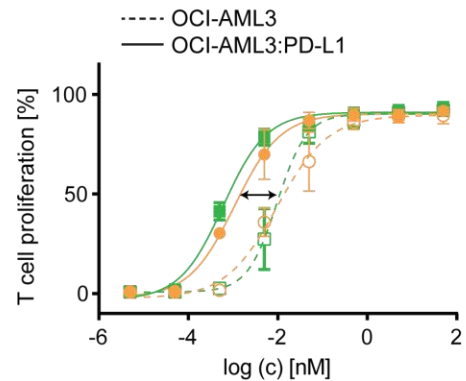


Figure 20: Dose-dependent proliferation of non-stimulated T cells.

(A) T cell proliferation in the presence of MOLM-13 and MOLM-13:PD-L1 cells at 5 pM concentration of CiTE antibody, sctb and control molecules or in the absence of target cells. Histograms show one out of three to four experiments with similar results. (B) Direct comparison of CiTE- and sctb-induced T cell proliferation on MOLM-13 and MOLM-13:PD-L1 and (C) OCI-AML3 and OCI-AML3:PD-L1 target cells. Experiments were performed for 96 h at an E:T ratio of 2:1 using CFSE-labeled non-stimulated HD T cells. The graphs show mean values of three to four independent experiments with SEM as error bars.

RESULTS

4.5.5. Sterical influence of N-terminal module in CiTE antibody

As highlighted in sections 4.5.3. and 4.5.4., the BiTE[®]-like molecule differed from CiTE antibody and sctb regarding the induction of cytotoxicity and T cell proliferation. Although all molecules possess an identical CD3 ϵ scFv, in the presence of MOLM-13 target cells the BiTE[®]-like molecule revealed a superior performance compared to the trispecific molecules (Figure 18 A and 20 A). On CD33^{dim} OCI-AML3 cells, these effects were not observed (Figure 19 A). We hypothesized that the deviations might be due to intramolecular properties and are a result of the additional modules that are fused to the N-terminus of the CD3 ϵ scFv. Thus, the binding of the CD3 ϵ scFv might be altered or the formation of the cytolytic synapse could be impaired due to partial sterical hindrance. To address this question, an α Her2. α CD3. α CD33 control was generated and compared to the BiTE[®]-like molecule with the intention to mimic the geometry of CiTE antibody and sctb. The attachment of a non-binding Her2 scFv to the N-terminus of the molecule induced a shift in the dose-response in redirected lysis and T cell proliferation assays to higher concentrations, indicating a worse performance of the molecule (Figure 21). This finding demonstrates that trispecific and bispecific formats might differ in their efficiency to engage T cells.

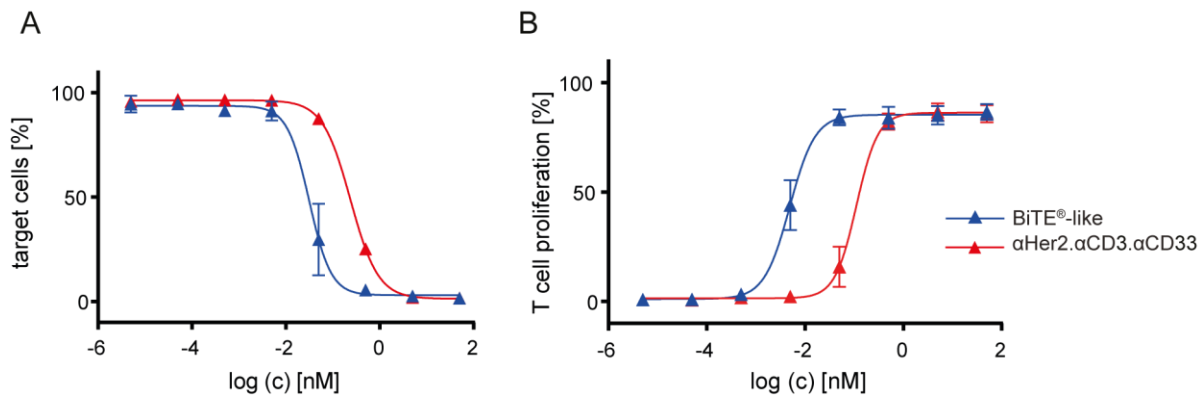


Figure 21: Comparison of α Her2. α CD3. α CD33 and BiTE[®]-like molecule.

The control α Her2. α CD3. α CD33 and the BiTE[®]-like molecule were compared in (A) 72 h redirected lysis assays and (B) 96 h T cell proliferation assays. HD T cells and OCI-AML3:PD-L1 cells were incubated at an E:T ratio of 2:1. Mean values of four (A) and three (B) independent experiments are shown. Error bars represent SEM.

4.5.6. CiTE-mediated increase in proinflammatory cytokine secretion

To investigate CiTE- and sctb-mediated redirection of T cells comprehensively, the release of proinflammatory cytokines was analyzed as a further hallmark of T cell activation. Therefore, IFN- γ and IL-2 release were quantified in the presence of MOLM-13 or MOLM-13:PD-L1 target

RESULTS

cells. To pay special attention to donor-dependent variations, IFN- γ release of three different T cell donors was determined separately. Cytokine levels were evaluated as fold change between the two cell lines to display the influence of PD-L1 expression, or as absolute levels on MOLM-13:PD-L1 cells (Figure 22).

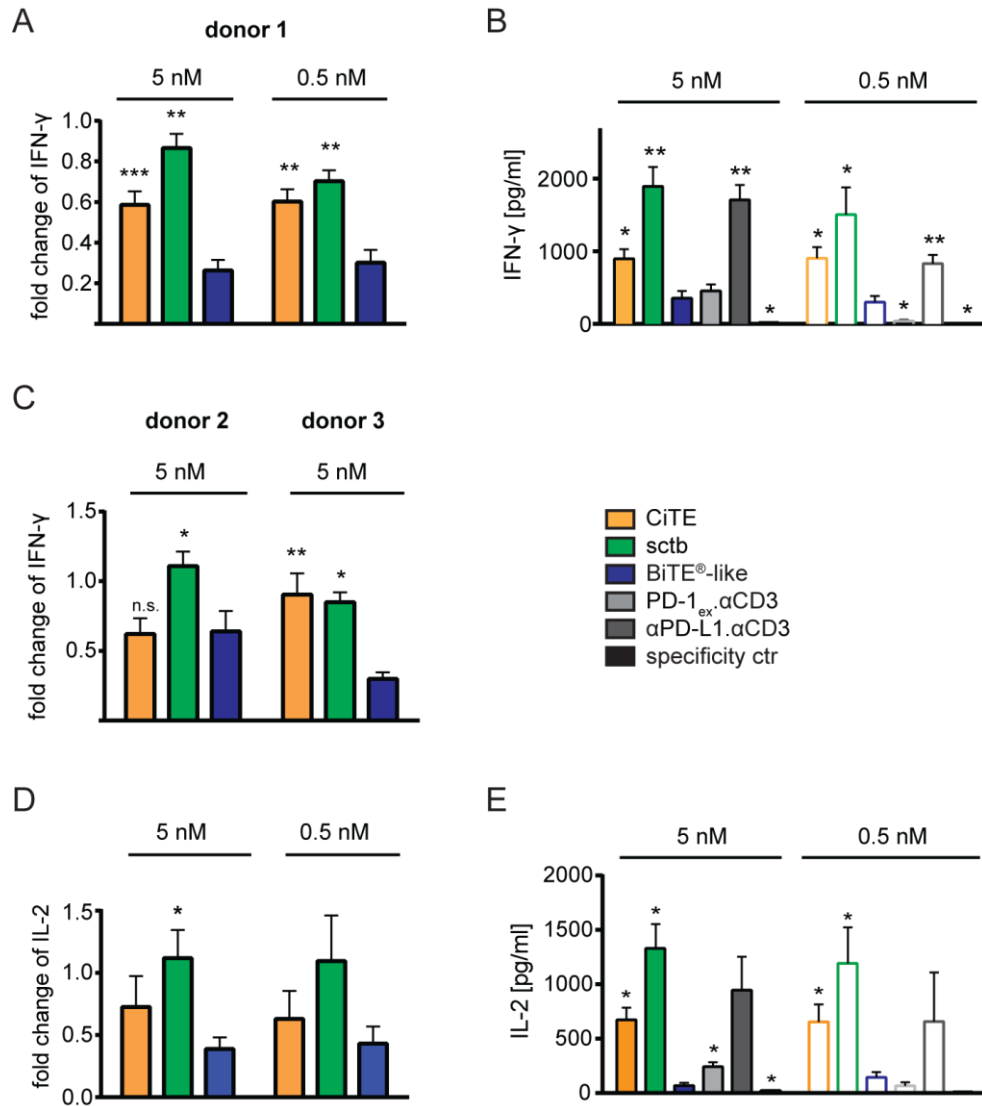


Figure 22: CiTE- and sctb-induced IFN- γ and IL-2 release.

(A) Fold change in IFN- γ levels (MOLM-13:PD-L1/MOLM-13) using T cells derived from donor 1. (B) Absolute IFN- γ levels on MOLM-13:PD-L1 target cells. (C) Fold change in IFN- γ levels (MOLM-13:PD-L1/MOLM-13) using T cells from donors 2 and 3. (D) Fold change in IL-2 levels (MOLM-13:PD-L1/MOLM-13). (E) Evaluation of absolute IL-2 levels on MOLM-13:PD-L1 target cells. Experiments were performed for 72 h at an E:T ratio of 2:1 using non-stimulated HD T cells. Bar charts of IFN- γ evaluation depict mean values of five independent experiments of the same donor, bar charts of IL-2 evaluation display four independent experiments with different HDs. Error bars indicate SEM. Statistics refer to the single application of the BiTE[®]-like molecule.

RESULTS

Notably, in the presence of the BiTE[®]-like molecule, PD-L1 led to a decrease in IFN- γ and IL-2 release (Figure 22 A, C, D). This reflects the inhibitory influence of the PD-1/PD-L1 interaction on T cells. IFN- γ quantification indicated that with effector cells from donors 1 and 3, both CiTE antibody and sctb induced a significantly higher fold change than the BiTE[®]-like molecule, whereas T cells from donor 2 revealed only a sctb-mediated increase (Figure 22 A, C). Thus, the heterogeneity between donors is expected to influence the efficiency of the molecules.

Since many clinical trials currently focus on the combination of checkpoint blockade and tumor-targeting agents, we combined the BiTE[®]-like molecule with the separate checkpoint blocking modules PD-1_{ex}-Fc fusion and PD-L1 scFv (Figure 23). Additionally, commercial PD-1 and PD-L1 blocking mABs were included.

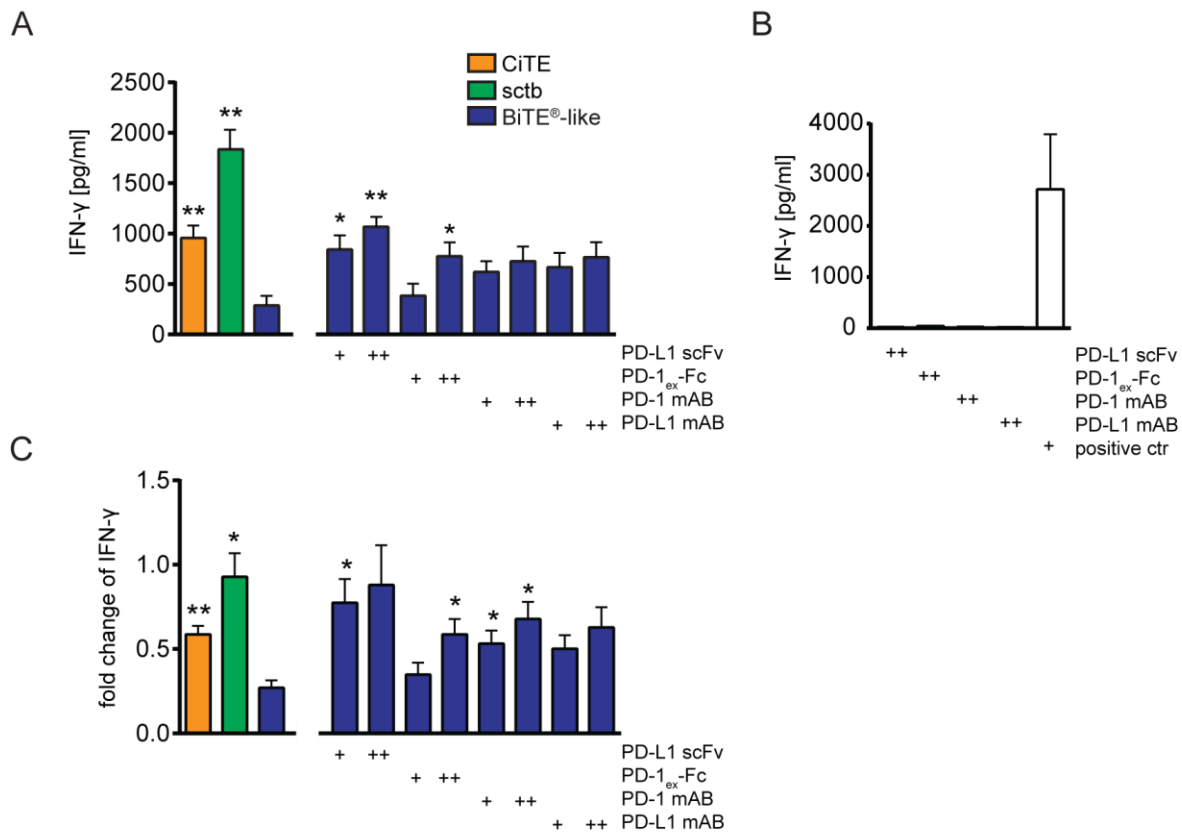


Figure 23: CiTE- and sctb-induced IFN- γ release in comparison to combinations with blocking agents.

(A) Absolute IFN- γ levels on MOLM-13:PD-L1 cells in the presence of 5 nM CiTE antibody, sctb, BiTE[®]-like molecule or combinations of BiTE[®]-like molecule with different PD-1/PD-L1 blocking agents at either equimolar ratio (+) or 50-fold surplus (++). (B) IFN- γ release in the presence of 250 nM blocking agents and MOLM-13:PD-L1 cells. (C) Fold change in IFN- γ levels (MOLM-13:PD-L1/MOLM-13). Experiments were performed for 72 h at an E:T ratio of 2:1 using non-stimulated HD T cells. Bar charts depict mean values of four independent experiments with SEM as error bars. Statistics refer to the single application of the BiTE[®]-like molecule.

RESULTS

The blocking agents were applied at equimolar concentration or 50-fold surplus, and control experiments confirmed that the molecules did not induce cytokine release by themselves (Figure 23 B). The combination of BiTE[®]-like molecule and PD-L1 scFv was able to induce a significant increase in IFN- γ release, whereas the low-affinity PD-1_{ex}-Fc only lead to elevated cytokine levels when applied in high excess (Figure 23 A). The addition of PD-1 and PD-L1 blocking mABs induced a similar response as the scFv. Notably, the CiTE antibody was able to raise IFN- γ levels to a similar extent than could be achieved with BiTE[®]-like molecule and a surplus of high-affinity blocking agents. Furthermore, not only the sctb but also the addition of the PD-L1 scFv induced similar IFN- γ levels in the presence and absence of PD-L1 (i.e. a fold change of ~1), which indicates complete blockade of the inhibitory axis (Figure 23 C). Still, the sctb was able to cause the highest absolute cytokine release on MOLM-13:PD-L1 cells (Figure 23 A). We thus assume that the CiTE- and sctb-mediated T cell activation is not only due to PD-L1 blockade but also to avidity-dependent binding. However, the individual contributions of these two effects could not be conclusively determined.

4.5.7. Selective lysis of CD33⁺PD-L1⁺ target cells

An important feature of the CiTE molecule in comparison to commercial PD-1 or PD-L1 blocking antibodies is its low-affinity for the inhibitory checkpoint ligand. We hypothesize to thereby circumvent systemic PD-L1-targeting and to avoid damage to PD-L1⁺ non-AML cells. To investigate potential on-target off-leukemia effects *in vitro*, preferential lysis was analyzed in a mixed target cell population of HEK293:PD-L1 and HEK293:CD33:PD-L1 cells, of which one cell line was labeled with Calcein AM. After incubation with pre-activated healthy donor T cells and increasing concentrations of molecules, specific lysis was determined by fluorescence readout of the released dye in the supernatant. The sctb mediated dose-dependent elimination of HEK293:PD-L1 target cells whereas no lysis could be observed when applying the CiTE antibody or BiTE[®]-like molecule (Figure 24 A). In contrast, HEK293:CD33:PD-L1 cells were depleted by all three molecules. Similar to the sctb, the high-affinity α PD-L1. α CD3 induced lysis of both target cell lines. PD-1_{ex}. α CD3 only led to elimination of target cells at elevated concentrations. This was also reflected in the direct comparison of specific lysis of PD-L1⁺ and CD33⁺PD-L1⁺ cells at 10 nM concentration (Figure 24 C). The sctb revealed killing of $24.5 \pm 4.4\%$ of HEK293:PD-L1 and $38.1 \pm 3.7\%$ of HEK293:CD33:PD-L1 cells, while CiTE and BiTE[®]-like molecule only mediated lysis of $38.4 \pm 3.7\%$ and $39.7 \pm 4.2\%$ of double-positive target cells, respectively. PD-L1⁺ cells

RESULTS

were only affected marginally. We assume that the increase of sctb-mediated lysis of double-positive targets is mainly due to an avidity effect. These results are a first proof that the PD-1_{ex} module in the CiTE antibody allows a high selectivity for CD33⁺PD-L1⁺ targets whereas the high-affinity PD-L1 scFv also addresses PD-L1⁺ cells that lack the expression of the leukemic antigen. *In vivo*, the administration of the CiTE antibody might therefore translate into a lowered risk to develop irAEs that are caused by systemic PD-L1 binding.

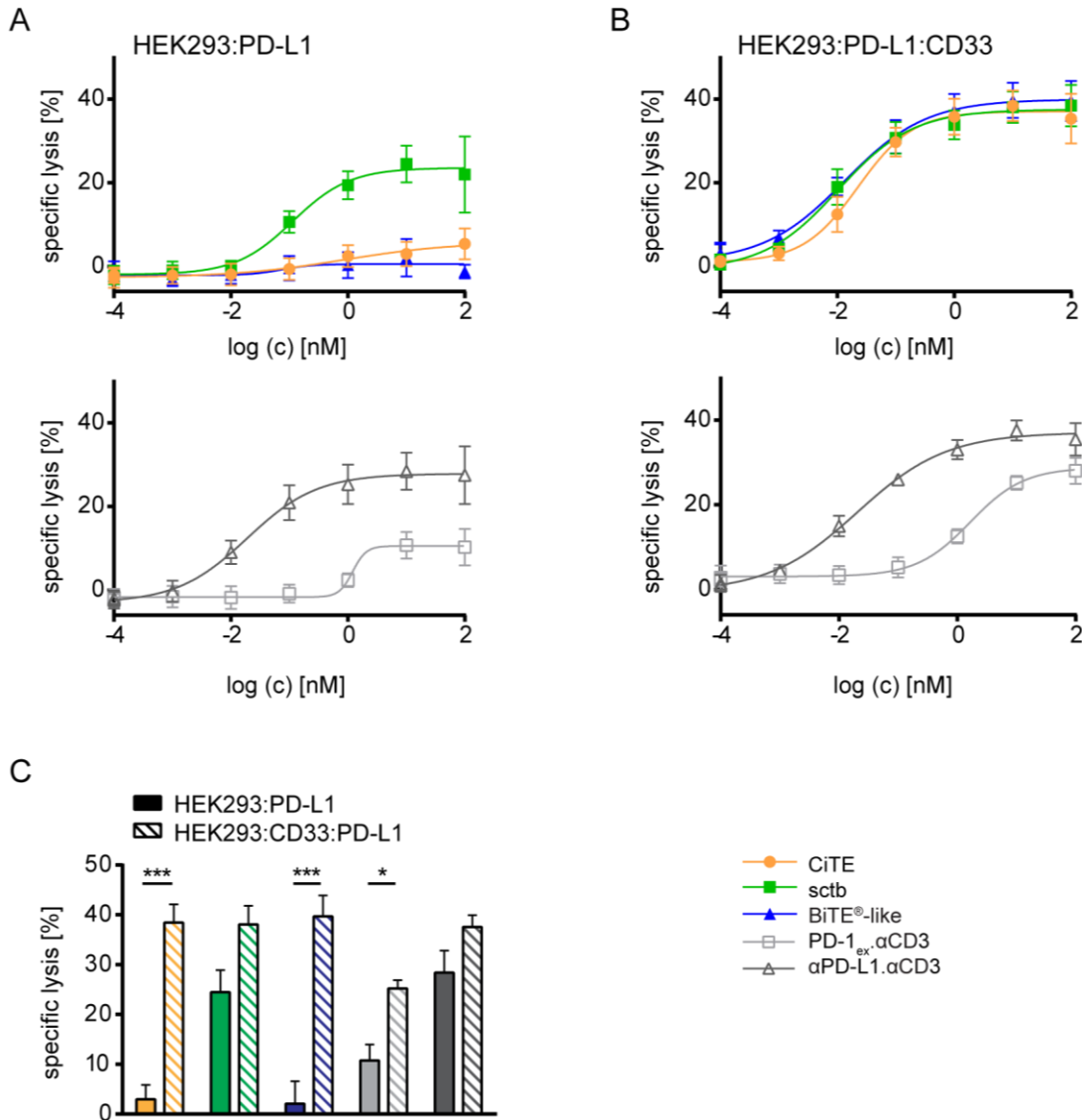


Figure 24: CiTE-induced preferential killing of CD33⁺PD-L1⁺ target cells.

(A) Preferential killing of HEK293:PD-L1 or (B) HEK293:CD33:PD-L1 in a mixed target cell population by pre-activated HD T cells and increasing concentrations of CiTE antibody, sctb or control molecules. (C) Specific lysis of HEK293:PD-L1 and HEK293:CD33:PD-L1 at 10 nM concentration of molecules. Experiments were performed for 4 h at an E:T ratio of 2:1. Graphs represent mean values of four independent experiments with SEM as error bars.

RESULTS

4.6. Selective lysis of primary AML patient samples

In the previous assays, the biological functionality of CiTE antibody and scTb was evaluated on cell lines. To provide clinically more relevant conditions, CiTE and scTb were further analyzed in an *ex vivo* co-culture of AML patient samples[§]. In a non-autologous setting, T cells were investigated regarding their PD-1 and AML cells regarding their PD-L1 expression. As a measure for T cell activation, IFN- γ levels were quantified in the supernatant.

Figure 25 A depicts the cytotoxic lysis of AML cells from an individual patient and illustrates the gating scheme for CD3⁺CD33⁻ T cells and CD3⁻CD33⁺ AML cells. On average, the CiTE revealed a slight increase in specific lysis compared to the BiTE[®]-like molecule, but only the scTb indicated a statistically significant benefit (Figure 25 B). This can be partially reasoned in the high heterogeneity between patients. Whereas the CiTE antibody was able to induce similar or superior AML cell lysis in 7 out of 8 patients (87.5%) compared to the BiTE[®]-like molecule, the scTb mediated an increased specific lysis in 8 out of 8 patients (100%) (Figure 25 C). Interestingly, the combination of the BiTE[®]-like molecule with a PD-L1 blocking mAb did not significantly increase target cell lysis in our setting. These results were also reflected in IFN- γ release (Figure 25 D).

On T cells, PD-1 levels were elevated in all conditions aside from the specificity control (Figure 25 E). The scTb triggered the highest PD-1 upregulation, and the CiTE slightly increased PD-1 levels compared to BiTE[®]-like molecule. The elevated PD-1 levels might be interpreted as reactive mechanism to an increased T cell activation as measured by elevated IFN- γ levels and cytotoxicity. Further, PD-L1 upregulation on AML cells could be detected in all conditions where the surface antigens were not masked by high-affinity blocking agents (Figure 25 F). Collectively, the CiTE antibody and to a higher extent the scTb were able to increase specific lysis of AML patient cells compared to the BiTE[®]-like molecule in a setting of adaptive immune resistance. Thus the two molecules might be an improvement to a BiTE[®]-like format with or without the combination with a PD-L1 mAb.

[§] Data were kindly provided by Christina Krupka, Laboratory of Marion Subklewe, Gene Center Munich, LMU München, Germany. Patient samples were provided by the Laboratory of Leukemia Diagnostics of the Department of Internal Medicine III of the Klinikum der Universität München, Germany

RESULTS

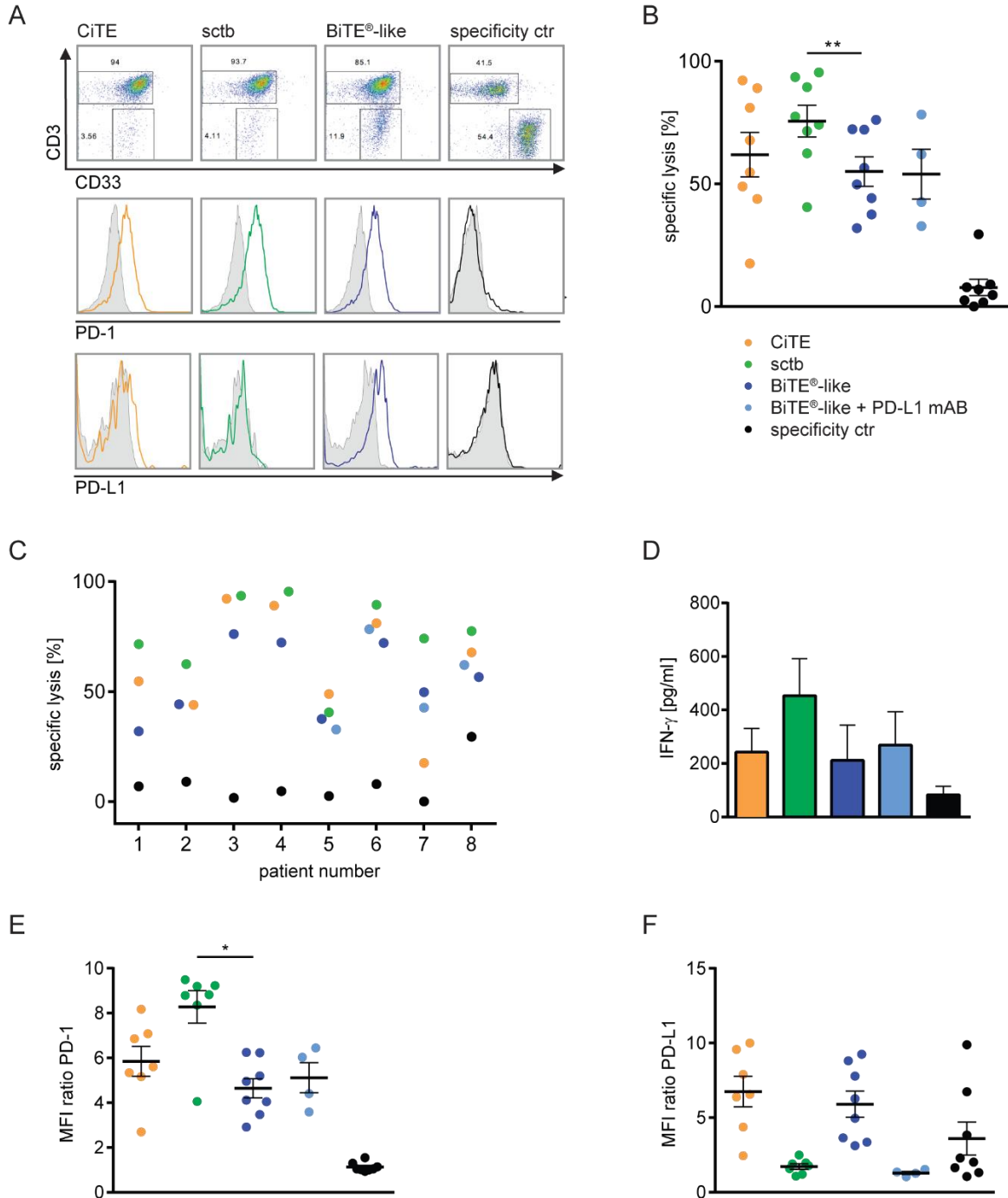


Figure 25: Biological functionality of CiTE, sctb and controls on primary AML patient samples.

(A) Cytotoxic lysis, PD-1 and PD-L1 upregulation induced by CiTE, sctb and controls on AML cells of an exemplary patient. (B) Specific lysis averaged over samples from eight patients. (C) Specific lysis of AML cells from individual patients. (D) IFN- γ release as determined on AML cells from four patients. (E) MFI-ratio of PD-1 expression on T cells. (F) MFI ratio of PD-L1 expression on AML cells. Experiments were performed for 3 to 4 days at an E:T ratio of 5:1 using non-stimulated HD T cells and patient-derived AML cells. CiTE, sctb and control molecules were applied at 10 nM and the PD-L1 mAb at 10 μ g/ml concentration. (B,C,E,F) represent values from eight, (D) from four experiments with SEM as error bars. Assays were performed by Christina Krupka.

RESULTS

4.7. Evaluation of the CiTE antibody in a murine AML xenograft model

To investigate the functionality of CiTE antibody and scfb *in vivo*, the molecules were evaluated in a murine xenograft model. Since both checkpoint blocking modules are described to be cross-reactive to murine PD-L1, the xenograft model was intended to cover two aspects:^{113,238,264} (1) the analysis of the efficiency to induce specific AML cell lysis *in vivo*, and (2) the potential development of irAEs^h.

The binding properties of the two checkpoint blocking modules were analyzed on Panc02OVA:mPD-L1 cells, which were engineered to express murine PD-L1 (Figure 26)ⁱ.

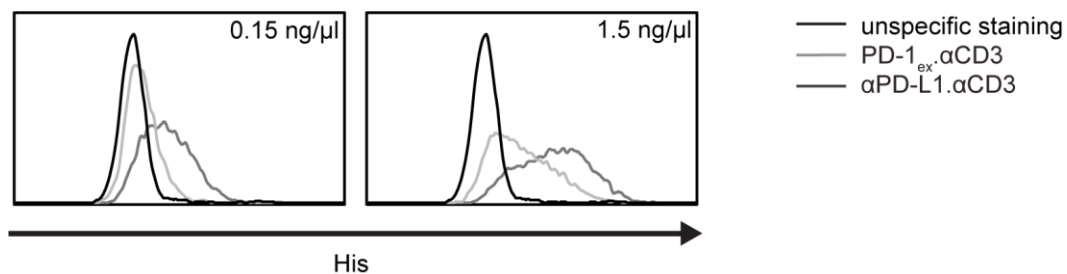


Figure 26: Cross-reactivity of human PD-1_{ex} and PD-L1 scFv with murine PD-L1.

Binding analysis of PD-1_{ex} in PD-1_{ex}.αCD3 and PD-L1 scFv in αPD-L1.αCD3 to Panc02OVA:mPD-L1 cells. Histograms show one out of three experiments with comparable results.

Therefore, PD-1_{ex}.αCD3 and αPD-L1.αCD3 were incubated with Panc02OVA:mPD-L1 cells and binding was assessed by flow cytometry. Both PD-1_{ex} and PD-L1 scFv interacted with the target cells, however, the scFv revealed a higher affinity to the antigen.

At primary diagnosis, only a subset of AML patients demonstrates PD-L1 expression, however, PD-L1 upregulation seems to play a critical role after first-line treatment.^{189,190,194-197} Thus, we consider a potential therapy with a CiTE antibody particularly suitable to counteract relapse. Furthermore, CD33 is not only expressed on bulk AML cells but also on LSCs, thus the CiTE molecule might also eliminate this cell population.⁷⁹ We chose an MRD-like setting to evaluate the efficiency of our molecules with an engraftment rate of <5% leukemic cells in the bone marrow.²⁶⁵ The study was conducted in accordance with the preclinical characterization of AMG 330 (Figure 27).⁷⁵ The daily treatment with 50 pmol (i.e. 1.7 pmol/g body weight) of CiTE antibody, scfb and control molecules was equivalent to 0.1 mg/kg of BiTE[®]-like molecule and therefore lay

^h Data were kindly provided by Katrin Deiser, Laboratory of Marion Subklewe, Gene Center Munich, LMU München, Germany

ⁱ Panc02OVA:mPD-L1 cells were kindly provided by Sebastian Kobold, Clinical Pharmacology, Department of Internal Medicine IV, Klinikum der LMU München, Germany

RESULTS

within the preclinically efficient range of AMG 330.⁷⁵ After 13 days, the mice were sacrificed and bone marrow and spleen were removed for further analysis.

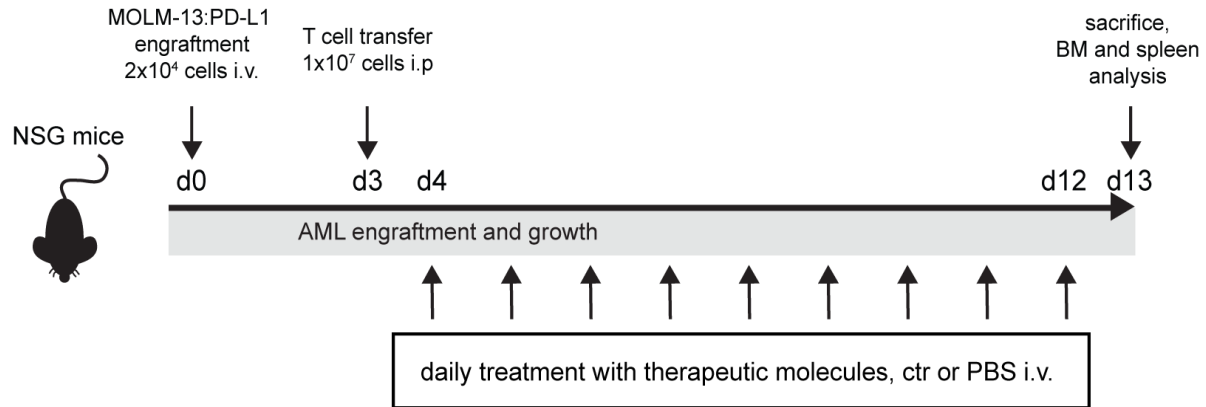


Figure 27: Experimental setup of *in vivo* studies.

Schedule of injection of MOLM-13:PD-L1 target cells, T cells and molecules into NSG mice.

Cytotoxic lysis of AML cells was evaluated by flow cytometry readout of residual CD45⁺CD33⁺ cells in the bone marrow. The CiTE antibody, sctb and BiTE[®]-like molecule evoked complete eradication of MOLM-13:PD-L1 cells, whereas the cohorts treated with specificity control or 1x PBS revealed a tumor engraftment of 1-3% in the bone marrow (Figure 28). Without treatment, the E:T ratio of human T cells and MOLM-13:PD-L1 cells at the time point of sacrifice was approximately 1:3 indicating an outgrowth of tumor cells (Figure 28 A).

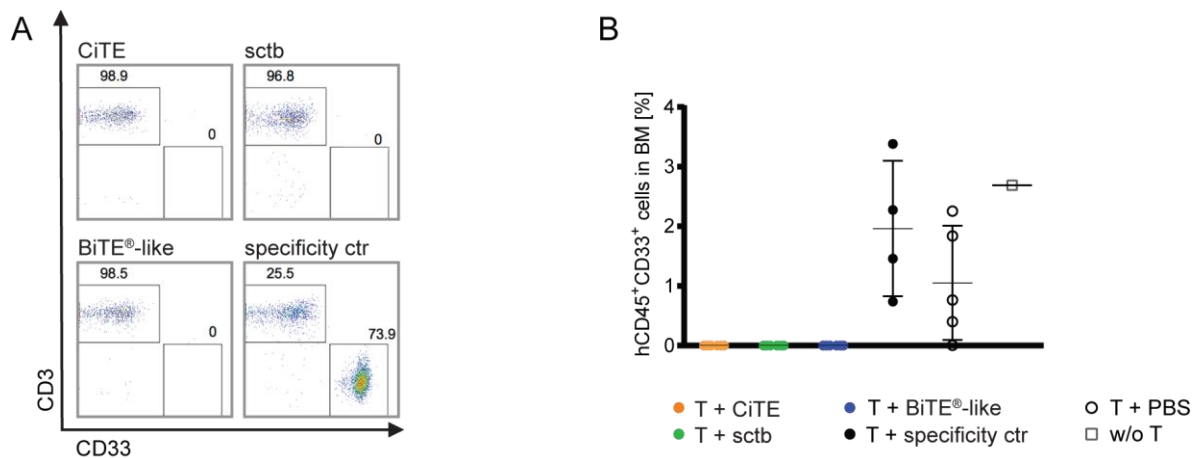


Figure 28: AML eradication *in vivo* mediated by CiTE antibody, sctb and BiTE[®]-like molecule.

(A) Exemplary evaluation of one mouse per treatment cohort. (B) Average of remaining target cells over treatment cohorts with SD as error bars. Experiment was performed by Katrin Deiser.

RESULTS

When monitoring the overall constitution of the mice, we observed a time-dependent decrease in relative body weight in the sctb treatment group whereas the body weight in all other cohorts remained stable (Figure 29).

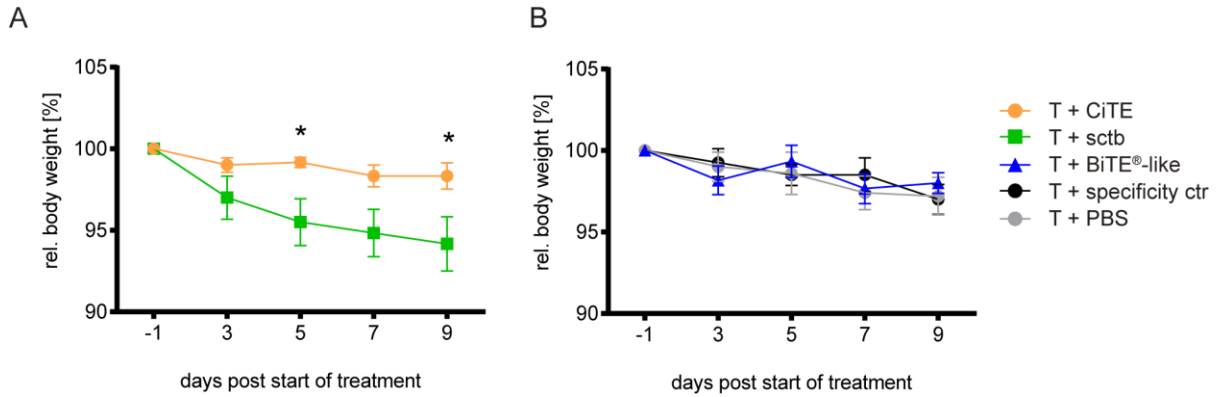


Figure 29: Monitoring of body weight during treatment period.

(A) Relative body weight in CiTE and sctb cohorts. (B) Relative body weight in control cohorts. Error bars indicate SEM. Data was obtained by Katrin Deiser.

In the sctb cohort PD-1 was significantly upregulated on CD4⁺ as well as CD4⁻ (i.e. CD8⁺) T cells, whereas PD-1 levels were low in all the other treatment groups. These findings were reflected on T cells derived from bone marrow and spleen (Figure 30).

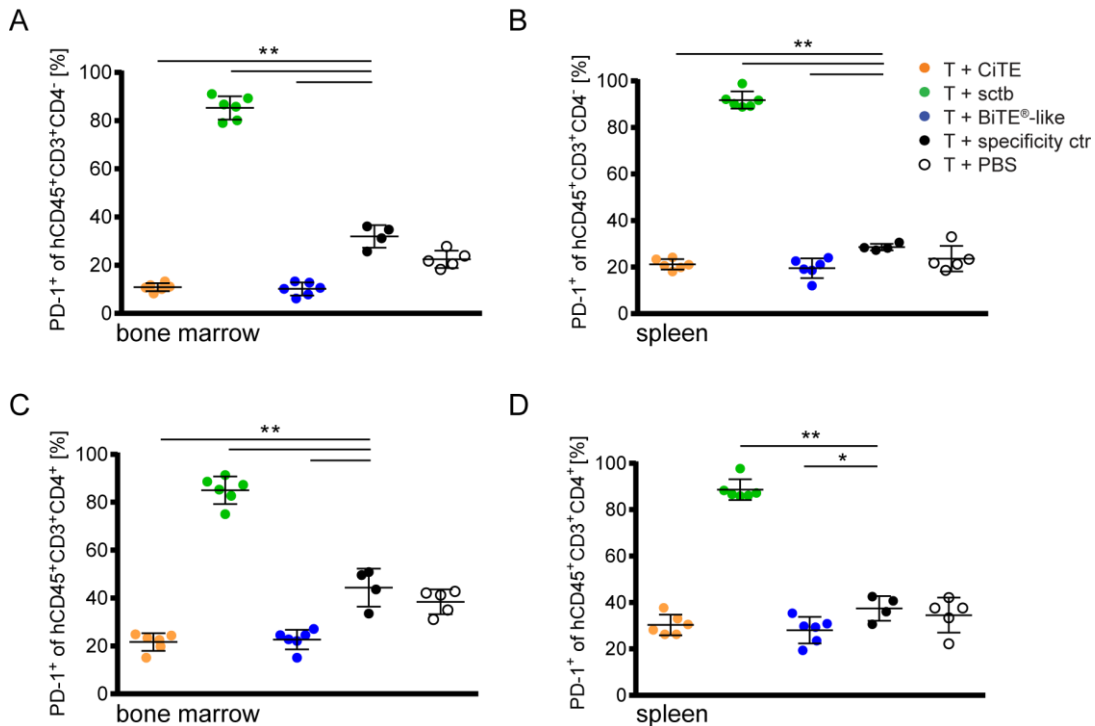


Figure 30: PD-1 expression on T cells of bone marrow and spleen.

PD-1 upregulation on CD4⁺ T cells of bone marrow (A) and spleen (B) as well as on CD4⁺ T cells of bone marrow (C) and spleen (D) as determined by flow cytometry with SD as error bars. Data was obtained by Katrin Deiser.

RESULTS

As exhaustion marker PD-1 upregulation points towards a prolonged antigen exposure in case of scfb treatment compared to CiTE antibody and BiTE[®]-like molecule, even though leukemia target cells were no longer detectable.

Evaluation of CD3 expression on T cells demonstrated a significant downregulation of CD3 on CD4⁺ (i.e. CD8⁺) T cells upon scfb treatment in both bone marrow and spleen, whereas in the other treatment groups only minor differences could be observed (Figure 31). On CD4⁺ T cells the CD3 expression levels were similar in all cohorts. Since CD3 is downregulated as a natural consequence of T cell activation, these findings suggest an increased activation of CD8⁺ T cells upon treatment with scfb.²⁶⁶⁻²⁶⁹

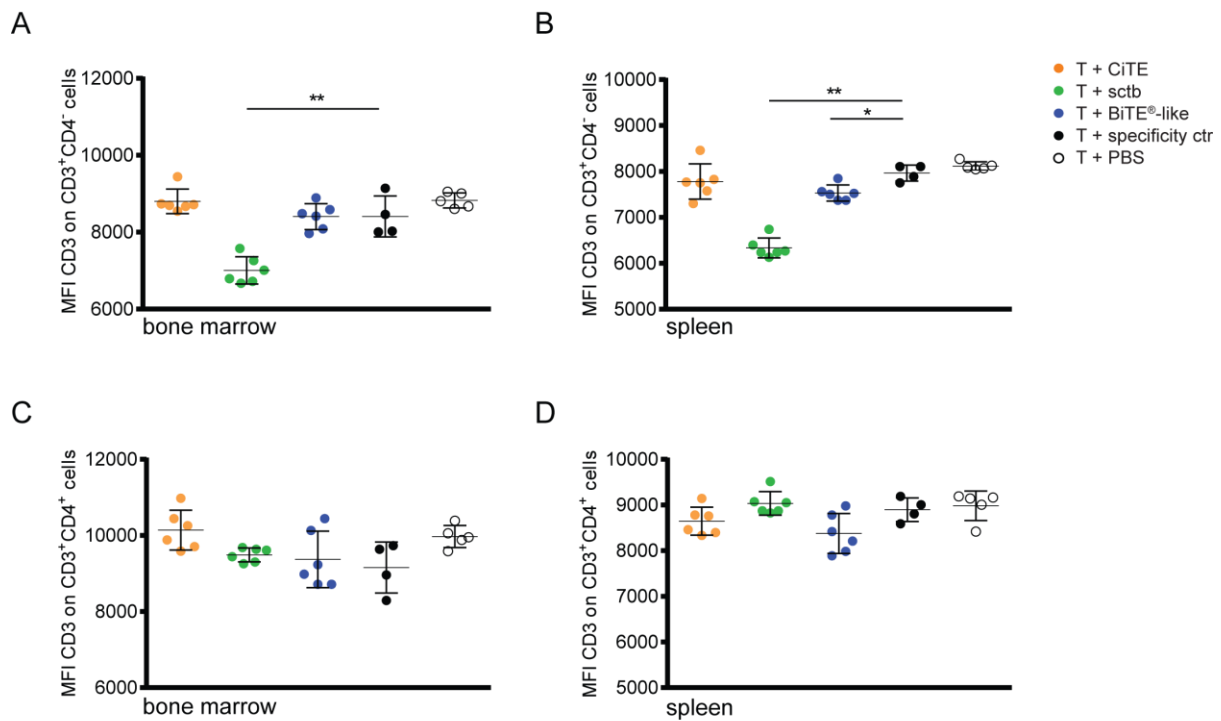


Figure 31: CD3 expression on T cells of bone marrow and spleen.

MFI of CD3 expression on CD4⁺ T cells of (A) bone marrow and (B) spleen as well as CD4⁺ T cells of (C) bone marrow and (D) spleen with SD as error bars. Data was generated by Katrin Deiser.

Although the three molecules evaluated in this study resemble each other in all binding modules aside from the checkpoint blocking arm, the scfb induced a different response. We hypothesize that the increase in T cell activation as well as the loss of body weight are due to an on-target off-leukemia effect caused by the PD-L1 scFv. Moreover, we reckon that the effect is restricted to the scfb and cannot be observed for the CiTE antibody due to the low binding affinity of PD-1_{ex}.

RESULTS

To exclude the possibility that the molecules target PD-L1 on the engrafted human T cells, PD-L1 levels were determined on T cells derived from bone marrow and spleen. Slight differences could be observed between the treatment groups, however, no increase in PD-L1 levels was detected (Figure 32). In fact, PD-L1 expression slightly decreased in the cohorts treated with CiTE antibody, sctb and BiTE[®]-like molecule.

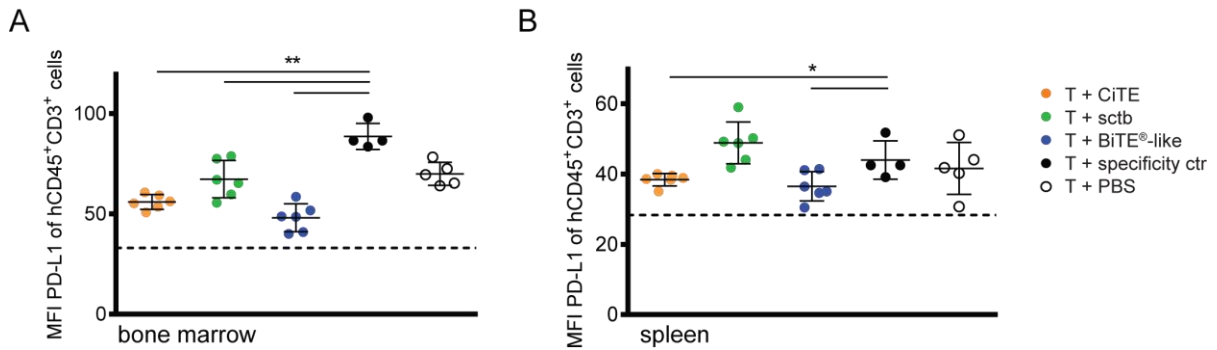


Figure 32: PD-L1 expression on T cells of bone marrow and spleen.

MFI of PD-L1 expression on CD45⁺CD3⁺ cells from (A) bone marrow and (B) spleen as measured by flow cytometry. Dashed line indicates MFI of isotype control with SD as error bars. Data was generated by Katrin Deiser.

Therefore, we hypothesize that the sctb-mediated effects were due to cross-reactivity of the high-affinity α PD-L1 binding arm to murine PD-L1. These effects could not be observed for the CiTE antibody, which we attribute to its low binding affinity to the checkpoint ligand.

Taken together, the CiTE antibody does not only possess a high potential to efficiently induce T cell effector functions against AML cell lines and primary AML patient samples *in vitro* but also *in vivo* in a murine xenograft model. It demonstrates a clear advantage compared to high-affinity PD-L1 binders by selectively targeting CD33⁺PD-L1⁺ cells. This may result in the specific lysis of AML blasts rather than PD-L1⁺ bystander cells and thereby presumably lead to a decrease of on-target off-leukemia events.

5. Discussion

In hematologic malignancies the development of successful immunotherapeutic strategies was hitherto limited to B-lymphoid neoplasias. The CD20-specific antibody rituximab was already approved in November 1997 for CD20⁺ B-cell non-Hodgkin lymphoma (NHL), and novel CD19-targeting agents such as the BiTE[®] blinatumomab and CD19-targeting chimeric antigen receptor (CAR) T cells have become available for the treatment of ALL in the last four years.^{63,270-272} New therapies are particularly necessitated in AML, where long-term survival rates are low and HSCT still represents the only curative option for non-favorable risk patients.²⁷³ Currently, monoclonal antibodies and derivatives thereof that target leukemia-associated antigens such as CD33 and CD123 as well as CAR T cells are clinically evaluated.^{212,220} The only immunotherapeutic agent that is available since September 2017 is GO (Mylotarg[®]), which has been approved for the treatment of newly diagnosed or r/r AML.^{226,231,232} Although CD33-targeting is considered highly promising, only thirty percent of patients respond to GO therapy after first relapse, which may be partially explained by the upregulation of PD-1 and PD-L1 in the leukemic microenvironment.^{195-197,229} Thus, PD-1 and PD-L1 blocking mABs are currently investigated in clinical trials as monotherapy and in combination with chemotherapy or other immunotherapeutic agents to achieve higher response rates in AML and increase survival rates.²³⁴

Despite the encouraging results from PD-1/PD-L1 blockade in various cancer types, a common drawback of all applied agents is their risk to induce irAEs, which can affect almost every organ.¹⁵⁶⁻¹⁶¹ The increasing use of systemically active immune checkpoint blocking mABs in the clinics will unavoidably lead to a higher number of cases that require intensive medical treatment. Thus, alternative therapeutic strategies to restrict irAEs are urgently needed. The novel CiTE antibody presented within this thesis approaches this problem by combining the high potential of T cell redirection with a local limitation of PD-1/PD-L1 blockade to the surface of leukemic cells.

5.1. Rationale for the novel CiTE format

The CiTE format is based on the established BiTE[®] scaffold, which already proved its high efficiency to redirect T cells independent of costimulatory signals.^{56,69,70,72,73,75,76,80} Since AML is often correlated with an immunosuppressed state, the synergistic effect of PD-1/PD-L1 blockade and CD3-mediated T cell activation appears particularly suited to trigger an efficient anti-cancer

DISCUSSION

immune response.^{186,187,189-191,198} We achieved a spatial limitation of immune checkpoint blockade to the cytolytic synapse by making use of the naturally occurring low affinity of PD-1_{ex}, which is not sufficient to bind to its ligands alone.¹¹⁵⁻¹¹⁷ Furthermore, PD-1_{ex} bears an advantage over conventional PD-L1-specific mABs in not only interfering with PD-L1 but also with PD-L2, which is also described to play a role in AML and other tumors but is hitherto less characterized.^{114,197} Aside from the low binding affinity for PD-L1, we also chose distinct affinities for the tumor-targeting and the T cell redirecting modules in agreement with the related BiTE[®] format.^{70,75,258} The selected CD33 scFv holds a high affinity for its ligand with measured K_D values of 29.4 nM and 31.0 nM, whereas the CD3ε scFv interacts with T cells with a comparably lower affinity of 121.3 nM. Thus, CiTE molecules are expected to primarily attach to the surface of CD33⁺ AML cells and form a matrix on which T cells can easily migrate, facilitating serial AML cell lysis as observed in *ex vivo* cytotoxicity assays and described previously for the BiTE[®] format.⁶⁹ By addressing T cells as effector population and inducing their proliferation, the CiTE antibody enables the amplification of the anti-cancer immune response. Moreover, T cells are able to directly interact with other immune cells and release proinflammatory cytokines.¹⁶ Other T cell redirecting therapeutics have been developed that have validated this therapeutic strategy, including BiTE[®]s, the trivalent TCB format and sctbs.^{56,67,68,75,86,87} In a different approach, antibodies containing extracellular domains of costimulatory T cell ligands such as 4-1BBL or OX40L, or extracellular domains of inhibitory receptors such as TIM-3 or PD-1 have been generated.²⁷⁴⁻²⁷⁶ The novelty of the presented CiTE antibody is that it is simultaneously capable of redirecting T cells and locally blocking an inhibitory immune checkpoint via the extracellular domain of a T cell immunoreceptor.

5.2. The CiTE format mediates T cell activation and cytotoxicity

In our studies, the CiTE antibody demonstrated a high efficiency to initiate T cell immune responses. It was able to activate T cells polyclonally and thus irrespective of their MHC:antigen specificity, as measured by the general upregulation of CD69 and CD25. This implies that a much larger effector T cell pool can be addressed than in a physiological immune response, where only T cells carrying the specific TCR are engaged.^{76,277} Since in AML after chemotherapy or HSCT T cell numbers are often reduced and low lymphocyte counts are associated with a poor prognosis, polyclonal activation and proliferation of remaining T cells might be particularly beneficial.²⁷⁸⁻²⁸⁰ Furthermore, CiTE-mediated T cell activation results in the release of IFN-γ and IL-2, thereby promoting a proinflammatory microenvironment and potentially leading to the attraction of other

DISCUSSION

immune cells to the tumor site. *In vitro*, the CiTE was able to specifically induce cytotoxic lysis of AML cells at very low concentrations with calculated EC₅₀ values between 2.3 pM and 132.5 pM. This is comparable to published values for BiTE[®] antibodies.^{70,75,76} Taking blinatumomab as reference, in a clinical application this might translate into effective therapeutic doses of around 15 µg/m²/day, which is significantly lower than conventional mABs.^{63,281,282} Notably, there is a considerable difference between EC₅₀ values, which were determined to be in the picomolar range, and the calculated dissociation constants of the separate tumor binding scFvs in the nanomolar range. This highlights the high biologic activity of the CiTE and suggests that a few molecules at the tumor site are already sufficient to induce T cell effector functions. In contrast, as example for conventional IgG antibodies rituximab was described to exhibit a 100,000-fold higher EC₅₀ value than the corresponding CD19xCD3 BiTE[®], indicating that Fc-induced tumor cell depletion through NK cells and macrophages is less potent than cytotoxic lysis by T cells.⁷⁰ An additional component that enhances CiTE-mediated T cell cytotoxicity is its ability to induce serial lysis of cancer cells, as demonstrated in assays with patient-derived AML cells. Similar to other T cell engagers, this is attributed to the low binding affinity of the CD3ε binding module compared to the tumor-targeting arm, allowing T cell migration between tumor cells.^{69,86}

It is important to mention that the CiTE antibody is able to induce cytotoxic lysis of target cells with varying target antigen densities. For the BiTE[®] AMG 330 it has been described that the kinetics of induced lysis correlate with CD33 surface levels, however, elimination of different AML cell lines with different CD33 antigen densities was still achieved.^{75,221} Similar results were obtained for the CiTE antibody. This is especially relevant since individuals reveal a large inter- and intra-patient heterogeneity regarding their CD33 expression.⁷⁹ In addition, the supposed source of relapse in many patients is a population of chemoresistant LSCs that expresses CD33 but at lower levels.⁷⁹ By depleting AML cells irrespective of absolute CD33 density, the CiTE might provide a promising strategy to eliminate remaining LSCs and thus prevent reoccurring disease outgrowth.^{79,213} First evidence for the efficient eradication of MRD was provided by the *in vivo* xenograft experiments that were performed as part of this study. By injecting MOLM-13:PD-L1 cells and obtaining 1-3% engraftment in the bone marrow, we were able to provide a model that resembled an MRD-positive state with <5% myeloblasts in the bone marrow.²⁶⁵ As the CiTE antibody was able to completely eradicate AML cells in our setting, we propose that it might also be a highly promising therapeutic to eliminate MRD cells in humans. However, future studies will have to elucidate safety and efficacy in preclinical models before transferring the CiTE format into

DISCUSSION

the clinics. From the current perspective similar patient groups that are addressed with GO might benefit from a CiTE therapy.²³² These include adult patients at relapse or elderly patients that cannot be treated with conventional therapies in particular, as GO monotherapy turned out to be advantageous in a randomized trial (EORTC-GIMEMA AML-19) with patients aged 62 years or older.^{232,283} Further, GO was efficient in newly diagnosed patients in combination with chemotherapy (e.g. studies ALFA-0701, MRC AML-15), wherefore accordingly a combination of CiTE and chemotherapeutic agents appears reasonable.^{231,232,284} However, due to the large heterogeneity within the disease we do not expect all patients to respond equally to CiTE administration.⁷⁹ This was already suggested by our *ex vivo* studies on primary AML patient samples, in which variable efficiency of AML depletion and differential upregulation of PD-1 on T cells as well as PD-L1 on AML cells were observed. Moreover, the release of proinflammatory cytokines by healthy donor T cells in response to CiTE-mediated activation indicated differences. The implementation of biomarker screenings might help to identify patients that benefit from CiTE therapy. These could include the quantification of CD33 expression and the determination of the responsiveness to PD-1/PD-L1 blockade, for instance by assessing the transcriptional IPRES signature.^{154,155}

5.3. Differences between CiTE and BiTE[®] format

By fusing a checkpoint blocking module to a BiTE[®]-like scaffold, we expected to increase T cell effector functions due to a joint effect of avidity-dependent target cell binding and local PD-1/PD-L1 checkpoint blockade. Indeed, in the presence of PD-L1⁺ AML cell lines the CiTE antibody induced a significant increase in the release of proinflammatory cytokines compared to the BiTE[®]-like molecule. Moreover, the CiTE displayed a higher efficiency in cytotoxicity induction on the majority of AML patient samples, and the high-affinity scfb contributed to our hypothesis by demonstrating the most efficient AML cell depletion. Since the synergy of avidity and blocking is the essential feature of the CiTE and the two mechanisms reinforce each other, the individual contribution of checkpoint blockade could not be assessed individually in these assays. Yet, the positive impact of PD-1/PD-L1 blockade on T cell redirection was demonstrated by recent *in vitro* studies. While PD-L1 expression reduced AMG 330-mediated effector functions, the combination with blocking agents was able to restore cytotoxicity.²³³ These findings were substantiated on primary AML patient samples, where the joint application of AMG 330 and blocking agents increased the efficiency of AML cell depletion.¹⁹⁴ Also in our hands the release of

DISCUSSION

proinflammatory cytokines was increased when combining a BiTE[®]-like molecule with checkpoint inhibitors. Importantly, the fusion of a PD-L1 blocking module in CiTE and sctb elevated IFN- γ levels to a similar or even higher extent. Thus, we estimate that the covalent fusion of a PD-L1 blocking module might increase the therapeutic benefit compared to BiTE[®] or combination therapies also *in vivo*.

In functional assays with MOLM-13 cells the CiTE molecule was, however, less efficient regarding the induction of cytotoxicity and T cell proliferation than the BiTE[®]-like molecule. To investigate whether this effect was due to general properties of the molecular scaffold, the BiTE[®]-like molecule was analyzed in comparison to a control molecule that based on the same trimodular geometry as the CiTE but in which PD-1_{ex} was replaced by a non-targeting scFv. Interestingly, the fusion of this module significantly decreased the performance of the molecule. We hypothesize that the additional binding arm might indeed slightly impair the formation of the cytolytic synapse either sterically, or via differences in the accessibility of the binding pocket of the CD3 ϵ scFv. Thus, in general a geometry as present in the BiTE[®] antibody might be more advantageous for T cell engagement than the trimodular CiTE format. Yet, these effects were only observable on cell lines and not on AML patient samples, wherefore they might not play a role in clinically relevant settings. In the presence of PD-L1 expression, no such effects were observed. Here, the direct fusion of a small blocking module might even bear a sterical advantage compared to combination therapies of BiTE[®] and blocking mABs.

5.4. The CiTE format increases selectivity for PD-L1⁺ AML cells

In the course of the more frequent clinical application of immune checkpoint inhibitors, clinicians become more and more aware of adverse events that require intensive medical care. These are often reasoned by on-target off-cancer toxicity due to PD-L1 upregulation in healthy tissues. Thus, novel strategies that implement the concept of immune checkpoint blockade in a cancer-restricted manner are of interest. Some approaches have already addressed this challenge but none of them have gained market approval yet. These include bispecific antibodies that simultaneously target two immune checkpoints such as PD-1 and TIM-3, or that address PD-1 and a TAA such as c-Met to increase tumor specificity.^{168,169} Another concept has been proposed that localizes a PD-L1 blocking antibody at the tumor site by attaching a binding arm against extracellular matrix proteins

DISCUSSION

in the tumor stroma.¹⁷⁰ Further, a recombinant myxoma virus has been engineered to carry a soluble form of PD-1, which is locally released from infected tumor cells.²⁸⁵

In the CiTE antibody we made use of the naturally occurring low affinity of PD-1_{ex} to its ligand, which is not sufficient to bind to PD-L1 expressing cells alone.¹¹⁵⁻¹¹⁷ We demonstrated that PD-1_{ex} only interacts with its target and blocks accessible binding sites when covalently linked to a high-affinity module. Thus, in comparison to high-affinity blocking agents the selectivity for leukemic cells can be significantly increased. *In vitro*, these findings were substantiated by showing that in the presence of PD-L1⁺ bystander cells, the CiTE exclusively induced lysis of AML cells, whereas the high-affinity scfb led to depletion of all target cells. Furthermore, the cross-reactivity of the PD-L1 blocking modules allowed us to evaluate potential irAEs in a murine model system.^{113,238,264} Similar to humans, PD-L1 expression in mice is widely distributed across different tissues.⁹⁶ Application of the CiTE did not provoke adverse events in our setting, whereas the high-affinity scfb revealed irAEs as indicated by relative body weight loss and the upregulation of PD-1 on T cells. These observations represent the first indication that in contrast to high-affinity PD-L1 binding agents the CiTE may not induce irAEs.

Aside from the prevention of irAEs that are a result of systemic PD-L1 blockade, the CiTE-mediated increase in selectivity for CD33⁺PD-L1⁺ cells might also bear the potential to reduce adverse events that originate from systemic CD33-targeting. This is particularly relevant since CD33 is also expressed on healthy myeloid cells and was detected on CD34⁺CD38⁻HSCs.^{79,215,286,287} As observed for GO, the general depletion of CD33⁺ cells consequentially results in myelosuppression as manifested in neutropenia and thrombocytopenia.^{218,288,289} In this regard, an interesting observation was that on PD-L1⁺ AML cells EC₅₀ values of CiTE were decreased by about one order of magnitude. We attribute this effect to avidity-dependent binding of PD-1_{ex} and the CD33 scFv. As CiTE and scfb behaved similar, this impact seems to be independent of the absolute binding affinity of the checkpoint blocking module. In carefully designed *in vivo* studies, the increase in efficiency might allow the exploration of a therapeutic concentration in which preferentially AML cells are targeted and healthy CD33⁺ cells are spared. Consequently, drug-associated cytopenias might be reduced while still sustaining therapeutic efficiency. It has previously been shown that bispecific dual-targeting agents with two high-affinity binding arms show a preference for double-positive cells.^{87,290} The novel feature of the CiTE is, that the low absolute affinity of PD-1_{ex} does not impair this effect compared to the high-affinity PD-L1 scFv in

DISCUSSION

the scfb. However, further investigations will have to clarify whether the measured concentrations are in a therapeutically relevant range and whether it is possible to determine a concentration in which LSCs are addressed but healthy CD33⁺ cells are spared.

Notably, CD33 is not only expressed on myeloid cells but also on activated T and NK cells, which might be detrimental for the specificity of the CiTE molecule.²⁹¹ However, publications on the BiTE[®] antibody AMG 330 reported that T cell activation is not correlated with CD33 upregulation, wherefore we also do not expect this mechanism to play a role for the CiTE antibody.⁷⁵ Apart from that, CD33 shedding has been observed in AML patients, which leads to the presence of soluble CD33 in the bone marrow plasma.²⁹² As it was demonstrated that this soluble form did not affect AMG 330 activity, we are confident that the same applies for the related CiTE format.⁷⁵

5.5. Benefit and risk of CiTE-mediated T cell activation

The activation of T cells by therapeutic antibodies bears the potential to initiate an anti-cancer immune response, however, the level of activation has to be carefully investigated. Lessons have been learned from a phase I clinical trial of the CD28 superagonist TGN1412, which was administered to six healthy volunteers at a dose that was 500-fold less than considered safe in animal models. Immediately after the first infusion, all patients developed a dramatic cytokine storm and subsequent multiorgan failure that required transfer to intensive care units.²⁹³⁻²⁹⁵ In this regard, one important safety aspect of the CiTE is that T cell activation crucially depends on the physical linkage to antigen-positive target cells. Similar to other currently investigated T cell engaging formats, the CiTE addresses T cells by binding to the ϵ subunit of CD3 in the TCR complex.^{68,70} Monoclonal CD3 antibodies as well as dimerized BiTE[®] molecules were shown to induce T cell activation by CD3 crosslinking, and the clinical application of OKT3 (i.e. muronomab; Orthoclone OKT3[®]), which is the parental antibody clone of blinatumomab and the presented CiTE, can result in severe side effects due to the development of CRS.^{73,262,263} However, we were able to demonstrate that monovalent CD3-targeting by the CiTE does not activate T cells in the absence of target cells or a tumor-targeting module *in vitro*, as measured by the upregulation of CD69 and CD25. Further, neither the release of proinflammatory cytokines such as IL-2 and IFN- γ nor T cell proliferation or cytotoxicity were detected. In accordance with the related BiTE[®] format, T cell activation was conditional on the crosslink to target cells.^{73,76} Yet, despite the absence

DISCUSSION

of extensive cytokine release *in vitro*, blinatumomab does induce CRS in some patients.⁸⁴ Thus, further studies also have to carefully evaluate CiTEs in this respect *in vivo*.

In line with T cell activation, we reported CiTE-mediated PD-1 upregulation on resting T cells and PD-L1 expression on primary patient-derived AML samples. This corresponds to publications that the expression of inhibitory immune checkpoints in AML does not originate from intrinsic oncogenic signaling but is rather a response to the inflammatory environment.¹⁸⁹⁻¹⁹¹ Particularly IFN- γ was shown to induce PD-L1 on AML cells *in vitro* and *in vivo*.¹⁸⁹⁻¹⁹¹ At this, inflammation cannot only be caused by an intrinsic anti-cancer response against cancer neoepitopes but also by artificial T cell engagement. Particularly in AML and ALL the correlation between targeted T cell activation and adaptive immune resistance has been demonstrated *in vitro*.^{194,296} To instantly counteract the inhibitory influence of PD-L1 upregulation, a combination of direct leukemia-targeting and PD-1/PD-L1 checkpoint inhibition appears reasonable. We were able to show that the fusion of a PD-L1 blocking module to a BiTE[®]-like scaffold significantly elevated T cell activation compared to a BiTE[®]-like molecule in the presence of PD-L1⁺ AML cells. The combination with blocking agents could increase IFN- γ and IL-2 levels induced by the BiTE[®]-like molecule, however, the highest cytokine release was achieved with the sctb. Importantly, also the CiTE was able to trigger similar cytokine levels compared to combination therapies, even if blocking agents were applied at a high surplus. An enhancement of T cell activation and associated proinflammatory cytokines might be beneficial in an immunosuppressed state to overcome PD-L1-mediated immune tolerance and restimulate the endogenous anti-cancer immune response. In AML, inhibitory ligands as well as the secretion of factors such as TGF- β and IL-10 and the increased abundance of T_{regs} and MDSCs contribute to an immunosuppressed state, thus a higher T cell activation might be particularly advantageous.^{188,193,203,204,297} Furthermore, after chemotherapy and HSCT the number of T cells is often decreased, which consequently lowers the probability of high cytokine levels that originate from activated T cells.²⁷⁸⁻²⁸⁰ A strong CiTE-mediated polyclonal activation is expected to lead to proliferation of remaining T cells, which could contribute to a restoration of the patient's effector T cell pool.

It has to be highlighted that the level of cytokine release seems to depend on the binding affinity of the PD-L1 blocking module, as the sctb revealed a stronger increase in IFN- γ and IL-2 levels compared to the BiTE[®]-like molecule than the CiTE antibody. Accordingly, the sctb is expected to bear a higher risk for CRS development than the CiTE. Moreover, the level of T cell activation

DISCUSSION

critically depends on the dosing regimen of a T cell engager. It thus appears conceivable that CiTEs might be applied at lower therapeutic doses than BiTE[®]s. Depending on the concentration, this might simultaneously favor the selective targeting of CD33⁺PD-L1⁺ cells and restrain binding to CD33⁺ or PD-L1⁺ non-AML cells. Carefully designed *in vivo* experiments in mice and non-human primates will have to be conducted before translating the CiTE format into clinical trials.

5.6. Optimization potential of the CiTE format

The CiTE format consists of two scFv modules and the extracellular domain of PD-1 that are connected by polypeptide linkers. In comparison to IgG based formats, it lacks the Fc part, which is accompanied by a lower molecular weight of roughly 75 kDa compared to 150 kDa. CiTE molecules are produced from one single polypeptide chain, whereas IgG antibodies assemble from two heavy and two light chains. The small molecular weight and the lack of an Fc portion is correlated with differences regarding predicted pharmacokinetic properties. In contrast to IgG antibodies, CiTEs are not expected to be adsorbed and endocytosed by FcR-bearing immune cells that represent a “sink” for the molecules.²⁹⁸ Still, it has to be considered that the CiTE moderately internalizes into PD-L1⁺ AML cells *in vitro*, which might lead to lower effective concentrations. A predictable characteristic of the format that differs from IgG molecules is a more rapid renal clearance from the bloodstream due to the small size and the correlated small hydrodynamic radius.²⁹⁹ The lack of an Fc region further contributes to a short plasma retention time. In contrast to the CiTE antibody, IgGs bind to neonatal Fc receptors (FcRn) after cellular uptake, which prevents the intracellular degradation and induces recirculation to the cell surface.^{33,300,301} Thus, conventional IgG-based mABs reveal a pharmacokinetic half-life of more than three weeks in humans.³⁰² In contrast, a scFv that possesses a similar architecture and size as the CiTE was described to exhibit a plasma half-life of four hours in the murine system, which was twice as long as the half-life of a bispecific scFv.⁶⁰ Still, in a clinical setting this might necessitate a frequent application or the administration as continuous infusion, as implemented for blinatumomab.^{63,82} Yet, the fast clearance might provide an advantage with regards to the control of exposure time. While an IgG antibody may remain in the blood system for several weeks after treatment discontinuation upon the detection of adverse events, CiTE therapy could be terminated immediately and the residual molecules cleared from the system within hours.⁶⁰ The smaller size also bears potential advantages compared to the larger mABs regarding tissue penetration, and it might facilitate binding of some epitopes that are more difficult to access for larger IgG

DISCUSSION

antibodies.^{58,59} Further studies will have to elucidate the potential and disadvantages of the comparably low molecular weight of CiTEs and elaborate on potential technologies to elongate plasma half-life. Possibilities include the chemical conjugation to polyethylene glycol (PEG) and a genetic fusion of a poly-amino acids such as proline-alanine-serine (PAS).^{303,304} Also coupling to a protein with a naturally occurring long half-life such as HSA or a domain that is capable of targeting such a protein by e.g. the fusion of an HSA-binding module can be found in other therapeutic formats and represent reasonable strategies.^{305,306}

Moreover, it is important to ensure that the CiTE antibody is stable as monomer, since dimerization of BiTE[®] molecules can lead to target cell-independent T cell activation.⁷³ After purification, we were able to obtain the CiTE antibody in a pure, monomeric state. Conventional storage of the protein at -80°C did not favor oligomer formation and incubation at physiological temperatures for several days did not lead to target cell-independent T cell activation. However, in the purification process multimers were detected by SEC. Since scFvs display a tendency to unfold at their V_H/V_L interface, it cannot be excluded that during long-term storage or *in vivo* application the Ig domains mispair with adjacent complementary Ig folds in a process called “protein domain swapping”.^{307,308} Consequently, this could lead to a mixture of different intramolecular folding states and oligomers. A consolidation of the functional monomeric state by stabilizing the scFvs might thus not only increase the total yield after purification but also the effective concentration of the protein in solution. Rational stabilization approaches include CDR grafting onto a stable framework, the introduction of point mutations in FRs or CDRs to stabilize the intrinsic domain folds, or stabilization of the V_H/V_L interface by e.g. the introduction of disulfide bonds.^{307,309,310} Still, changes in the amino acid sequence of scFvs have to be carefully designed to avoid worsening of expression yield and protein affinity.

5.7. Future directions of the CiTE format

In the present study we reported the *de novo* generation of the CiTE antibody format. By targeting CD33 on AML cells and simultaneously blocking the PD-1/PD-L1 immune checkpoint with PD-1_{ex}, we were able to locally restrict checkpoint blockade to the cytolytic synapse. We demonstrated that the CiTE induces efficient T cell-mediated cytotoxicity *in vitro* and *in vivo* and it exhibits a high selectivity for CD33⁺PD-L1⁺ cells. Thus we propose the CiTE format as highly promising therapeutic approach for AML treatment and hypothesize that induced irAEs are low.

DISCUSSION

However, future preclinical studies will have to be performed to obtain a reliable prognosis regarding efficiency and safety in humans. Although the CiTE antibody has been analyzed on samples derived from different patients, a larger number of individuals will have to be screened to representatively investigate the role of inter-patient heterogeneity.⁷⁹ Further, the performed xenograft experiments were well suited for proof-of-concept evaluation but they do not reflect the physiological tumor microenvironment and the interplay of tumor cells and immune system.³¹¹ Thus, in a next step, the CiTE molecule should be investigated in a humanized mouse model. Here a human immune system is established by transplantation of human peripheral blood lymphocytes or HSCs into immunodeficient or irradiated mice.^{311,312} HSCs are mainly derived from bone marrow fetal liver and umbilical cord blood.³¹² The injection of patient-derived xenografts (PDX) instead of human cell lines would further allow the inclusion of the genetic diversity within AML.³¹¹ Apart from that, established murine AML model systems could be used that inherit the main genetic aberrations that have been found in AML.^{311,313,314} The most conclusive evaluation could be provided by studies in non-human primates as this system is more similar to human. Due to the encouraging results of our initial AML xenograft studies, we are confident that the CiTE strategy might also succeed in such more advanced *in vivo* models.

Collectively, the *in vitro* and *in vivo* evaluation that was performed within this thesis demonstrated that the CiTE antibody induces highly efficient and specific elimination of AML cells. We consider this molecular format to be a promising strategy for AML treatment that may have significant benefits compared to conventional chemotherapy and should be further explored in combination approaches or as monotherapy.

6. References

1. Parish CR. Cancer immunotherapy: the past, the present and the future. *Immunol Cell Biol.* 2003;81(2):106-113.
2. Coley WB. The treatment of malignant tumors by repeated inoculations of erysipelas. With a report of ten original cases. 1893. *Clin Orthop Relat Res.* 1991(262):3-11.
3. Decker WK, Safdar A. Bioimmunoadjuvants for the treatment of neoplastic and infectious disease: Coley's legacy revisited. *Cytokine Growth Factor Rev.* 2009;20(4):271-281.
4. Morales A, Eidinger D, Bruce AW. Intracavitary Bacillus Calmette-Guerin in the treatment of superficial bladder tumors. *J Urol.* 1976;116(2):180-183.
5. Kamat AM, Lamm DL. Immunotherapy for bladder cancer. *Curr Urol Rep.* 2001;2(1):62-69.
6. Bassi P. BCG (Bacillus of Calmette Guerin) therapy of high-risk superficial bladder cancer. *Surg Oncol.* 2002;11(1-2):77-83.
7. Ehrlich P. Ueber den jetzigen Stand der Karzinomforschung. *Ned Tijdschr Geneesk.* 1909;5:73-290.
8. Dunn GP, Bruce AT, Ikeda H, Old LJ, Schreiber RD. Cancer immunoediting: from immunosurveillance to tumor escape. *Nat Immunol.* 2002;3(11):991-998.
9. Burnet FM. Immunological aspects of malignant disease. *Lancet.* 1967;1(7501):1171-1174.
10. Lawrence HS. *Cellular and Humoral Aspects of Hypersensitivity.* New York: A Hoeber-Harper Book; 1959.
11. Urban JL, Schreiber H. Tumor antigens. *Annu Rev Immunol.* 1992;10:617-644.
12. Boon T, Cerottini JC, Van den Eynde B, van der Bruggen P, Van Pel A. Tumor antigens recognized by T lymphocytes. *Annu Rev Immunol.* 1994;12:337-365.
13. Fenton RG, Longo DL. Genetic instability and tumor cell variation: implications for immunotherapy. *J Natl Cancer Inst.* 1995;87(4):241-243.
14. Stoler DL, Chen N, Basik M, et al. The onset and extent of genomic instability in sporadic colorectal tumor progression. *Proc Natl Acad Sci U S A.* 1999;96(26):15121-15126.
15. Kohler G, Milstein C. Continuous cultures of fused cells secreting antibody of predefined specificity. *Nature.* 1975;256(5517):495-497.
16. Murphy K, Travers P, Walport M. *Janeway's Immunobiology.* Vol 7: Garland Science; 2008.
17. Leavy O. Therapeutic antibodies: past, present and future. *Nat Rev Immunol.* 2010;10(5):297.
18. Schroff RW, Foon KA, Beatty SM, Oldham RK, Morgan AC, Jr. Human anti-murine immunoglobulin responses in patients receiving monoclonal antibody therapy. *Cancer Res.* 1985;45(2):879-885.
19. Chames P, Van Regenmortel M, Weiss E, Baty D. Therapeutic antibodies: successes, limitations and hopes for the future. *Br J Pharmacol.* 2009;157(2):220-233.
20. Winter G, Milstein C. Man-made antibodies. *Nature.* 1991;349(6307):293-299.
21. Orlandi R, Gussow DH, Jones PT, Winter G. Cloning immunoglobulin variable domains for expression by the polymerase chain reaction. *Proc Natl Acad Sci U S A.* 1989;86(10):3833-3837.
22. Skerra A, Pluckthun A. Assembly of a functional immunoglobulin Fv fragment in *Escherichia coli.* *Science.* 1988;240(4855):1038-1041.
23. Neuberger MS, Williams GT, Mitchell EB, Jouhal SS, Flanagan JG, Rabbitts TH. A hapten-specific chimaeric IgE antibody with human physiological effector function. *Nature.* 1985;314(6008):268-270.
24. Jones PT, Dear PH, Foote J, Neuberger MS, Winter G. Replacing the complementarity-determining regions in a human antibody with those from a mouse. *Nature.* 1986;321(6069):522-525.

REFERENCES

25. McCafferty J, Griffiths AD, Winter G, Chiswell DJ. Phage antibodies: filamentous phage displaying antibody variable domains. *Nature*. 1990;348(6301):552-554.
26. Hoogenboom HR, Chames P. Natural and designer binding sites made by phage display technology. *Immunol Today*. 2000;21(8):371-378.
27. Kesik-Brodacka M. Progress in biopharmaceutical development. *Biotechnol Appl Biochem*. 2017.
28. Martin U. 2016 Sales of Recombinant Therapeutic Antibodies & Proteins. *La Merie Biologics*. 2017.
29. Lu LL, Suscovich TJ, Fortune SM, Alter G. Beyond binding: antibody effector functions in infectious diseases. *Nat Rev Immunol*. 2017.
30. Val IJd, Jedrzejewski PM, Exley K, et al. Application of Quality by Design Paradigm to the Manufacture of Protein Therapeutics. In: Petrescu S, ed. *Glycosylation*. Rijeka: InTech; 2012:Ch. 16.
31. Mimura Y, Katoh T, Saldova R, et al. Glycosylation engineering of therapeutic IgG antibodies: challenges for the safety, functionality and efficacy. *Protein Cell*. 2017.
32. Jefferis R. Glycosylation as a strategy to improve antibody-based therapeutics. *Nat Rev Drug Discov*. 2009;8(3):226-234.
33. Weiner LM, Surana R, Wang S. Monoclonal antibodies: versatile platforms for cancer immunotherapy. *Nat Rev Immunol*. 2010;10(5):317-327.
34. Scott AM, Wolchok JD, Old LJ. Antibody therapy of cancer. *Nat Rev Cancer*. 2012;12(4):278-287.
35. DiLillo DJ, Ravetch JV. Fc-Receptor Interactions Regulate Both Cytotoxic and Immunomodulatory Therapeutic Antibody Effector Functions. *Cancer Immunol Res*. 2015;3(7):704-713.
36. Joffre OP, Segura E, Savina A, Amigorena S. Cross-presentation by dendritic cells. *Nat Rev Immunol*. 2012;12(8):557-569.
37. Dhodapkar KM, Krasovsky J, Williamson B, Dhodapkar MV. Antitumor monoclonal antibodies enhance cross-presentation of cellular antigens and the generation of myeloma-specific killer T cells by dendritic cells. *J Exp Med*. 2002;195(1):125-133.
38. Brode S, Macary PA. Cross-presentation: dendritic cells and macrophages bite off more than they can chew! *Immunology*. 2004;112(3):345-351.
39. Brinkmann U, Kontermann RE. The making of bispecific antibodies. *MAbs*. 2017;9(2):182-212.
40. Kontermann R. Dual targeting strategies with bispecific antibodies. *mAbs*. 2012;4(2).
41. Klein C, Sustmann C, Thomas M, et al. Progress in overcoming the chain association issue in bispecific heterodimeric IgG antibodies. *MAbs*. 2012;4(6):653-663.
42. Chelius D, Ruf P, Gruber P, et al. Structural and functional characterization of the trifunctional antibody catumaxomab. *MAbs*. 2010;2(3):309-319.
43. Schaefer W, Volger HR, Lorenz S, et al. Heavy and light chain pairing of bivalent quadroma and knobs-into-holes antibodies analyzed by UHR-ESI-QTOF mass spectrometry. *MAbs*. 2016;8(1):49-55.
44. De Lau WB, Heije K, Neefjes JJ, Oosterwegel M, Rozemuller E, Bast BJ. Absence of preferential homologous H/L chain association in hybrid hybridomas. *J Immunol*. 1991;146(3):906-914.
45. Ridgway JB, Presta LG, Carter P. 'Knobs-into-holes' engineering of antibody CH3 domains for heavy chain heterodimerization. *Protein Eng*. 1996;9(7):617-621.
46. Kontermann RE, Brinkmann U. Bispecific antibodies. *Drug Discov Today*. 2015;20(7):838-847.
47. Schaefer W, Regula JT, Bahner M, et al. Immunoglobulin domain crossover as a generic approach for the production of bispecific IgG antibodies. *Proc Natl Acad Sci U S A*. 2011;108(27):11187-11192.

REFERENCES

48. Liu Z, Leng EC, Gunasekaran K, et al. A novel antibody engineering strategy for making monovalent bispecific heterodimeric IgG antibodies by electrostatic steering mechanism. *J Biol Chem.* 2015;290(12):7535-7562.
49. Lewis SM, Wu X, Pustilnik A, et al. Generation of bispecific IgG antibodies by structure-based design of an orthogonal Fab interface. *Nat Biotechnol.* 2014;32(2):191-198.
50. Gunasekaran K, Pentony M, Shen M, et al. Enhancing antibody Fc heterodimer formation through electrostatic steering effects: applications to bispecific molecules and monovalent IgG. *J Biol Chem.* 2010;285(25):19637-19646.
51. Huston JS, Levinson D, Mudgett-Hunter M, et al. Protein engineering of antibody binding sites: recovery of specific activity in an anti-digoxin single-chain Fv analogue produced in *Escherichia coli*. *Proc Natl Acad Sci U S A.* 1988;85(16):5879-5883.
52. Ahmad ZA, Yeap SK, Ali AM, Ho WY, Alitheen NB, Hamid M. scFv antibody: principles and clinical application. *Clin Dev Immunol.* 2012;2012:980250.
53. Saerens D, Ghassabeh GH, Muyldermans S. Single-domain antibodies as building blocks for novel therapeutics. *Curr Opin Pharmacol.* 2008;8(5):600-608.
54. Holliger P, Prospero T, Winter G. "Diabodies": small bivalent and bispecific antibody fragments. *Proc Natl Acad Sci U S A.* 1993;90(14):6444-6448.
55. Johnson S, Burke S, Huang L, et al. Effector cell recruitment with novel Fv-based dual-affinity re-targeting protein leads to potent tumor cytotoxicity and in vivo B-cell depletion. *J Mol Biol.* 2010;399(3):436-449.
56. Loffler A, Kufer P, Lutterbuse R, et al. A recombinant bispecific single-chain antibody, CD19 x CD3, induces rapid and high lymphoma-directed cytotoxicity by unstimulated T lymphocytes. *Blood.* 2000;95(6):2098-2103.
57. Oates J, Jakobsen BK. ImmTACs: Novel bi-specific agents for targeted cancer therapy. *Oncoimmunology.* 2013;2(2):e22891.
58. Spiess C, Zhai Q, Carter PJ. Alternative molecular formats and therapeutic applications for bispecific antibodies. *Mol Immunol.* 2015;67(2 Pt A):95-106.
59. Coppieters K, Dreier T, Silence K, et al. Formatted anti-tumor necrosis factor alpha VHH proteins derived from camelids show superior potency and targeting to inflamed joints in a murine model of collagen-induced arthritis. *Arthritis Rheum.* 2006;54(6):1856-1866.
60. Kellner C, Bruenke J, Stieglmaier J, et al. A novel CD19-directed recombinant bispecific antibody derivative with enhanced immune effector functions for human leukemic cells. *J Immunother.* 2008;31(9):871-884.
61. Todorovska A, Roovers RC, Dolezal O, Kortt AA, Hoogenboom HR, Hudson PJ. Design and application of diabodies, triabodies and tetrabodies for cancer targeting. *J Immunol Methods.* 2001;248(1-2):47-66.
62. Kipriyanov SM, Moldenhauer G, Schuhmacher J, et al. Bispecific tandem diabody for tumor therapy with improved antigen binding and pharmacokinetics. *J Mol Biol.* 1999;293(1):41-56.
63. Sanford M. Blinatumomab: first global approval. *Drugs.* 2015;75(3):321-327.
64. Staerz UD, Bevan MJ. Hybrid hybridoma producing a bispecific monoclonal antibody that can focus effector T-cell activity. *Proc Natl Acad Sci U S A.* 1986;83(5):1453-1457.
65. Segal DM, Weiner GJ, Weiner LM. Bispecific antibodies in cancer therapy. *Curr Opin Immunol.* 1999;11(5):558-562.
66. Seimetz D. Novel monoclonal antibodies for cancer treatment: the trifunctional antibody catumaxomab (removab). *J Cancer.* 2011;2:309-316.
67. Bacac M, Fauti T, Sam J, et al. A Novel Carcinoembryonic Antigen T-Cell Bispecific Antibody (CEA TCB) for the Treatment of Solid Tumors. *Clin Cancer Res.* 2016;22(13):3286-3297.
68. Bacac M, Klein C, Umana P. CEA TCB: A novel head-to-tail 2:1 T cell bispecific antibody for treatment of CEA-positive solid tumors. *Oncoimmunology.* 2016;5(8):e1203498.

REFERENCES

69. Hoffmann P, Hofmeister R, Brischwein K, et al. Serial killing of tumor cells by cytotoxic T cells redirected with a CD19-/CD3-bispecific single-chain antibody construct. *Int J Cancer*. 2005;115(1):98-104.
70. Dreier T, Lorenczewski G, Brandl C, et al. Extremely potent, rapid and costimulation-independent cytotoxic T-cell response against lymphoma cells catalyzed by a single-chain bispecific antibody. *Int J Cancer*. 2002;100(6):690-697.
71. Chames P, Baty D. Bispecific antibodies for cancer therapy: the light at the end of the tunnel? *MAbs*. 2009;1(6):539-547.
72. Dreier T, Baeuerle PA, Fichtner I, et al. T cell costimulus-independent and very efficacious inhibition of tumor growth in mice bearing subcutaneous or leukemic human B cell lymphoma xenografts by a CD19-/CD3- bispecific single-chain antibody construct. *J Immunol*. 2003;170(8):4397-4402.
73. Brischwein K, Parr L, Pflanz S, et al. Strictly target cell-dependent activation of T cells by bispecific single-chain antibody constructs of the BiTE class. *J Immunother*. 2007;30(8):798-807.
74. Ross SL, Sherman M, McElroy PL, et al. Bispecific T cell engager (BiTE(R)) antibody constructs can mediate bystander tumor cell killing. *PLoS One*. 2017;12(8):e0183390.
75. Friedrich M, Henn A, Raum T, et al. Preclinical characterization of AMG 330, a CD3/CD33-bispecific T-cell-engaging antibody with potential for treatment of acute myelogenous leukemia. *Mol Cancer Ther*. 2014;13(6):1549-1557.
76. Brischwein K, Schlereth B, Guller B, et al. MT110: a novel bispecific single-chain antibody construct with high efficacy in eradicating established tumors. *Mol Immunol*. 2006;43(8):1129-1143.
77. Oberst MD, Fuhrmann S, Mulgrew K, et al. CEA/CD3 bispecific antibody MEDI-565/AMG 211 activation of T cells and subsequent killing of human tumors is independent of mutations commonly found in colorectal adenocarcinomas. *MAbs*. 2014;6(6):1571-1584.
78. Lutterbuese R, Raum T, Kischel R, et al. T cell-engaging BiTE antibodies specific for EGFR potently eliminate KRAS- and BRAF-mutated colorectal cancer cells. *Proc Natl Acad Sci U S A*. 2010;107(28):12605-12610.
79. Krupka C, Kufer P, Kischel R, et al. CD33 target validation and sustained depletion of AML blasts in long-term cultures by the bispecific T-cell-engaging antibody AMG 330. *Blood*. 2014;123(3):356-365.
80. Aigner M, Feulner J, Schaffer S, et al. T lymphocytes can be effectively recruited for ex vivo and in vivo lysis of AML blasts by a novel CD33/CD3-bispecific BiTE antibody construct. *Leukemia*. 2013;27(5):1107-1115.
81. Friedrich M, Raum T, Lutterbuese R, et al. Regression of human prostate cancer xenografts in mice by AMG 212/BAY2010112, a novel PSMA/CD3-Bispecific BiTE antibody cross-reactive with non-human primate antigens. *Mol Cancer Ther*. 2012;11(12):2664-2673.
82. Smits NC, Sentman CL. Bispecific T-Cell Engagers (BiTEs) as Treatment of B-Cell Lymphoma. *J Clin Oncol*. 2016;34(10):1131-1133.
83. Klinger M, Brandl C, Zugmaier G, et al. Immunopharmacologic response of patients with B-lineage acute lymphoblastic leukemia to continuous infusion of T cell-engaging CD19/CD3-bispecific BiTE antibody blinatumomab. *Blood*. 2012;119(26):6226-6233.
84. Teachey DT, Rheingold SR, Maude SL, et al. Cytokine release syndrome after blinatumomab treatment related to abnormal macrophage activation and ameliorated with cytokine-directed therapy. *Blood*. 2013;121(26):5154-5157.
85. Goebeler ME, Knop S, Viardot A, et al. Bispecific T-Cell Engager (BiTE) Antibody Construct Blinatumomab for the Treatment of Patients With Relapsed/Refractory Non-Hodgkin Lymphoma: Final Results From a Phase I Study. *J Clin Oncol*. 2016;34(10):1104-1111.

REFERENCES

86. Roskopf CC, Schiller CB, Braciak TA, et al. T cell-recruiting triplebody 19-3-19 mediates serial lysis of malignant B-lymphoid cells by a single T cell. *Oncotarget*. 2014;5(15):6466-6483.
87. Roskopf CC, Braciak TA, Fenn NC, et al. Dual-targeting triplebody 33-3-19 mediates selective lysis of biphenotypic CD19+ CD33+ leukemia cells. *Oncotarget*. 2016;7(16):22579-22589.
88. Jenkins MK, Schwartz RH. Antigen presentation by chemically modified splenocytes induces antigen-specific T cell unresponsiveness in vitro and in vivo. *J Exp Med*. 1987;165(2):302-319.
89. Schwartz RH. T cell anergy. *Annu Rev Immunol*. 2003;21:305-334.
90. Chaput N, Louafi S, Bardier A, et al. Identification of CD8+CD25+Foxp3+ suppressive T cells in colorectal cancer tissue. *Gut*. 2009;58(4):520-529.
91. Kuniwa Y, Miyahara Y, Wang HY, et al. CD8+ Foxp3+ regulatory T cells mediate immunosuppression in prostate cancer. *Clin Cancer Res*. 2007;13(23):6947-6958.
92. Churlaud G, Pitoiset F, Jebbawi F, et al. Human and Mouse CD8(+)/CD25(+)/FOXP3(+) Regulatory T Cells at Steady State and during Interleukin-2 Therapy. *Front Immunol*. 2015;6:171.
93. Pardoll DM. The blockade of immune checkpoints in cancer immunotherapy. *Nat Rev Cancer*. 2012;12(4):252-264.
94. Chen DS, Mellman I. Oncology meets immunology: the cancer-immunity cycle. *Immunity*. 2013;39(1):1-10.
95. Greenwald RJ, Freeman GJ, Sharpe AH. The B7 family revisited. *Annu Rev Immunol*. 2005;23:515-548.
96. Keir ME, Butte MJ, Freeman GJ, Sharpe AH. PD-1 and its ligands in tolerance and immunity. *Annu Rev Immunol*. 2008;26:677-704.
97. Sharpe AH, Freeman GJ. The B7-CD28 superfamily. *Nat Rev Immunol*. 2002;2(2):116-126.
98. June CH, Warshauer JT, Bluestone JA. Is autoimmunity the Achilles' heel of cancer immunotherapy? *Nat Med*. 2017;23(5):540-547.
99. Kim R, Emi M, Tanabe K. Cancer immunoediting from immune surveillance to immune escape. *Immunology*. 2007;121(1):1-14.
100. Cerwenka A, Lanier LL. Natural killer cells, viruses and cancer. *Nat Rev Immunol*. 2001;1(1):41-49.
101. Street SE, Hayakawa Y, Zhan Y, et al. Innate immune surveillance of spontaneous B cell lymphomas by natural killer cells and gammadelta T cells. *J Exp Med*. 2004;199(6):879-884.
102. Qin Z, Schwartzkopff J, Pradera F, et al. A critical requirement of interferon gamma-mediated angiostasis for tumor rejection by CD8+ T cells. *Cancer Res*. 2003;63(14):4095-4100.
103. Gollob JA, Sciambi CJ, Huang Z, Dressman HK. Gene expression changes and signaling events associated with the direct antimelanoma effect of IFN-gamma. *Cancer Res*. 2005;65(19):8869-8877.
104. Motz GT, Coukos G. Deciphering and reversing tumor immune suppression. *Immunity*. 2013;39(1):61-73.
105. Alsaab HO, Sau S, Alzhrani R, et al. PD-1 and PD-L1 Checkpoint Signaling Inhibition for Cancer Immunotherapy: Mechanism, Combinations, and Clinical Outcome. *Front Pharmacol*. 2017;8:561.
106. Martin AM, Nirschl TR, Nirschl CJ, et al. Paucity of PD-L1 expression in prostate cancer: innate and adaptive immune resistance. *Prostate Cancer Prostatic Dis*. 2015;18(4):325-332.
107. Zou W, Chen L. Inhibitory B7-family molecules in the tumour microenvironment. *Nat Rev Immunol*. 2008;8(6):467-477.
108. Mellman I, Coukos G, Dranoff G. Cancer immunotherapy comes of age. *Nature*. 2011;480(7378):480-489.

REFERENCES

109. Agata Y, Kawasaki A, Nishimura H, et al. Expression of the PD-1 antigen on the surface of stimulated mouse T and B lymphocytes. *Int Immunol*. 1996;8(5):765-772.
110. Okazaki T, Honjo T. PD-1 and PD-1 ligands: from discovery to clinical application. *Int Immunol*. 2007;19(7):813-824.
111. Nielsen C, Ohm-Laursen L, Barington T, Husby S, Lillevang ST. Alternative splice variants of the human PD-1 gene. *Cell Immunol*. 2005;235(2):109-116.
112. Lazar-Molnar E, Yan Q, Cao E, Ramagopal U, Nathenson SG, Almo SC. Crystal structure of the complex between programmed death-1 (PD-1) and its ligand PD-L2. *Proc Natl Acad Sci U S A*. 2008;105(30):10483-10488.
113. Freeman GJ, Long AJ, Iwai Y, et al. Engagement of the PD-1 immunoinhibitory receptor by a novel B7 family member leads to negative regulation of lymphocyte activation. *J Exp Med*. 2000;192(7):1027-1034.
114. Latchman Y, Wood CR, Chernova T, et al. PD-L2 is a second ligand for PD-1 and inhibits T cell activation. *Nat Immunol*. 2001;2(3):261-268.
115. Zak KM, Grudnik P, Magiera K, Domling A, Dubin G, Holak TA. Structural Biology of the Immune Checkpoint Receptor PD-1 and Its Ligands PD-L1/PD-L2. *Structure*. 2017;25(8):1163-1174.
116. Lin DY, Tanaka Y, Iwasaki M, et al. The PD-1/PD-L1 complex resembles the antigen-binding Fv domains of antibodies and T cell receptors. *Proc Natl Acad Sci U S A*. 2008;105(8):3011-3016.
117. Cheng X, Veverka V, Radhakrishnan A, et al. Structure and interactions of the human programmed cell death 1 receptor. *J Biol Chem*. 2013;288(17):11771-11785.
118. Chen L. Co-inhibitory molecules of the B7-CD28 family in the control of T-cell immunity. *Nat Rev Immunol*. 2004;4(5):336-347.
119. Lim TS, Chew V, Sieow JL, et al. PD-1 expression on dendritic cells suppresses CD8(+) T cell function and antitumor immunity. *Oncimmunology*. 2016;5(3):e1085146.
120. Sharpe AH, Pauken KE. The diverse functions of the PD1 inhibitory pathway. *Nat Rev Immunol*. 2017.
121. Barber DL, Wherry EJ, Masopust D, et al. Restoring function in exhausted CD8 T cells during chronic viral infection. *Nature*. 2006;439(7077):682-687.
122. Crawford A, Angelosanto JM, Kao C, et al. Molecular and transcriptional basis of CD4(+) T cell dysfunction during chronic infection. *Immunity*. 2014;40(2):289-302.
123. Pauken KE, Wherry EJ. Overcoming T cell exhaustion in infection and cancer. *Trends Immunol*. 2015;36(4):265-276.
124. Francisco LM, Sage PT, Sharpe AH. The PD-1 pathway in tolerance and autoimmunity. *Immunol Rev*. 2010;236:219-242.
125. Boussiotis VA, Chatterjee P, Li L. Biochemical signaling of PD-1 on T cells and its functional implications. *Cancer J*. 2014;20(4):265-271.
126. Patel SP, Kurzrock R. PD-L1 Expression as a Predictive Biomarker in Cancer Immunotherapy. *Mol Cancer Ther*. 2015;14(4):847-856.
127. Zhou ZJ, Zhan P, Song Y. PD-L1 over-expression and survival in patients with non-small cell lung cancer: a meta-analysis. *Transl Lung Cancer Res*. 2015;4(2):203-208.
128. Zhang M, Dong Y, Liu H, et al. The clinicopathological and prognostic significance of PD-L1 expression in gastric cancer: a meta-analysis of 10 studies with 1,901 patients. *Sci Rep*. 2016;6:37933.
129. Jin Y, Zhao J, Shi X, Yu X. Prognostic value of programmed death ligand 1 in patients with solid tumors: A meta-analysis. *J Cancer Res Ther*. 2015;11 Suppl 1:C38-43.
130. Sabatier R, Finetti P, Mamessier E, et al. Prognostic and predictive value of PDL1 expression in breast cancer. *Oncotarget*. 2015;6(7):5449-5464.
131. Dolan DE, Gupta S. PD-1 pathway inhibitors: changing the landscape of cancer immunotherapy. *Cancer Control*. 2014;21(3):231-237.

REFERENCES

132. Okazaki T, Maeda A, Nishimura H, Kurosaki T, Honjo T. PD-1 immunoreceptor inhibits B cell receptor-mediated signaling by recruiting src homology 2-domain-containing tyrosine phosphatase 2 to phosphotyrosine. *Proc Natl Acad Sci U S A*. 2001;98(24):13866-13871.
133. Yokosuka T, Takamatsu M, Kobayashi-Imanishi W, Hashimoto-Tane A, Azuma M, Saito T. Programmed cell death 1 forms negative costimulatory microclusters that directly inhibit T cell receptor signaling by recruiting phosphatase SHP2. *J Exp Med*. 2012;209(6):1201-1217.
134. Riley JL. PD-1 signaling in primary T cells. *Immunol Rev*. 2009;229(1):114-125.
135. Mezzadra R, Sun C, Jae LT, et al. Identification of CMTM6 and CMTM4 as PD-L1 protein regulators. *Nature*. 2017;549(7670):106-110.
136. Coelho MA, de Carne Trecesson S, Rana S, et al. Oncogenic RAS Signaling Promotes Tumor Immuno-resistance by Stabilizing PD-L1 mRNA. *Immunity*. 2017;47(6):1083-1099 e1086.
137. Chinai JM, Janakiram M, Chen F, Chen W, Kaplan M, Zang X. New immunotherapies targeting the PD-1 pathway. *Trends Pharmacol Sci*. 2015;36(9):587-595.
138. Butte MJ, Keir ME, Phamduy TB, Sharpe AH, Freeman GJ. Programmed death-1 ligand 1 interacts specifically with the B7-1 costimulatory molecule to inhibit T cell responses. *Immunity*. 2007;27(1):111-122.
139. Xiao Y, Yu S, Zhu B, et al. RGMB is a novel binding partner for PD-L2 and its engagement with PD-L2 promotes respiratory tolerance. *J Exp Med*. 2014;211(5):943-959.
140. Velu V, Titanji K, Zhu B, et al. Enhancing SIV-specific immunity in vivo by PD-1 blockade. *Nature*. 2009;458(7235):206-210.
141. Brahmer JR, Tykodi SS, Chow LQ, et al. Safety and activity of anti-PD-L1 antibody in patients with advanced cancer. *N Engl J Med*. 2012;366(26):2455-2465.
142. Raedler LA. Opdivo (Nivolumab): Second PD-1 Inhibitor Receives FDA Approval for Unresectable or Metastatic Melanoma. *Am Health Drug Benefits*. 2015;8(Spec Feature):180-183.
143. Raedler LA. Keytruda (Pembrolizumab): First PD-1 Inhibitor Approved for Previously Treated Unresectable or Metastatic Melanoma. *Am Health Drug Benefits*. 2015;8(Spec Feature):96-100.
144. Syed YY. Durvalumab: First Global Approval. *Drugs*. 2017;77(12):1369-1376.
145. Ning YM, Suzman D, Maher VE, et al. FDA Approval Summary: Atezolizumab for the Treatment of Patients with Progressive Advanced Urothelial Carcinoma after Platinum-Containing Chemotherapy. *Oncologist*. 2017;22(6):743-749.
146. Kim ES. Avelumab: First Global Approval. *Drugs*. 2017;77(8):929-937.
147. Topalian SL, Hodi FS, Brahmer JR, et al. Safety, activity, and immune correlates of anti-PD-1 antibody in cancer. *N Engl J Med*. 2012;366(26):2443-2454.
148. Wartewig T, Kurgys Z, Keppler S, et al. PD-1 is a haploinsufficient suppressor of T cell lymphomagenesis. *Nature*. 2017.
149. Wolchok JD, Chiarion-Sileni V, Gonzalez R, et al. Overall Survival with Combined Nivolumab and Ipilimumab in Advanced Melanoma. *N Engl J Med*. 2017;377(14):1345-1356.
150. Swart M, Verbrugge I, Beltman JB. Combination Approaches with Immune-Checkpoint Blockade in Cancer Therapy. *Front Oncol*. 2016;6:233.
151. Chamoto K, Chowdhury PS, Kumar A, et al. Mitochondrial activation chemicals synergize with surface receptor PD-1 blockade for T cell-dependent antitumor activity. *Proc Natl Acad Sci U S A*. 2017;114(5):E761-E770.
152. Yang W, Bai Y, Xiong Y, et al. Potentiating the antitumor response of CD8(+) T cells by modulating cholesterol metabolism. *Nature*. 2016;531(7596):651-655.
153. Blank CU, Haanen JB, Ribas A, Schumacher TN. CANCER IMMUNOLOGY. The "cancer immunogram". *Science*. 2016;352(6286):658-660.
154. Hugo W, Zaretsky JM, Sun L, et al. Genomic and Transcriptomic Features of Response to Anti-PD-1 Therapy in Metastatic Melanoma. *Cell*. 2016;165(1):35-44.

REFERENCES

155. Bu X, Mahoney KM, Freeman GJ. Learning from PD-1 Resistance: New Combination Strategies. *Trends Mol Med.* 2016;22(6):448-451.
156. Naidoo J, Wang X, Woo KM, et al. Pneumonitis in Patients Treated With Anti-Programmed Death-1/Programmed Death Ligand 1 Therapy. *J Clin Oncol.* 2017;35(7):709-717.
157. Matson DR, Accola MA, Rehrauer WM, Corliss RF. Fatal Myocarditis Following Treatment with the PD-1 Inhibitor Nivolumab. *J Forensic Sci.* 2017.
158. Gettinger SN, Horn L, Gandhi L, et al. Overall Survival and Long-Term Safety of Nivolumab (Anti-Programmed Death 1 Antibody, BMS-936558, ONO-4538) in Patients With Previously Treated Advanced Non-Small-Cell Lung Cancer. *J Clin Oncol.* 2015;33(18):2004-2012.
159. Hamid O, Robert C, Daud A, et al. Safety and tumor responses with lambrolizumab (anti-PD-1) in melanoma. *N Engl J Med.* 2013;369(2):134-144.
160. Weber JS, Hodi FS, Wolchok JD, et al. Safety Profile of Nivolumab Monotherapy: A Pooled Analysis of Patients With Advanced Melanoma. *J Clin Oncol.* 2017;35(7):785-792.
161. Tajiri K, Aonuma K, Sekine I. Immune checkpoint inhibitor-related myocarditis. *Jpn J Clin Oncol.* 2017:1-6.
162. Weber JS, Yang JC, Atkins MB, Disis ML. Toxicities of Immunotherapy for the Practitioner. *J Clin Oncol.* 2015;33(18):2092-2099.
163. Nishimura H, Nose M, Hiai H, Minato N, Honjo T. Development of lupus-like autoimmune diseases by disruption of the PD-1 gene encoding an ITIM motif-carrying immunoreceptor. *Immunity.* 1999;11(2):141-151.
164. Wang J, Yoshida T, Nakaki F, Hiai H, Okazaki T, Honjo T. Establishment of NOD-Pdcd1^{-/-} mice as an efficient animal model of type I diabetes. *Proc Natl Acad Sci U S A.* 2005;102(33):11823-11828.
165. Latchman YE, Liang SC, Wu Y, et al. PD-L1-deficient mice show that PD-L1 on T cells, antigen-presenting cells, and host tissues negatively regulates T cells. *Proc Natl Acad Sci U S A.* 2004;101(29):10691-10696.
166. Tahoori MT, Pourfathollah AA, Akhlaghi M, Daneshmandi S, Nicknam MH, Soleimanifar N. Association of programmed cell death-1 (PDCD-1) gene polymorphisms with rheumatoid arthritis in Iranian patients. *Clin Exp Rheumatol.* 2011;29(5):763-767.
167. Prokunina L, Castillejo-Lopez C, Oberg F, et al. A regulatory polymorphism in PDCD1 is associated with susceptibility to systemic lupus erythematosus in humans. *Nat Genet.* 2002;32(4):666-669.
168. Kuchroo VK, Anderson AC, Inventors; The Brigham And Women's Hospital, Inc., assignee. Bi-specific antibodies against tim-3 and pd-1 for immunotherapy in chronic immune conditions. 2016.
169. Sun ZJ, Wu Y, Hou WH, et al. A novel bispecific c-MET/PD-1 antibody with therapeutic potential in solid cancer. *Oncotarget.* 2017;8(17):29067-29079.
170. Ishihara J, Fukunaga K, Ishihara A, et al. Matrix-binding checkpoint immunotherapies enhance antitumor efficacy and reduce adverse events. *Sci Transl Med.* 2017;9(415).
171. Buske C, Spiekermann K, Braess J, Hiddemann W. Akute myeloische Leukämie. In: Hiddemann W, Bartram CR, eds. *Die Onkologie - Teil 2.* Vol 2. Heidelberg, Germany: Springer Medizin Verlag; 2010:1822.
172. Dohner H, Weisdorf DJ, Bloomfield CD. Acute Myeloid Leukemia. *N Engl J Med.* 2015;373(12):1136-1152.
173. De Kouchkovsky I, Abdul-Hay M. 'Acute myeloid leukemia: a comprehensive review and 2016 update'. *Blood Cancer J.* 2016;6(7):e441.
174. Bennett JM, Catovsky D, Daniel MT, et al. Proposals for the classification of the acute leukaemias. French-American-British (FAB) co-operative group. *Br J Haematol.* 1976;33(4):451-458.
175. Sabattini E, Bacci F, Sagranso C, Pileri SA. WHO classification of tumours of haematopoietic and lymphoid tissues in 2008: an overview. *Pathologica.* 2010;102(3):83-87.

REFERENCES

176. Arber DA, Orazi A, Hasserjian R, et al. The 2016 revision to the World Health Organization classification of myeloid neoplasms and acute leukemia. *Blood*. 2016;127(20):2391-2405.
177. Dohner H, Estey EH, Amadori S, et al. Diagnosis and management of acute myeloid leukemia in adults: recommendations from an international expert panel, on behalf of the European LeukemiaNet. *Blood*. 2010;115(3):453-474.
178. Roboz GJ. Current treatment of acute myeloid leukemia. *Curr Opin Oncol*. 2012;24(6):711-719.
179. Feller N, van der Pol MA, van Stijn A, et al. MRD parameters using immunophenotypic detection methods are highly reliable in predicting survival in acute myeloid leukaemia. *Leukemia*. 2004;18(8):1380-1390.
180. Pollyea DA, Gutman JA, Gore L, Smith CA, Jordan CT. Targeting acute myeloid leukemia stem cells: a review and principles for the development of clinical trials. *Haematologica*. 2014;99(8):1277-1284.
181. Bonnet D, Dick JE. Human acute myeloid leukemia is organized as a hierarchy that originates from a primitive hematopoietic cell. *Nat Med*. 1997;3(7):730-737.
182. Stahl M, Kim TK, Zeidan AM. Update on acute myeloid leukemia stem cells: New discoveries and therapeutic opportunities. *World J Stem Cells*. 2016;8(10):316-331.
183. Tallman MS, Gilliland DG, Rowe JM. Drug therapy for acute myeloid leukemia. *Blood*. 2005;106(4):1154-1163.
184. Lichtenegger FS, Krupka C, Haubner S, Kohnke T, Subklewe M. Recent developments in immunotherapy of acute myeloid leukemia. *J Hematol Oncol*. 2017;10(1):142.
185. Ustun C, Miller JS, Munn DH, Weisdorf DJ, Blazar BR. Regulatory T cells in acute myelogenous leukemia: is it time for immunomodulation? *Blood*. 2011;118(19):5084-5095.
186. Zhou Q, Munger ME, Highfill SL, et al. Program death-1 signaling and regulatory T cells collaborate to resist the function of adoptively transferred cytotoxic T lymphocytes in advanced acute myeloid leukemia. *Blood*. 2010;116(14):2484-2493.
187. Zhang L, Gajewski TF, Kline J. PD-1/PD-L1 interactions inhibit antitumor immune responses in a murine acute myeloid leukemia model. *Blood*. 2009;114(8):1545-1552.
188. Buggins AG, Milojkovic D, Arno MJ, et al. Microenvironment produced by acute myeloid leukemia cells prevents T cell activation and proliferation by inhibition of NF-kappaB, c-Myc, and pRb pathways. *J Immunol*. 2001;167(10):6021-6030.
189. Berthon C, Driss V, Liu J, et al. In acute myeloid leukemia, B7-H1 (PD-L1) protection of blasts from cytotoxic T cells is induced by TLR ligands and interferon-gamma and can be reversed using MEK inhibitors. *Cancer Immunol Immunother*. 2010;59(12):1839-1849.
190. Norde WJ, Maas F, Hobo W, et al. PD-1/PD-L1 interactions contribute to functional T-cell impairment in patients who relapse with cancer after allogeneic stem cell transplantation. *Cancer Res*. 2011;71(15):5111-5122.
191. Kronig H, Kremmler L, Haller B, et al. Interferon-induced programmed death-ligand 1 (PD-L1/B7-H1) expression increases on human acute myeloid leukemia blast cells during treatment. *Eur J Haematol*. 2014;92(3):195-203.
192. El Kholy NM, Sallam MM, Ahmed MB, et al. Expression of indoleamine 2,3-dioxygenase in acute myeloid leukemia and the effect of its inhibition on cultured leukemia blast cells. *Med Oncol*. 2011;28(1):270-278.
193. Mussai F, De Santo C, Abu-Dayyeh I, et al. Acute myeloid leukemia creates an arginase-dependent immunosuppressive microenvironment. *Blood*. 2013;122(5):749-758.
194. Krupka C, Kufer P, Kischel R, et al. Blockade of the PD-1/PD-L1 axis augments lysis of AML cells by the CD33/CD3 BiTE antibody construct AMG 330: reversing a T-cell-induced immune escape mechanism. *Leukemia*. 2016;30(2):484-491.
195. Schnorfeil FM, Lichtenegger FS, Emmerig K, et al. T cells are functionally not impaired in AML: increased PD-1 expression is only seen at time of relapse and correlates with a shift towards the memory T cell compartment. *J Hematol Oncol*. 2015;8:93.

REFERENCES

196. Chen X, Liu S, Wang L, Zhang W, Ji Y, Ma X. Clinical significance of B7-H1 (PD-L1) expression in human acute leukemia. *Cancer Biol Ther.* 2008;7(5):622-627.
197. Yang H, Bueso-Ramos C, DiNardo C, et al. Expression of PD-L1, PD-L2, PD-1 and CTLA4 in myelodysplastic syndromes is enhanced by treatment with hypomethylating agents. *Leukemia.* 2014;28(6):1280-1288.
198. Coles SJ, Gilmour MN, Reid R, et al. The immunosuppressive ligands PD-L1 and CD200 are linked in AML T-cell immunosuppression: identification of a new immunotherapeutic synapse. *Leukemia.* 2015;29(9):1952-1954.
199. Perez-Garcia A, Brunet S, Berlanga JJ, et al. CTLA-4 genotype and relapse incidence in patients with acute myeloid leukemia in first complete remission after induction chemotherapy. *Leukemia.* 2009;23(3):486-491.
200. Isidori A, Loscocco F, Ciciarello M, et al. Renewing the immunological approach to AML treatment: from novel pathways to innovative therapies. *Cancer Research Frontiers.* 2016;2(2):226-251.
201. Iachininoto MG, Nuzzolo ER, Bonanno G, et al. Cyclooxygenase-2 (COX-2) inhibition constrains indoleamine 2,3-dioxygenase 1 (IDO1) activity in acute myeloid leukaemia cells. *Molecules.* 2013;18(9):10132-10145.
202. Sehgal A, Whiteside TL, Boyiadzis M. Programmed death-1 checkpoint blockade in acute myeloid leukemia. *Expert Opin Biol Ther.* 2015;15(8):1191-1203.
203. Sun H, Li Y, Zhang ZF, et al. Increase in myeloid-derived suppressor cells (MDSCs) associated with minimal residual disease (MRD) detection in adult acute myeloid leukemia. *Int J Hematol.* 2015;102(5):579-586.
204. Szczepanski MJ, Szajnik M, Czystowska M, et al. Increased frequency and suppression by regulatory T cells in patients with acute myelogenous leukemia. *Clin Cancer Res.* 2009;15(10):3325-3332.
205. Shenghui Z, Yixiang H, Jianbo W, et al. Elevated frequencies of CD4(+) CD25(+) CD127lo regulatory T cells is associated to poor prognosis in patients with acute myeloid leukemia. *Int J Cancer.* 2011;129(6):1373-1381.
206. Zhou Q, Bucher C, Munger ME, et al. Depletion of endogenous tumor-associated regulatory T cells improves the efficacy of adoptive cytotoxic T-cell immunotherapy in murine acute myeloid leukemia. *Blood.* 2009;114(18):3793-3802.
207. Kolb HJ, Schattenberg A, Goldman JM, et al. Graft-versus-leukemia effect of donor lymphocyte transfusions in marrow grafted patients. *Blood.* 1995;86(5):2041-2050.
208. Makita M, Azuma T, Hamaguchi H, et al. Leukemia-associated fusion proteins, dek-can and bcr-abl, represent immunogenic HLA-DR-restricted epitopes recognized by fusion peptide-specific CD4+ T lymphocytes. *Leukemia.* 2002;16(12):2400-2407.
209. Graf C, Heidel F, Tenzer S, et al. A neoepitope generated by an FLT3 internal tandem duplication (FLT3-ITD) is recognized by leukemia-reactive autologous CD8+ T cells. *Blood.* 2007;109(7):2985-2988.
210. Greiner J, Ono Y, Hofmann S, et al. Mutated regions of nucleophosmin 1 elicit both CD4(+) and CD8(+) T-cell responses in patients with acute myeloid leukemia. *Blood.* 2012;120(6):1282-1289.
211. von Lindern M, Fornerod M, van Baal S, et al. The translocation (6;9), associated with a specific subtype of acute myeloid leukemia, results in the fusion of two genes, dek and can, and the expression of a chimeric, leukemia-specific dek-can mRNA. *Mol Cell Biol.* 1992;12(4):1687-1697.
212. Hoseini SS, Cheung NK. Acute myeloid leukemia targets for bispecific antibodies. *Blood Cancer J.* 2017;7(4):e552.
213. Hauswirth AW, Florian S, Printz D, et al. Expression of the target receptor CD33 in CD34+/CD38-/CD123+ AML stem cells. *Eur J Clin Invest.* 2007;37(1):73-82.

REFERENCES

214. Munoz L, Nomdedeu JF, Lopez O, et al. Interleukin-3 receptor alpha chain (CD123) is widely expressed in hematologic malignancies. *Haematologica*. 2001;86(12):1261-1269.
215. Taussig DC, Pearce DJ, Simpson C, et al. Hematopoietic stem cells express multiple myeloid markers: implications for the origin and targeted therapy of acute myeloid leukemia. *Blood*. 2005;106(13):4086-4092.
216. Jordan CT, Upchurch D, Szilvassy SJ, et al. The interleukin-3 receptor alpha chain is a unique marker for human acute myelogenous leukemia stem cells. *Leukemia*. 2000;14(10):1777-1784.
217. Bernstein ID. Monoclonal antibodies to the myeloid stem cells: therapeutic implications of CMA-676, a humanized anti-CD33 antibody calicheamicin conjugate. *Leukemia*. 2000;14(3):474-475.
218. Laszlo GS, Estey EH, Walter RB. The past and future of CD33 as therapeutic target in acute myeloid leukemia. *Blood Rev*. 2014;28(4):143-153.
219. Feldman EJ, Brandwein J, Stone R, et al. Phase III randomized multicenter study of a humanized anti-CD33 monoclonal antibody, lintuzumab, in combination with chemotherapy, versus chemotherapy alone in patients with refractory or first-relapsed acute myeloid leukemia. *J Clin Oncol*. 2005;23(18):4110-4116.
220. Kenderian SS, Ruella M, Shestova O, et al. CD33-specific chimeric antigen receptor T cells exhibit potent preclinical activity against human acute myeloid leukemia. *Leukemia*. 2015;29(8):1637-1647.
221. Laszlo GS, Gudgeon CJ, Harrington KH, et al. Cellular determinants for preclinical activity of a novel CD33/CD3 bispecific T-cell engager (BiTE) antibody, AMG 330, against human AML. *Blood*. 2014;123(4):554-561.
222. Scheinberg DA, Lovett D, Divgi CR, et al. A phase I trial of monoclonal antibody M195 in acute myelogenous leukemia: specific bone marrow targeting and internalization of radionuclide. *J Clin Oncol*. 1991;9(3):478-490.
223. Sekeres MA, Lancet JE, Wood BL, et al. Randomized phase IIb study of low-dose cytarabine and lintuzumab versus low-dose cytarabine and placebo in older adults with untreated acute myeloid leukemia. *Haematologica*. 2013;98(1):119-128.
224. van Der Velden VH, te Marvelde JG, Hoogeveen PG, et al. Targeting of the CD33-calicheamicin immunoconjugate Mylotarg (CMA-676) in acute myeloid leukemia: in vivo and in vitro saturation and internalization by leukemic and normal myeloid cells. *Blood*. 2001;97(10):3197-3204.
225. Loke J, Khan JN, Wilson JS, Craddock C, Wheatley K. Mylotarg has potent anti-leukaemic effect: a systematic review and meta-analysis of anti-CD33 antibody treatment in acute myeloid leukaemia. *Ann Hematol*. 2015;94(3):361-373.
226. Gemtuzumab Ozogamicin Makes a Comeback. *Cancer Discov*. 2017.
227. Hamann PR, Hinman LM, Hollander I, et al. Gemtuzumab ozogamicin, a potent and selective anti-CD33 antibody-calicheamicin conjugate for treatment of acute myeloid leukemia. *Bioconjug Chem*. 2002;13(1):47-58.
228. Zein N, Sinha AM, McGahren WJ, Ellestad GA. Calicheamicin gamma 1I: an antitumor antibiotic that cleaves double-stranded DNA site specifically. *Science*. 1988;240(4856):1198-1201.
229. Sievers EL, Larson RA, Stadtmauer EA, et al. Efficacy and safety of gemtuzumab ozogamicin in patients with CD33-positive acute myeloid leukemia in first relapse. *J Clin Oncol*. 2001;19(13):3244-3254.
230. Petersdorf SH, Kopecky KJ, Slovak M, et al. A phase 3 study of gemtuzumab ozogamicin during induction and postconsolidation therapy in younger patients with acute myeloid leukemia. *Blood*. 2013;121(24):4854-4860.

REFERENCES

231. Castaigne S, Pautas C, Terre C, et al. Effect of gemtuzumab ozogamicin on survival of adult patients with de-novo acute myeloid leukaemia (ALFA-0701): a randomised, open-label, phase 3 study. *Lancet*. 2012;379(9825):1508-1516.
232. Godwin CD, Gale RP, Walter RB. Gemtuzumab ozogamicin in acute myeloid leukemia. *Leukemia*. 2017;31(9):1855-1868.
233. Laszlo GS, Gudgeon CJ, Harrington KH, Walter RB. T-cell ligands modulate the cytolytic activity of the CD33/CD3 BiTE antibody construct, AMG 330. *Blood Cancer J*. 2015;5:e340.
234. Hobo W, Hutten TJA, Schaap NPM, Dolstra H. Immune checkpoint molecules in acute myeloid leukaemia: managing the double-edged sword. *Br J Haematol*. 2018.
235. Knaus HA, Kanakry CG, Luznik L, Gojo I. Immunomodulatory Drugs: Immune Checkpoint Agents in Acute Leukemia. *Curr Drug Targets*. 2017;18(3):315-331.
236. Pianko MJ, Liu Y, Bagchi S, Lesokhin AM. Immune checkpoint blockade for hematologic malignancies: a review. *Stem Cell Investig*. 2017;4:32.
237. Krebber A, Bornhauser S, Burmester J, et al. Reliable cloning of functional antibody variable domains from hybridomas and spleen cell repertoires employing a reengineered phage display system. *J Immunol Methods*. 1997;201(1):35-55.
238. Irving B, Chiu H, Maecker H, et al., Inventors; Genentech, Inc. (South San Francisco, CA, US), assignee. Anti-PD-L1 antibodies, compositions and articles of manufacture. 2012.
239. Zugmaier G, Degenhard E, Inventors; Amgen Research (Munich), assignee. Treatment of acute lymphoblastic leukemia. 2009.
240. Singer H, Kellner C, Lanig H, et al. Effective elimination of acute myeloid leukemic cells by recombinant bispecific antibody derivatives directed against CD33 and CD16. *J Immunother*. 2010;33(6):599-608.
241. Carter P, Presta L, Gorman CM, et al. Humanization of an anti-p185HER2 antibody for human cancer therapy. *Proc Natl Acad Sci U S A*. 1992;89(10):4285-4289.
242. Green MR, Sambrook J, Sambrook J. *Molecular cloning : a laboratory manual*. Cold Spring Harbor, N.Y.: Cold Spring Harbor Laboratory Press; 2012.
243. Hanahan D. Studies on transformation of *Escherichia coli* with plasmids. *J Mol Biol*. 1983;166(4):557-580.
244. Hillen W, Gatz C, Altschmied L, Schollmeier K, Meier I. Control of expression of the Tn10-encoded tetracycline resistance genes. Equilibrium and kinetic investigation of the regulatory reactions. *J Mol Biol*. 1983;169(3):707-721.
245. Jacobs C, Duewell P, Heckelsmiller K, et al. An ISCOM vaccine combined with a TLR9 agonist breaks immune evasion mediated by regulatory T cells in an orthotopic model of pancreatic carcinoma. *Int J Cancer*. 2011;128(4):897-907.
246. World Medical A. World Medical Association Declaration of Helsinki: ethical principles for medical research involving human subjects. *JAMA*. 2013;310(20):2191-2194.
247. Laemmli UK. Cleavage of structural proteins during the assembly of the head of bacteriophage T4. *Nature*. 1970;227(5259):680-685.
248. Boivin S, Kozak S, Meijers R. Optimization of protein purification and characterization using Thermofluor screens. *Protein Expr Purif*. 2013;91(2):192-206.
249. Olejniczak SH, Stewart CC, Donohue K, Czuczman MS. A quantitative exploration of surface antigen expression in common B-cell malignancies using flow cytometry. *Immunol Invest*. 2006;35(1):93-114.
250. Benedict CA, MacKrell AJ, Anderson WF. Determination of the binding affinity of an anti-CD34 single-chain antibody using a novel, flow cytometry based assay. *J Immunol Methods*. 1997;201(2):223-231.
251. Schubert I, Saul D, Nowecki S, Mackensen A, Fey GH, Oduncu FS. A dual-targeting triplebody mediates preferential redirected lysis of antigen double-positive over single-positive leukemic cells. *MAbs*. 2014;6(1):286-296.

REFERENCES

252. van Gosliga D, Schepers H, Rizo A, van der Kolk D, Vellenga E, Schuringa JJ. Establishing long-term cultures with self-renewing acute myeloid leukemia stem/progenitor cells. *Exp Hematol.* 2007;35(10):1538-1549.
253. Amsellem S, Pflumio F, Bardinet D, et al. Ex vivo expansion of human hematopoietic stem cells by direct delivery of the HOXB4 homeoprotein. *Nat Med.* 2003;9(11):1423-1427.
254. Funayama K, Shimane M, Nomura H, Asano S. An evidence for adhesion-mediated acquisition of acute myeloid leukemic stem cell-like immaturities. *Biochem Biophys Res Commun.* 2010;392(3):271-276.
255. Chomel JC, Bonnet ML, Sorel N, et al. Leukemic stem cell persistence in chronic myeloid leukemia patients with sustained undetectable molecular residual disease. *Blood.* 2011;118(13):3657-3660.
256. Sandhofer N, Metzeler KH, Rothenberg M, et al. Dual PI3K/mTOR inhibition shows antileukemic activity in MLL-rearranged acute myeloid leukemia. *Leukemia.* 2015;29(4):828-838.
257. Kugler M, Stein C, Kellner C, et al. A recombinant trispesific single-chain Fv derivative directed against CD123 and CD33 mediates effective elimination of acute myeloid leukaemia cells by dual targeting. *Br J Haematol.* 2010;150(5):574-586.
258. Schubert I, Kellner C, Stein C, et al. A single-chain triplebody with specificity for CD19 and CD33 mediates effective lysis of mixed lineage leukemia cells by dual targeting. *MAbs.* 2011;3(1):21-30.
259. Contreras-Sandoval AM, Merino M, Vasquez M, Troconiz IF, Berraondo P, Garrido MJ. Correlation between anti-PD-L1 tumor concentrations and tumor-specific and nonspecific biomarkers in a melanoma mouse model. *Oncotarget.* 2016;7(47):76891-76901.
260. Walter RB, Raden BW, Kamikura DM, Cooper JA, Bernstein ID. Influence of CD33 expression levels and ITIM-dependent internalization on gemtuzumab ozogamicin-induced cytotoxicity. *Blood.* 2005;105(3):1295-1302.
261. Ponce LP, Fenn NC, Moritz N, et al. SIRPalpha-antibody fusion proteins stimulate phagocytosis and promote elimination of acute myeloid leukemia cells. *Oncotarget.* 2017.
262. Tsoukas CD, Landgraf B, Bentin J, et al. Activation of resting T lymphocytes by anti-CD3 (T3) antibodies in the absence of monocytes. *J Immunol.* 1985;135(3):1719-1723.
263. Bugelski PJ, Achuthanandam R, Capocasale RJ, Treacy G, Bouman-Thio E. Monoclonal antibody-induced cytokine-release syndrome. *Expert Rev Clin Immunol.* 2009;5(5):499-521.
264. Zhang X, Schwartz JC, Guo X, et al. Structural and functional analysis of the costimulatory receptor programmed death-1. *Immunity.* 2004;20(3):337-347.
265. Ommen HB. Monitoring minimal residual disease in acute myeloid leukaemia: a review of the current evolving strategies. *Ther Adv Hematol.* 2016;7(1):3-16.
266. Valitutti S, Muller S, Salio M, Lanzavecchia A. Degradation of T cell receptor (TCR)-CD3-zeta complexes after antigenic stimulation. *J Exp Med.* 1997;185(10):1859-1864.
267. Favier B, Burroughs NJ, Wedderburn L, Valitutti S. TCR dynamics on the surface of living T cells. *Int Immunol.* 2001;13(12):1525-1532.
268. Liu H, Rhodes M, Wiest DL, Vignali DA. On the dynamics of TCR:CD3 complex cell surface expression and downmodulation. *Immunity.* 2000;13(5):665-675.
269. Valitutti S, Muller S, Cella M, Padovan E, Lanzavecchia A. Serial triggering of many T-cell receptors by a few peptide-MHC complexes. *Nature.* 1995;375(6527):148-151.
270. Storz U. Rituximab: how approval history is reflected by a corresponding patent filing strategy. *MAbs.* 2014;6(4):820-837.
271. Davila ML, Riviere I, Wang X, et al. Efficacy and toxicity management of 19-28z CAR T cell therapy in B cell acute lymphoblastic leukemia. *Sci Transl Med.* 2014;6(224):224ra225.
272. Frey NV, Porter DL. CAR T-cells merge into the fast lane of cancer care. *Am J Hematol.* 2016;91(1):146-150.

REFERENCES

273. Stelljes M, Krug U, Beelen DW, et al. Allogeneic transplantation versus chemotherapy as postremission therapy for acute myeloid leukemia: a prospective matched pairs analysis. *J Clin Oncol.* 2014;32(4):288-296.
274. Hornig N, Kermer V, Frey K, Diebold P, Kontermann RE, Muller D. Combination of a bispecific antibody and costimulatory antibody-ligand fusion proteins for targeted cancer immunotherapy. *J Immunother.* 2012;35(5):418-429.
275. Schreiber T, Fromm G, De Silva SS, Schilling N. Compositions and methods for adjoining type i and type ii extracellular domains as heterologous chimeric proteins. Google Patents; 2017.
276. Arndt C, Feldmann A, von Bonin M, et al. Costimulation improves the killing capability of T cells redirected to tumor cells expressing low levels of CD33: description of a novel modular targeting system. *Leukemia.* 2014;28(1):59-69.
277. Offner S, Hofmeister R, Romaniuk A, Kufer P, Baeuerle PA. Induction of regular cytolytic T cell synapses by bispecific single-chain antibody constructs on MHC class I-negative tumor cells. *Mol Immunol.* 2006;43(6):763-771.
278. Behl D, Porrata LF, Markovic SN, et al. Absolute lymphocyte count recovery after induction chemotherapy predicts superior survival in acute myelogenous leukemia. *Leukemia.* 2006;20(1):29-34.
279. Bruserud O, Ulvestad E, Berentsen S, Bergheim J, Nesthus I. T-lymphocyte functions in acute leukaemia patients with severe chemotherapy-induced cytopenia: characterization of clonogenic T-cell proliferation. *Scand J Immunol.* 1998;47(1):54-62.
280. Porrata LF, Litzow MR, Tefferi A, et al. Early lymphocyte recovery is a predictive factor for prolonged survival after autologous hematopoietic stem cell transplantation for acute myelogenous leukemia. *Leukemia.* 2002;16(7):1311-1318.
281. Ribera JM, Ferrer A, Ribera J, Genesca E. Profile of blinatumomab and its potential in the treatment of relapsed/refractory acute lymphoblastic leukemia. *Onco Targets Ther.* 2015;8:1567-1574.
282. McLaughlin P, Grillo-Lopez AJ, Link BK, et al. Rituximab chimeric anti-CD20 monoclonal antibody therapy for relapsed indolent lymphoma: half of patients respond to a four-dose treatment program. *J Clin Oncol.* 1998;16(8):2825-2833.
283. Amadori S, Suci S, Selleslag D, et al. Gemtuzumab Ozogamicin Versus Best Supportive Care in Older Patients With Newly Diagnosed Acute Myeloid Leukemia Unsuitable for Intensive Chemotherapy: Results of the Randomized Phase III EORTC-GIMEMA AML-19 Trial. *J Clin Oncol.* 2016;34(9):972-979.
284. Burnett AK, Hills RK, Milligan D, et al. Identification of patients with acute myeloblastic leukemia who benefit from the addition of gemtuzumab ozogamicin: results of the MRC AML15 trial. *J Clin Oncol.* 2011;29(4):369-377.
285. Bartee MY, Dunlap KM, Bartee E. Tumor-Localized Secretion of Soluble PD1 Enhances Oncolytic Virotherapy. *Cancer Res.* 2017;77(11):2952-2963.
286. Ehninger A, Kramer M, Rollig C, et al. Distribution and levels of cell surface expression of CD33 and CD123 in acute myeloid leukemia. *Blood Cancer J.* 2014;4:e218.
287. Freeman SD, Kelm S, Barber EK, Crocker PR. Characterization of CD33 as a new member of the sialoadhesin family of cellular interaction molecules. *Blood.* 1995;85(8):2005-2012.
288. Taksin AL, Legrand O, Raffoux E, et al. High efficacy and safety profile of fractionated doses of Mylotarg as induction therapy in patients with relapsed acute myeloblastic leukemia: a prospective study of the alfa group. *Leukemia.* 2007;21(1):66-71.
289. Larson RA, Sievers EL, Stadtmauer EA, et al. Final report of the efficacy and safety of gemtuzumab ozogamicin (Mylotarg) in patients with CD33-positive acute myeloid leukemia in first recurrence. *Cancer.* 2005;104(7):1442-1452.

REFERENCES

290. Gupta P, Goldenberg DM, Rossi EA, et al. Dual-targeting immunotherapy of lymphoma: potent cytotoxicity of anti-CD20/CD74 bispecific antibodies in mantle cell and other lymphomas. *Blood*. 2012;119(16):3767-3778.
291. Hernandez-Caselles T, Martinez-Esparza M, Perez-Oliva AB, et al. A study of CD33 (SIGLEC-3) antigen expression and function on activated human T and NK cells: two isoforms of CD33 are generated by alternative splicing. *J Leukoc Biol*. 2006;79(1):46-58.
292. Biedermann B, Gil D, Bowen DT, Crocker PR. Analysis of the CD33-related siglec family reveals that Siglec-9 is an endocytic receptor expressed on subsets of acute myeloid leukemia cells and absent from normal hematopoietic progenitors. *Leuk Res*. 2007;31(2):211-220.
293. Attarwala H. TGN1412: From Discovery to Disaster. *J Young Pharm*. 2010;2(3):332-336.
294. Suntharalingam G, Perry MR, Ward S, et al. Cytokine storm in a phase 1 trial of the anti-CD28 monoclonal antibody TGN1412. *The New England journal of medicine*. 2006;355(10):1018-1028.
295. Stebbings R, Poole S, Thorpe R. Safety of biologics, lessons learnt from TGN1412. *Curr Opin Biotechnol*. 2009;20(6):673-677.
296. Kohnke T, Krupka C, Tischer J, Knosel T, Subklewe M. Increase of PD-L1 expressing B-precursor ALL cells in a patient resistant to the CD19/CD3-bispecific T cell engager antibody blinatumomab. *J Hematol Oncol*. 2015;8:111.
297. Chen X, Kline DE, Kline J. Peripheral T-cell tolerance in hosts with acute myeloid leukemia. *Oncoimmunology*. 2013;2(8):e25445.
298. Molfetta R, Quatrini L, Gasparrini F, Zitti B, Santoni A, Paolini R. Regulation of fc receptor endocytic trafficking by ubiquitination. *Front Immunol*. 2014;5:449.
299. Unverdorben F, Richter F, Hutt M, et al. Pharmacokinetic properties of IgG and various Fc fusion proteins in mice. *MAbs*. 2016;8(1):120-128.
300. Keizer RJ, Huitema ADR, Schellens JHM, Beijnen JH. Clinical Pharmacokinetics of Therapeutic Monoclonal Antibodies. *Clinical Pharmacokinetics*. 2010;49(8):493-507.
301. Ghetie V, Ward ES. Multiple roles for the major histocompatibility complex class I- related receptor FcRn. *Annu Rev Immunol*. 2000;18:739-766.
302. Mankarious S, Lee M, Fischer S, et al. The half-lives of IgG subclasses and specific antibodies in patients with primary immunodeficiency who are receiving intravenously administered immunoglobulin. *J Lab Clin Med*. 1988;112(5):634-640.
303. Caliceti P, Veronese FM. Pharmacokinetic and biodistribution properties of poly(ethylene glycol)-protein conjugates. *Adv Drug Deliv Rev*. 2003;55(10):1261-1277.
304. Schlapschy M, Binder U, Borger C, et al. PASylation: a biological alternative to PEGylation for extending the plasma half-life of pharmaceutically active proteins. *Protein Eng Des Sel*. 2013;26(8):489-501.
305. Rogers B, Dong D, Li Z, Li Z. Recombinant human serum albumin fusion proteins and novel applications in drug delivery and therapy. *Curr Pharm Des*. 2015;21(14):1899-1907.
306. Andersen JT, Pehrson R, Tolmachev V, Daba MB, Abrahmsen L, Ekblad C. Extending half-life by indirect targeting of the neonatal Fc receptor (FcRn) using a minimal albumin binding domain. *J Biol Chem*. 2011;286(7):5234-5241.
307. Worn A, Pluckthun A. Stability engineering of antibody single-chain Fv fragments. *J Mol Biol*. 2001;305(5):989-1010.
308. Ewert S, Honegger A, Pluckthun A. Stability improvement of antibodies for extracellular and intracellular applications: CDR grafting to stable frameworks and structure-based framework engineering. *Methods*. 2004;34(2):184-199.
309. Young NM, MacKenzie CR, Narang SA, Oomen RP, Baenziger JE. Thermal stabilization of a single-chain Fv antibody fragment by introduction of a disulphide bond. *FEBS Lett*. 1995;377(2):135-139.
310. Zhao JX, Yang L, Gu ZN, et al. Stabilization of the single-chain fragment variable by an interdomain disulfide bond and its effect on antibody affinity. *Int J Mol Sci*. 2010;12(1):1-11.

REFERENCES

311. Kohnken R, Porcu P, Mishra A. Overview of the Use of Murine Models in Leukemia and Lymphoma Research. *Front Oncol.* 2017;7:22.
312. Brehm MA, Wiles MV, Greiner DL, Shultz LD. Generation of improved humanized mouse models for human infectious diseases. *J Immunol Methods.* 2014;410:3-17.
313. Basova P, Pospisil V, Savvulidi F, et al. Aggressive acute myeloid leukemia in PU.1/p53 double-mutant mice. *Oncogene.* 2014;33(39):4735-4745.
314. Beurlet S, Omidvar N, Gorombeï P, et al. BCL-2 inhibition with ABT-737 prolongs survival in an NRAS/BCL-2 mouse model of AML by targeting primitive LSK and progenitor cells. *Blood.* 2013;122(16):2864-2876.

ABBREVIATIONS

7. List of abbreviations

ADC	antibody-drug conjugate	c-Met	cellular-mesenchymal to
ADCC	antibody-dependent cellular cytotoxicity		epithelial transition factor
ADCP	antibody-dependent cellular phagocytosis	CMTM	chemokine-like factor-like MARVEL transmembrane domain-containing protein
ALL	acute lymphoblastic leukemia	CNS	central nervous system
AML	acute myeloid leukemia	COX-2	cyclooxygenase-2
AP-1	activator protein-1	CRS	cytokine release syndrome
APC	antigen presenting cell	CTL	cytotoxic T lymphocyte
BATF	basic leucine zipper transcriptional factor ATF-like	CTLA-4	cytotoxic T lymphocyte- associated protein-4
BCG	Bacille Calmette-Guérin	DART	dual-affinity receptor re- targeting
BCR	B cell receptor	DC	dendritic cell
BiTE [®]	bispecific T cell engager	E:T	effector-to-target cell ratio
BM	bone marrow	EMA	European Medicines Agency
C	constant	Fab	fragment for antigen binding
CalichDMH	N-acetyl-g-calicheamicin dimethyl hydrazide	FAB	French-American-British
CAR	chimeric antigen receptor	Fc	fragment crystallizable
CD	cluster of differentiation	FcR	Fc receptor
CDC	complement-dependent cytotoxicity	FcRn	neonatal Fc receptor
CDR	complementarity-determining region	FcγR	Fc gamma receptor
CEA	carcinoembryonic antigen	FDA	U.S. Food and Drug Administration
C _H	constant region of Ig heavy chain	Flt3	FSM-like tyrosine kinase 3
C _L	constant region of Ig light chain	FR	framework region
CLR	C-type lectin receptor	GO	gemtuzumab ozogamicin
		GvL	graft-versus-leukemia
		H	heavy
		HAMA	human anti-mouse antibody

ABBREVIATIONS

HSA	human serum albumin		complex
HSC	hematopoietic stem cell	MRD	minimal residual disease
HSCT	hematopoietic stem cell transplantation	NFAT	nuclear factor of activated T cells
HV	hypervariable	NF- κ B	nuclear factor- κ B
i.v.	intravenous	NHL	non-Hodgkin's lymphoma
ICOS	inducible co-stimulator	NK	natural killer
IDO	indoleamine 2,3-dioxygenase	NOD	non-obese diabetic
IFN	interferon	NPM1	nucleophosmin 1
Ig	immunoglobulin	NSCLC	non-small-cell lung cancer
IL	interleukin	NSG	NOD scid gamma
ImmTAC [®]	immune mobilizing monoclonal T-cell receptors against cancer	NTA	nitrilotriacetic acid
IPRES	Innate PD-1 RESistance	ORF	open reading frame
irAE	immune-related adverse event	OS	overall survival
ITD	internal tandem duplication	PAGE	polyacrylamide gel electrophoresis
ITIM	immunoreceptor tyrosine-based inhibitory motif	PAS	proline-alanine-serine
ITSM	immunoreceptor tyrosine-based switch motif	PB	peripheral blood
K _D	equilibrium dissociation constant	PBMC	peripheral blood mononuclear cell
kih	knobs-into-holes	PD-1	programmed death-1
L	light	PD-L	programmed death-ligand
LAA	leukemia-associated antigen	PEG	polyethylene glycol
LB	lysogeny broth	PGE ₂	prostaglandine E ₂
LSC	leukemic stem cell	PI3K	phosphoinositide 3-kinase
mAb	monoclonal antibody	PKC θ	protein kinase C θ
MBL	mannose-binding lectin	r/r	relapsed or refractory
MDSC	myeloid-derived suppressor cell	RAS	rat sarcoma
MHC	major histocompatibility	RDL	redirected lysis
		RGMB	repulsive guidance molecule B
		scFv	single-chain variable fragment
		sctb	single-chain triplebody
		SDS	sodium dodecyl sulfate

ABBREVIATIONS

SHP-2	src homology 2-domain- containing tyrosine phosphatase	T_H	T helper cell
SEC	size exclusion chromatography	TIM-3	T-cell immunoglobulin and mucin-domain containing
Siglec	sialic acid-binding immunoglobulin-like lectin	TNF	tumor necrosis factor
SNP	single-nucleotide polymorphism	TNFR	tumor necrosis factor receptor
TAA	tumor-associated antigen	T_{reg}	regulatory T cell
TandAb [®]	tetravalent bispecific tandem diabody.	tris	tris-hydroxymethyl- aminomethane
TCB	T cell bispecific	V	variable
TCR	T cell receptor	V_H	variable region of Ig heavy chain
TDLN	tumor-draining lymph node	V_L	variable region of Ig light chain
TGF	transforming growth factor	WHO	World Health Organization

8. Acknowledgements

First of all, I want to thank my supervisor Prof. Dr. Karl-Peter Hopfner for the chance to work on the new concept of local T cell immune checkpoint blockade and the continuous support during my PhD project. I am especially grateful for the freedom to establish my experiments and to design my research, which allowed me to develop my own ideas.

I would like to express my gratitude to Prof. Dr. Marion Subklewe for the great collaboration and the helpful scientific input. Moreover, I want to thank Dr. Christina Krupka and Dr. Katrin Deiser for scientific discussions and the time they invested in the evaluation of my molecules on patient samples and in mouse studies.

Special thanks go to PD Dr. Sebastian Kobold for fruitful scientific discussions and for being my second supervisor. Together with Prof. Dr. Elfriede Nößner I also want to thank him for valuable advice in my Thesis Advisory Committee. In addition, I want to thank Dr. Felicitas Rataj and Constanze Heise for the contribution to my project.

I am very grateful to the members of the antibody subgroup. I want to especially thank Alexandra Schele for her advice in protein biochemistry, and Dr. Nadja Fenn for her input during the whole project and the writing process of the manuscript. Many thanks also go to Laia Pascual Ponce, Dr. Nadine Magauer, Dr. Claudia Roskopf, Saskia Schmitt, Siret Tahk and Simon Dedic. It was a great pleasure to work with you! Moreover, I want to thank Dr. Charlotte Lässig, David Drexler and Adrian Bandera. I really enjoyed our conversations about science and a lot of other things. Furthermore, I want to thank all the other lab members of the AG Hopfner who supported me during my thesis. Thanks a lot for your advice and the good working atmosphere, you are a great team!

Ganz besonders möchte ich mich bei meinen Eltern, Franziska und Markus bedanken, die mich in jeglicher Situation unterstützt haben. Ohne euch wäre diese Arbeit nicht möglich gewesen.